

66-482777
DD-482777
ASD-TDR-63-159

EPN
MATERIALS CENTER TECHNICAL LIBRARY
OFFICIAL FILE COPY

WIND TUNNEL STUDY OF
PARACHUTE CLUSTERING

TECHNICAL DOCUMENTARY REPORT ASD-TDR-63-159

April 1963

Flight Accessories Laboratory
Directorate of Aeromechanics
Aeronautical Systems Division
Air Force Systems Command
Wright-Patterson Air Force Base, Ohio

Project No. 6065, Task No. 606502

(Prepared under Contract No. AF 33(657)-7985
by Technology Incorporated, Dayton, Ohio.
Authors: J. F. Braun and W. B. Walcott)

NOTICES

When Government drawings, specifications, or other data are used for any purpose other than in connection with a definitely related Government procurement operation, the United States Government thereby incurs no responsibility nor any obligation whatsoever; and the fact that the Government may have formulated, furnished, or in any way supplied the said drawings, specifications, or other data, is not to be regarded by implication or otherwise as in any manner licensing the holder or any other person or corporation, or conveying any rights or permission to manufacture, use, or sell any patented invention that may in any way be related thereto.

Qualified requesters may obtain copies of this report from the Armed Services Technical Information Agency, (ASTIA), Arlington Hall Station, Arlington 12, Virginia.

This report has been released to the Office of Technical Services, U.S. Department of Commerce, Washington 25, D. C. , for sale to the general public.

Copies of this report should not be returned to the Aeronautical Systems Division unless return is required by security considerations, contractual obligations, or notice on a specific document.

FOREWORD

This report was initiated by the Retardation and Recovery Branch, Flight Accessories Laboratory, Directorate of Aeromechanics, Deputy for Technology, Aeronautical Systems Division, Wright-Patterson Air Force Base, Ohio. The testing effort and the subsequent review and analysis of the data upon which the report is based were accomplished by Technology Incorporated, Dayton, Ohio, under Air Force Contract Number AF 33(657)-7985, Project Number 6065, "Performance and Design of Deployable Aerodynamic Decelerators," Task Number 606502, "Subsonic Parachute Performance Parameters."

Mr. Lawrence L. Watson of the Aeronautical Systems Division was the project engineer. Mr. K. L. Rickey, project manager of Technology Incorporated, was in charge of the work covered under this contract.

The authors are appreciative of the contributions of the following associates: Mr. Ronald Ruff, who conducted the wind tunnel tests; Mr. Krishan Joshi, who supervised the data reduction; and Mr. Dale Bazill, who designed the balance and sting.

ABSTRACT

Four types of canopies were tested in a 12-foot vertical wind tunnel at a velocity of approximately 100 feet per second to determine the static stability and drag characteristics of multiple canopies in various clustered arrangements under captive and equilibrium test conditions. Solid Flat Circular, Extended Skirt, Ringslot, and Circular Flat Ribbon were the types of canopy tested. Canopies of each type were tested individually and in clusters ranging from two to seven canopies per cluster. A special two-component balance was fabricated to measure the pitching moment and tangential force over an angle-of-attack range of ± 25 degrees. The effects of riser length, angle-of-attack, reefing ratio, and the number of canopies in a cluster on the tangential force and static stability are discussed. Also, the characteristics peculiar to the solid type of canopies (Solid Flat Circular and Extended Skirt) and to the ribbon type of canopies (Ringslot and Circular Flat Ribbon) are noted.

Publication of this technical documentary report does not constitute Air Force approval of the report's findings or conclusions. It is published only for the exchange and stimulation of ideas.



GEORGE A. SOLT, JR.

Chief, Aerodynamic Decelerator Branch
Flight Accessories Laboratory

TABLE OF CONTENTS

<u>Section</u>		<u>Page</u>
1	Introduction	1
2	Procedure	1
2.1	General	1
2.2	Sign Convention	4
2.3	Model Parachute Canopies	4
2.4	Description of the ASD Vertical Wind Tunnel	7
2.5	Instrumentation	8
2.6	Testing Procedure, Captive Tests	8
2.7	Testing Procedure, Equilibrium Tests	9
2.8	Pressure Survey Before and After the Two-Component Balance Installation	10
2.9	Aerodynamic Tare Determination	11
2.10	Data Reduction	11
3	Results	14
3.1	General	14
3.2	Order of Results Presentation	15
3.3	Constant Dynamic Pressure as Opposed to Constant Velocity	17
3.4	Parachute Cluster Orientation	17
4	Data Discussion	62
4.1	General	62
4.2	Data Accuracy	62
4.2.1	Over-all Data Accuracy	62
4.2.2	Raw Data Recordings and Measurements	62
4.2.3	Dynamic Pressure	62
4.2.4	Other Factors Related to Data Accuracy	63
4.3	Solid Canopies (Circular Flat and Extended Skirt)	63
4.4	Ribbon Canopies (Circular Flat and Ringslot)	66
4.5	Over-all Comparisons	69
5	Conclusions and Recommendations	70
5.1	Conclusions	70
5.2	Recommendations	70
	Appendix I. Parachute Instrumentation System	73
	Appendix II. Model Parachute Description	79

LIST OF ILLUSTRATIONS

<u>Figure</u>		<u>Page</u>
1	Graphic Presentation of Sign Convention Employed in this Parachute Cluster Study	2
2	View Showing Mechanical Arrangement Maintaining the Fixed Canopy Separation of a Cluster of Five Extended Skirt Type of Canopies	3
3	Typical View of Five Extended Skirt Type of Canopies in a Cluster: Reefing Ratio (D_r/D_o) - 0.5 and Riser Length - $1.5 D_o$	3
4	Scene Showing Configuration with Adjustable Suspended Weight for Equilibrium Tests	4
5	Orthogonal Views of Model Two-Cluster Parachute Arrangement	5
6	Two-Component Balance Seen at the Base of the Parachute Cluster Configuration	6
7	Sectional Drawing of the ASD Vertical Wind Tunnel Indicating the Air Flow Direction	7
8	Drawings Depicting Arrangements of Canopy Clusters with Respect to Strut and Travel Direction	9
9	Dynamic Pressure Survey of the ASD Vertical Wind Tunnel before Installation of Two-Component Balance	12
10	Dynamic Pressure Survey of the ASD Vertical Wind Tunnel after Installation of Two-Component Balance	13
11	View of Five Extended Skirt Canopies Illustrating Onset of Collapse	15
12	Variation of Tangential Force and Moment Coefficients with Angle-of-Attack: Canopy Type - Flat Circular, Cluster - one; Reefing Ratio - none; Riser Length - $0 D_o$	18
13	Variation of Tangential Force and Moment Coefficients with Angle-of-Attack: Canopy Type - Flat Circular; Cluster - one, Reefing Ratio - 0.5; Riser Length - $0 D_o$	18

LIST OF ILLUSTRATIONS (cont'd)

<u>Figure</u>		<u>Page</u>
14	Variation of Tangential Force and Moment Coefficients with Angle-of-Attack: Canopy Type - Flat Circular; Cluster - one; Reefing Ratio - 0.3; Riser Length - 0 D_0	19
15	Variation of Tangential Force and Moment Coefficients with Angle-of-Attack: Canopy Type - Flat Circular; Cluster - one; Reefing Ratio - 0.2; Riser Length - 0 D_0	19
16	Variation of Tangential Force and Moment Coefficients with Angle-of-Attack: Canopy Type - Flat Circular; Cluster - two; Reefing Ratio - none; Riser Length - 0.5 D_0	20
17	Variation of Tangential Force and Moment Coefficients with Angle-of-Attack: Canopy Type - Flat Circular; Cluster - two; Reefing Ratio - 0.5; Riser Length - 0.5 D_0	20
18	Variation of Tangential Force and Moment Coefficients with Angle-of-Attack: Canopy Type - Flat Circular; Cluster - two; Reefing Ratio - 0.3; Riser Length - 0.5 D_0	21
19	Variation of Tangential Force and Moment Coefficients with Angle-of-Attack: Canopy Type - Flat Circular; Cluster - three; Reefing Ratio - none; Riser Length - 1.0 D_0	21
20	Variation of Tangential Force and Moment Coefficients with Angle-of-Attack: Canopy Type - Flat Circular; Cluster - three; Reefing Ratio - none; Riser Length - 0.5 D_0	22
21	Variation of Tangential Force and Moment Coefficients with Angle-of-Attack: Canopy Type - Flat Circular; Cluster - three; Reefing Ratio - 0.5; Riser Length - 1.0 D_0	22
22	Variation of Tangential Force and Moment Coefficients with Angle-of-Attack: Canopy Type - Flat Circular; Cluster - three; Reefing Ratio - 0.5; Riser Length - 0.5 D_0	23

LIST OF ILLUSTRATIONS (cont'd)

<u>Figure</u>		<u>Page</u>
23	Variation of Tangential Force and Moment Coefficients with Angle-of-Attack: Canopy Type - Flat Circular; Cluster - three; Reefing Ratio - 0.3; Riser Length - 1.0 D_0	23
24	Variation of Tangential Force and Moment Coefficients with Angle-of-Attack: Canopy Type - Flat Circular; Cluster - three; Reefing Ratio - Riser Length - 0.5 D_0	24
25	Variation of Tangential Force and Moment Coefficients with Angle-of-Attack: Canopy Type - Flat Circular; Cluster - five; Reefing Ratio - none; Riser Length - 1.5 D_0	24
26	Variation of Tangential Force and Moment Coefficients with Angle-of-Attack: Canopy Type - Flat Circular; Cluster - five; Reefing Ratio - none; Riser Length - 1.0 D_0	25
27	Variation of Tangential Force and Moment Coefficients with Angle-of-Attack: Canopy Type - Flat Circular; Cluster - five; Reefing Ratio - none; Riser Length - 0.5 D_0	25
28	Variation of Tangential Force and Moment Coefficients with Angle-of-Attack: Canopy Type - Flat Circular; Cluster - five; Reefing Ratio - 0.5; Riser Length - 1.5 D_0	26
29	Variation of Tangential Force and Moment Coefficients with Angle-of-Attack: Canopy Type - Flat Circular; Cluster - five; Reefing Ratio - 0.5; Riser Length - 1.0 D_0	26
30	Variation of Tangential Force and Moment Coefficients with Angle-of-Attack: Canopy Type - Flat Circular; Cluster - five; Reefing Ratio - 0.5; Riser Length - 0.5 D_0	27
31	Variation of Tangential Force and Moment Coefficients with Angle-of-Attack: Canopy Type - Flat Circular; Cluster - five; Reefing Ratio - 0.3; Riser Length - 1.5 D_0	27

LIST OF ILLUSTRATIONS (cont'd)

<u>Figure</u>		<u>Page</u>
32	Variation of Tangential Force and Moment Coefficients with Angle-of-Attack: Canopy Type - Flat Circular; Cluster - five; Reefing Ratio - 0.3; Riser Length - 1.0 D_0	28
33	Variation of Tangential Force and Moment Coefficients with Angle-of-Attack: Canopy Type - Flat Circular; Cluster - five; Reefing Ratio - 0.3; Riser Length - 0.5 D_0	28
34	Variation of Tangential Force and Moment Coefficients with Angle-of-Attack: Canopy Type - Flat Circular; Cluster - seven; Reefing Ratio - none; Riser Length - 1.5 D_0	29
35	Variation of Tangential Force and Moment Coefficients with Angle-of-Attack: Canopy Type - Flat Circular; Cluster - seven; Reefing Ratio - none; Riser Length - 1.0 D_0	29
36	Variation of Tangential Force and Moment Coefficients with Angle-of-Attack: Canopy Type - Flat Circular; Cluster - seven; Reefing Ratio - 0.5; Riser Length - 1.5 D_0	30
37	Variation of Tangential Force and Moment Coefficients with Angle-of-Attack: Canopy Type - Flat Circular; Cluster - seven; Reefing Ratio - 0.5; Riser Length - 1.0 D_0	30
38	Variation of Tangential Force and Moment Coefficients with Angle-of-Attack: Canopy Type - Flat Circular; Cluster - seven; Reefing Ratio - 0.3; Riser Length - 1.5 D_0	31
39	Variation of Tangential Force and Moment Coefficients with Angle-of-Attack: Canopy Type - Flat Circular; Cluster - seven; Reefing Ratio - 0.3; Riser Length - 1.0 D_0	31
40	Variation of Tangential Force and Moment Coefficients with Angle-of-Attack: Canopy Type - Extended Skirt; Cluster - one; Reefing Ratio - none; Riser Length - 0 D_0	32

LIST OF ILLUSTRATIONS (cont'd)

<u>Figure</u>		<u>Page</u>
41	Variation of Tangential Force and Moment Coefficients with Angle-of-Attack: Canopy Type - Extended Skirt; Cluster - one; Reefing Ratio - 0.5; Riser Length - $0.7 D_0$	32
42	Variation of Tangential Force and Moment Coefficients with Angle-of-Attack: Canopy Type - Extended Skirt; Cluster - one; Reefing Ratio - 0.3; Riser Length - $0 D_0$	33
43	Variation of Tangential Force and Moment Coefficients with Angle-of-Attack: Canopy Type - Extended Skirt; Cluster - one; Reefing Ratio - 0.2; Riser Length - $0 D_0$	33
44	Variation of Tangential Force and Moment Coefficients with Angle-of-Attack: Canopy Type - Extended Skirt; Cluster - two; Reefing Ratio - none; Riser Length - $0.5 D_0$	34
45	Variation of Tangential Force and Moment Coefficients with Angle-of-Attack: Canopy Type - Extended Skirt; Cluster - two; Reefing Ratio - 0.5; Riser Length - $0.5 D_0$	34
46	Variation of Tangential Force and Moment Coefficients with Angle-of-Attack: Canopy Type - Extended Skirt; Cluster - two; Reefing Ratio - 0.3; Riser Length - $0.5 D_0$	35
47	Variation of Tangential Force and Moment Coefficients with Angle-of-Attack: Canopy Type - Extended Skirt; Cluster - three; Reefing Ratio - none; Riser Length - $1.0 D_0$	35
48	Variation of Tangential Force and Moment Coefficients with Angle-of-Attack: Canopy Type - Extended Skirt; Cluster - three; Reefing Ratio - none; Riser Length - $0.5 D_0$	36
49	Variation of Tangential Force and Moment Coefficients with Angle-of-Attack: Canopy Type - Extended Skirt; Cluster - three; Reefing Ratio - 0.5; Riser Length - $1.0 D_0$	36

LIST OF ILLUSTRATIONS (cont'd)

<u>Figure</u>		<u>Page</u>
50	Variation of Tangential Force and Moment Coefficients with Angle-of-Attack: Canopy Type - Extended Skirt; Cluster - three; Reefing Ratio - 0.5; Riser Length - $0.5 D_0$	37
51	Variation of Tangential Force and Moment Coefficients with Angle-of-Attack: Canopy Type - Extended Skirt; Cluster - three; Reefing Ratio - 0.3; Riser Length - $1.0 D_0$	37
52	Variation of Tangential Force and Moment Coefficients with Angle-of-Attack: Canopy Type - Extended Skirt; Cluster - three; Reefing Ratio - 0.3; Riser Length - $0.5 D_0$	38
53	Variation of Tangential Force and Moment Coefficients with Angle-of-Attack: Canopy Type - Extended Skirt; Cluster - five; Reefing Ratio - none; Riser Length - $1.5 D_0$	38
54	Variation of Tangential Force and Moment Coefficients with Angle-of-Attack: Canopy Type - Extended Skirt; Cluster - five; Reefing Ratio - none; Riser Length - $1.0 D_0$	39
55	Variation of Tangential Force and Moment Coefficients with Angle-of-Attack: Canopy Type - Extended Skirt; Cluster - five; Reefing Ratio - none; Riser Length - $0.5 D_0$	39
56	Variation of Tangential Force and Moment Coefficients with Angle-of-Attack: Canopy Type - Extended Skirt; Cluster - five; Reefing Ratio - 0.5; Riser Length - $1.5 D_0$	40
57	Variation of Tangential Force and Moment Coefficients with Angle-of-Attack: Canopy Type - Extended Skirt; Cluster - five; Reefing Ratio - 0.5; Riser Length - $1.0 D_0$	40
58	Variation of Tangential Force and Moment Coefficients with Angle-of-Attack: Canopy Type - Extended Skirt; Cluster - five, Reefing Ratio - 0.5; Riser Length - $0.5 D_0$	41

LIST OF ILLUSTRATIONS (cont'd)

<u>Figure</u>		<u>Page</u>
59	Variation of Tangential Force and Moment Coefficients with Angle-of-Attack: Canopy Type - Extended Skirt; Cluster - five; Reefing Ratio - 0.3; Riser Length - 1.5 D_0	41
60	Variation of Tangential Force and Moment Coefficients with Angle-of-Attack: Canopy Type - Extended Skirt; Cluster - five; Reefing Ratio - 0.3; Riser Length - 1.0 D_0	42
61	Variation of Tangential Force and Moment Coefficients with Angle-of-Attack: Canopy Type - Extended Skirt; Cluster - five; Reefing Ratio - 0.3; Riser Length - 0.5 D_0	42
62	Variation of Tangential Force and Moment Coefficients with Angle-of-Attack: Canopy Type - Ribbon; Cluster; - one; Reefing Ratio - none; Riser Length - 0 D_0	43
63	Variation of Tangential Force and Moment Coefficients with Angle-of-Attack: Canopy Type - Ribbon; Cluster - one; Reefing Ratio - 0.5; Riser Length - 0 D_0	43
64	Variation of Tangential Force and Moment Coefficients with Angle-of-Attack: Canopy Type - Ribbon; Cluster - one; Reefing Ratio - 0.3; Riser Length - 0 D_0	44
65	Variation of Tangential Force and Moment Coefficients with Angle-of-Attack: Canopy Type - Ribbon; Cluster - one; Reefing Ratio - 0.2; Riser Length - 0 D_0	44
66	Variation of Tangential Force and Moment Coefficients with Angle-of-Attack: Canopy Type - Ribbon; Cluster - two; Reefing Ratio - none; Riser Length - 0.5 D_0	45
67	Variation of Tangential Force and Moment Coefficients with Angle-of-Attack: Canopy Type - Ribbon; Cluster - two; Reefing Ratio - 0.5; Riser Length - 0.5 D_0	45
68	Variation of Tangential Force and Moment Coefficients with Angle-of-Attack: Canopy Type - Ribbon; Cluster - three; Reefing Ratio - none; Riser Length - 1.0 D_0	46

LIST OF ILLUSTRATIONS (cont'd)

<u>Figure</u>		<u>Page</u>
69	Variation of Tangential Force and Moment Coefficients with Angle-of-Attack: Canopy Type - Ribbon; Cluster - three; Reefing Ratio - none; Riser Length - $0.5 D_0$	46
70	Variation of Tangential Force and Moment Coefficients with Angle-of-Attack: Canopy Type - Ribbon; Cluster - three; Reefing Ratio - 0.5; Riser Length - $1.0 D_0$	47
71	Variation of Tangential Force and Moment Coefficients with Angle-of-Attack: Canopy Type - Ribbon; Cluster - three; Reefing Ratio - 0.5; Riser Length - $0.5 D_0$	47
72	Variation of Tangential Force and Moment Coefficients with Angle-of-Attack: Canopy Type - Ribbon; Cluster - five; Reefing Ratio - none; Riser Length - $1.5 D_0$	48
73	Variation of Tangential Force and Moment Coefficients with Angle-of-Attack: Canopy Type - Ribbon; Cluster - five; Reefing Ratio - none; Riser Length - $1.0 D_0$	48
74	Variation of Tangential Force and Moment Coefficients with Angle-of-Attack: Canopy Type - Ribbon; Cluster - five; Reefing Ratio - none; Riser Length - $0.5 D_0$	49
75	Variation of Tangential Force and Moment Coefficients with Angle-of-Attack: Canopy Type - Ribbon; Cluster - five; Reefing Ratio - 0.5; Riser Length - $1.5 D_0$	49
76	Variation of Tangential Force and Moment Coefficients with Angle-of-Attack: Canopy Type - Ribbon; Cluster - five; Reefing Ratio - 0.5; Riser Length - $1.0 D_0$	50
77	Variation of Tangential Force and Moment Coefficients with Angle-of-Attack: Canopy Type - Ringslot; Cluster - one; Reefing Ratio - none; Riser Length - $0 D_0$	50
78	Variation of Tangential Force and Moment Coefficients with Angle-of-Attack: Canopy Type - Ringslot; Cluster - one; Reefing Ratio - 0.5; Riser Length - $0 D_0$	51
79	Variation of Tangential Force and Moment Coefficients with Angle-of-Attack: Canopy Type - Ringslot; Cluster - one; Reefing Ratio - 0.3; Riser Length - $0 D_0$	51

LIST OF ILLUSTRATIONS (cont'd)

<u>Figure</u>		<u>Page</u>
80	Variation of Tangential Force and Moment Coefficients with Angle-of-Attack: Canopy Type - Ringslot; Cluster - one; Reefing Ratio - 0.3; Riser Length - 0 D_0	52
81	Variation of Tangential Force and Moment Coefficients with Angle-of-Attack: Canopy Type - Ringslot; Cluster - two; Reefing Ratio - none; Riser Length - 0.5 D_0	52
82	Variation of Tangential Force and Moment Coefficients with Angle-of-Attack: Canopy Type - Ringslot; Cluster - three; Reefing Ratio - none; Riser Length - 1.0 D_0	53
83	Variation of Tangential Force and Moment Coefficients with Angle-of-Attack: Canopy Type - Ringslot; Cluster - three; Reefing Ratio - none; Riser Length - 0.5 D_0	53
84	Variation of Tangential Force and Moment Coefficients with Angle-of-Attack: Canopy Type - Ringslot; Cluster - three; Reefing Ratio - 0.5; Riser Length - 1.0 D_0	54
85	Variation of Tangential Force and Moment Coefficients with Angle-of-Attack: Canopy Type - Ringslot; Cluster - three; Reefing Ratio - 0.5; Riser Length - 0.5 D_0	54
86	Variation of Tangential Force and Moment Coefficients with Angle-of-Attack: Canopy Type - Ringslot; Cluster - three; Reefing Ratio - 0.3; Riser Length - 1.0 D_0	55
87	Variation of Tangential Force and Moment Coefficients with Angle-of-Attack: Canopy Type - Ringslot; Cluster - three; Reefing Ratio - 0.3; Riser Length - 0.5 D_0	55
88	Variation of Tangential Force and Moment Coefficients with Angle-of-Attack: Canopy Type - Ringslot; Cluster - five; Reefing Ratio - none; Riser Length - 1.5 D_0	56
89	Variation of Tangential Force and Moment Coefficients with Angle-of-Attack: Canopy Type - Ringslot; Cluster - five; Reefing Ratio - none; Riser Length - 1.0 D_0	56
90	Variation of Drag Coefficient with Reefing Ratio and Riser Length, Equilibrium Test: Canopy Type - Flat Circular; No. of Canopies in a Cluster - one	57

LIST OF ILLUSTRATIONS (cont'd)

<u>Figure</u>		<u>Page</u>
91	Variation of Drag Coefficient with Reefing Ratio and Riser Length, Equilibrium Test: Canopy Type - Flat Circular; No. of Canopies in a Cluster - two	57
92	Variation of Drag Coefficient with Reefing Ratio and Riser Length, Equilibrium Test: Canopy Type - Flat Circular; No. of Canopies in a Cluster - three	57
93	Variation of Drag Coefficient with Reefing Ratio and Riser Length, Equilibrium Test: Canopy Type - Flat Circular; No. of Canopies in a Cluster - four	57
94	Variation of Drag Coefficient with Reefing Ratio and Riser Length, Equilibrium Test: Canopy Type - Extended Skirt; No. of Canopies in a Cluster - one	58
95	Variation of Drag Coefficient with Reefing Ratio and Riser Length, Equilibrium Test: Canopy Type - Extended Skirt; No. of Canopies in a Cluster - two	58
96	Variation of Drag Coefficient with Reefing Ratio and Riser Length, Equilibrium Test: Canopy Type - Extended Skirt; No. of Canopies in a Cluster - three	58
97	Variation of Drag Coefficient with Reefing Ratio and Riser Length, Equilibrium Test: Canopy Type - Extended Skirt; No. of Canopies in a Cluster - four	58
98	Variation of Drag Coefficient with Reefing Ratio and Riser Length, Equilibrium Test: Canopy Type - Ribbon; No. of Canopies in a Cluster - one	59
99	Variation of Drag Coefficient with Reefing Ratio and Riser Length, Equilibrium Test: Canopy Type - Ribbon; No. of Canopies in a Cluster - two	59
100	Variation of Drag Coefficient with Reefing Ratio and Riser Length, Equilibrium Test: Canopy Type - Ribbon; No. of Canopies in a Cluster - three	59
101	Variation of Drag Coefficient with Reefing Ratio and Riser Length, Equilibrium Test: Canopy Type - Ribbon; No. of Canopies in a Cluster - four	59

LIST OF ILLUSTRATIONS (cont'd)

<u>Figure</u>		<u>Page</u>
102	Variation of Drag Coefficient with Reefing Ratio and Riser Length, Equilibrium Test: Canopy Type - Ribbon; No. of Canopies in a Cluster - five	60
103	Variation of Drag Coefficient with Reefing Ratio and Riser Length, Equilibrium Test: Canopy Type - Ringslot; No. of Canopies in a Cluster - one	60
104	Variation of Drag Coefficient with Reefing Ratio and Riser Length, Equilibrium Test: Canopy Type - Ringslot; No. of Canopies in a Cluster - two	60
105	Variation of Drag Coefficient with Reefing Ratio and Riser Length, Equilibrium Test: Canopy Type - Ringslot; No. of Canopies in a Cluster - three	60
106	Variation of Drag Coefficient with Reefing Ratio and Riser Length, Equilibrium Test: Canopy Type - Ringslot; No. of Canopies in a Cluster - four	61
107	Variation of Drag Coefficient with Reefing Ratio and Riser Length, Equilibrium Test: Canopy Type - Ringslot; No. of Canopies in a Cluster - five	61
108	Variation of Drag Coefficient with Reefing Ratio and Riser Length, Equilibrium Test: Canopy Type - Ringslot; No. of Canopies in a Cluster - six	61
109	Variation of Drag Coefficient with Reefing Ratio and Riser Length, Equilibrium Test: Canopy Type - Ringslot; No. of Canopies in a Cluster - seven	61
110	Graph for Flat Circular Type of Canopy Depicting Effect of Reefing Ratio and Number of Canopies in a Cluster on Drag Coefficient	64
111	Graph for Extended Skirt Type of Canopy Depicting Effect of Reefing Ratio and Number of Canopies in a Cluster on Drag Coefficient	64
112	Effect of Reefing Ratio on Static Stability of Flat Circular Type of Canopy Shown Graphically	65

LIST OF ILLUSTRATIONS (cont'd)

<u>Figure</u>		<u>Page</u>
113	Effect of Reefing Ratio on Static Stability of Extended Skirt Type of Canopy Shown Graphically	65
114	Plot Illustrating Effect of Number of Canopies in a Cluster on Static Stability of Flat Circular Type of Canopy	65
115	Plot Illustrating Effect of Number of Canopies in a Cluster on Static Stability of Extended Skirt Type of Canopy	65
116	Effect of Riser Length on Static Stability of Flat Circular Type of Canopy Presented Graphically	66
117	Effect of Riser Length on Static Stability of Extended Skirt Type of Canopy Presented Graphically	66
118	Graph for Ribbon Type of Canopy Depicting Effect of Reefing Ratio and Number of Canopies in a Cluster on Drag Coefficient	67
119	Graph for Ringslot Type of Canopy Depicting Effect of Reefing Ratio and Number of Canopies in a Cluster on Drag Coefficient	67
120	Effect of Reefing Ratio on Static Stability of Ribbon Type of Canopy Shown Graphically	67
121	Effect of Reefing Ratio on Static Stability of Ringslot Type of Canopy Shown Graphically	67
122	Plot Illustrating Effect of Number of Canopies in a Cluster on Static Stability of Ribbon Type of Canopy	68
123	Plot Illustrating Effect of Number of Canopies in a Cluster on Static Stability of Ringslot Type of Canopy	68
124	Effect of Riser Length on Static Stability of Ribbon Type of Canopy Presented Graphically	68
125	Effect of Riser Length on Static Stability of Ringslot Type of Canopy Presented Graphically	68
126	Illustration of the Balance Assembly for Parachute Positioning and Load Sensing	75

LIST OF ILLUSTRATIONS (cont'd)

<u>Figure</u>		<u>Page</u>
127	View Showing Installation of Two-Component Balance with Hydraulic Control Console Seen to the Right	74
128	Illustration of Typical Strain Gage Sensing Element	74
129	Block Diagram of Recording Instrumentation System . . .	75
130	Plan View of Wind Tunnel Indicating Camera Locations as Related to other Equipment	76
131	Typical Tangential Force Calibration Curve for Transducer and Sting No. 3	77
132	Typical Moment Calibration Curve for Transducer and Sting No. 2	77
133	Drawing Depicting Circuitry for Secondary Calibration . .	77
134	Typical Patterns for Gore Configurations	79
135	View Showing Measuring Technique for Flat Pattern Canopies	80
136	View Showing Measuring Technique for Extended Skirt Canopies	80

LIST OF TABLES

<u>Table</u>		<u>Page</u>
I	Model Parachute Description	6
II	Summary of Captive and Equilibrium Tests on Flat Circular Type of Canopies	16
III	Summary of Captive and Equilibrium Tests on Extended Skirt Type of Canopies	16
IV	Summary of Captive and Equilibrium Tests on Ribbon Type of Canopies	16
V	Summary of Captive and Equilibrium Tests on Ringslot Type of Canopies	16
VI	Sensing Element Calibrations for Tangential Force and Pitching Moment	78

LIST OF SYMBOLS

<u>Symbol</u>	<u>Concept</u>	<u>Dimensions</u>
C_{D_0}	Drag Coefficient Based on Nominal Surface Area	none
C_{M_0}	Pitching Moment Coefficient Based on Nominal Surface Area	none
C_{N_0}	Normal Force Coefficient Based on Nominal Surface Area	none
C_{T_0}	Tangential Force Coefficient Based on Nominal Surface Area	none
D_0	Nominal Diameter	feet
D_r	Reefed Diameter	feet
D_r/D_0	Reefing Ratio	none
F_T	Tangential Force	pounds
l_r	Riser Length	inches
q	Dynamic Pressure	pounds/feet ²
S_0	Nominal Surface Area	feet ²
V	Velocity	feet/second
W	Weight of Parachute Assembly plus Suspended Weight	pounds
α	Angle-of-Attack	degrees

SECTION 1

INTRODUCTION

Past research on parachute clustering has been quite limited and has dealt primarily with the performance of clustered solid cloth type of parachute canopies for terminal descent deceleration of air dropped loads.

The objective of this study was to gather additional information on parachute clustering, especially data related to the effects of number and type of parachute canopies in a cluster, reefing ratios, and riser lengths upon the static stability and drag coefficient of the configuration in subsonic flow. To obtain comparative data, all tests were conducted under controlled conditions in the Aeronautical Systems Division (ASD) Vertical Wind Tunnel.

Four different types of parachute canopies were employed in this study: Solid Flat, Extended Skirt, Ringslot, and Ribbon. Parachute canopies of these types with various riser lengths, reefing ratios, cluster configurations, and at different angles of attack were tested. The riser length varied from 0 D_0 to 1.5 D_0 and the reefing ratio, D_r/D_0 , ranged from 0.2 to 0.5. These reefing ratios were employed in all canopy configurations; in addition, nonreefed canopies in single and clustered configurations were tested. The configurations were tested at various angles of attack, ranging from -25 to +25 degrees, unless the canopy skirt began to collapse.

The majority of the test points were obtained during captive tests where the tangential force and pitching moment of the cluster configurations were measured by means of a two-component balance and recorded. These forces were subsequently reduced to coefficient form.

Equilibrium tests (free floating) which also were performed during the experimental testing program permitted the comparison of the data obtained during these tests with the data acquired during the captive tests.

This study also involved the development of a measuring system capable of sensing and recording accurately the forces acting tangentially to parachute canopies and the pitching moments of the canopies.

SECTION 2

PROCEDURE

2.1 General

During the captive test series, the model parachute canopies were attached to a two-component balance in the ASD Vertical Wind Tunnel and positioned at various angles of attack, α , defined as the

angle between a chosen geometrical center plane of the canopy cluster and the plane parallel to the direction of air flow through the moment center, as depicted in Figure 1. The model canopies were fixed on the two-component balance so that the projected confluence point of the canopy suspension lines or of the risers would always be at the moment center. Canopy separation was purposely maintained by a mechanical positioner located at the top of the sting. Figure 2 shows the mechanical positioner maintaining fixed canopy separation of a cluster of five Extended Skirt type of parachute canopies reefed to $D_r/D_o = 0.3$. The parameters measured during each test were the angle of attack, the pitching moment, and the force acting tangentially to the chosen geometric center plane of the clustered configuration.

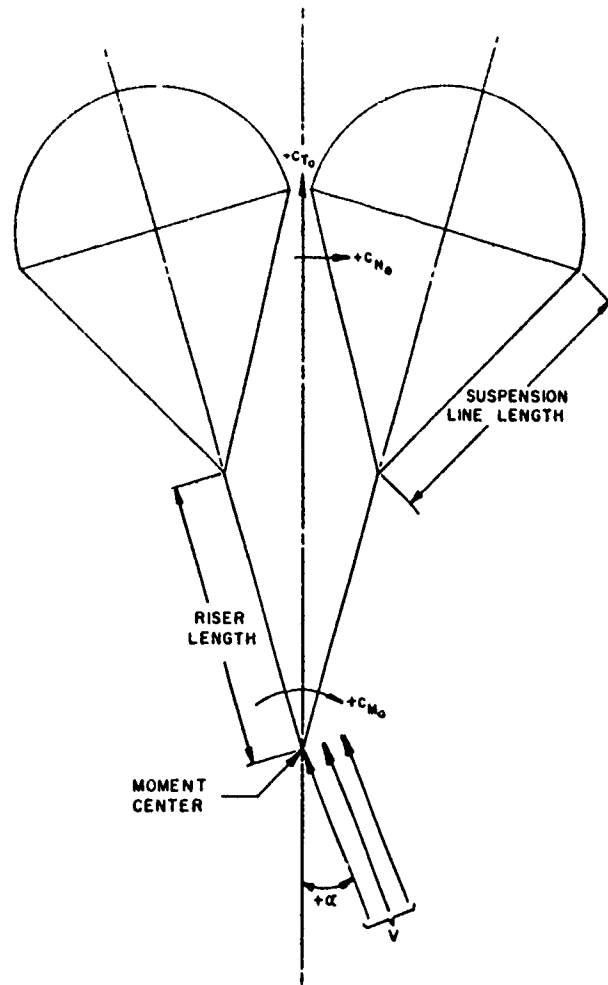


Figure 1. Graphic Presentation of Sign Convention Employed in This Parachute Cluster Study

Angles of attack were varied from -25 to +25 degrees unless the canopy skirt began to collapse before these limits. All tests were performed at a constant air velocity of approximately 100 feet per second.

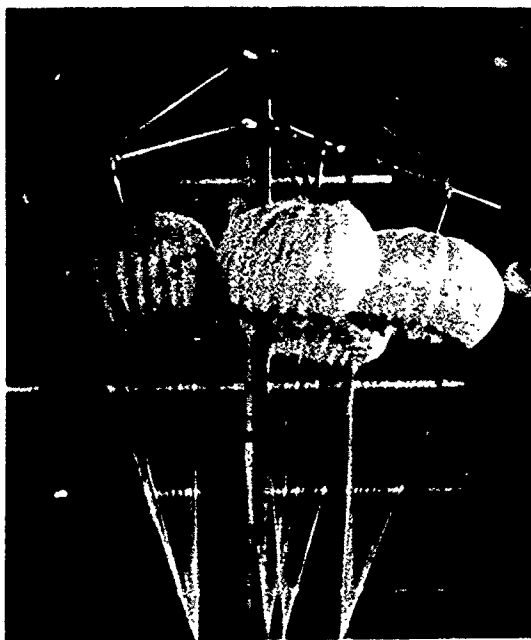


Figure 2.

View Showing Mechanical Arrangement Maintaining Fixed Canopy Separation of a Cluster of Five Extended Skirt Type of Canopies

The number of canopies in the clustered configurations ranged from one to seven. These configurations had four different riser lengths and three reefing ratios, in addition to the nonreefed canopies. Riser lengths were zero, $0.5 D_0$, $1 D_0$, $1.5 D_0$ and reefing ratios, D_r/D_0 , were 0.2, 0.3, and 0.5.

Figure 3 shows a cluster of five Extended Skirt type of canopies reefed at $D_r/D_0 = 0.5$ at an angle of attack of 10 degrees and a riser length of $1.5 D_0$.

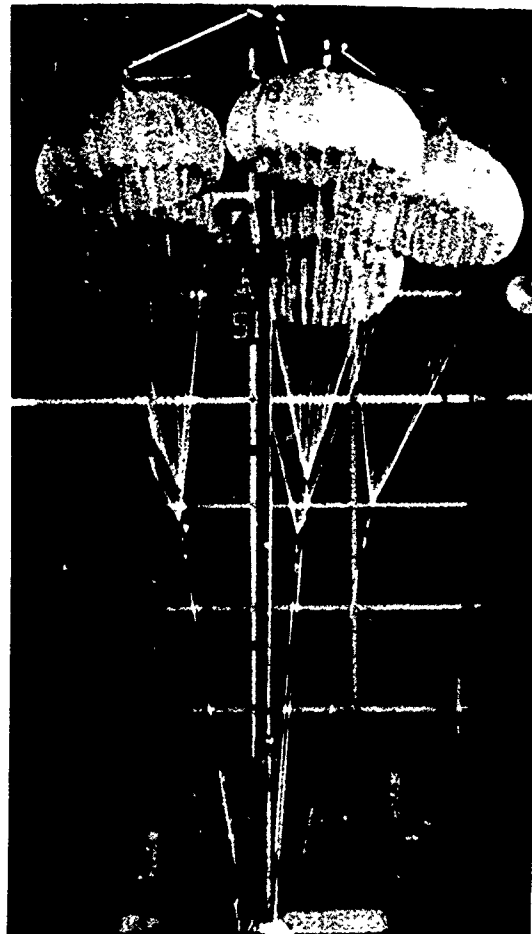


Figure 3.

Typical View of Five Extended Skirt Type of Canopies in a Cluster: Reefing Ratio (D_r/D_0) - 0.5 and Riser Length - $1.5 D_0$

Furthermore, to supplement the data obtained during captive tests, a series of equilibrium tests were conducted. These tests were conducted primarily for canopy configurations which exhibited no, or marginal, inflation during the captive tests; marginal inflations occurring were with canopy configurations having small reefing ratios. Figure 4 shows a reefed canopy cluster in a typical equilibrium test configuration.

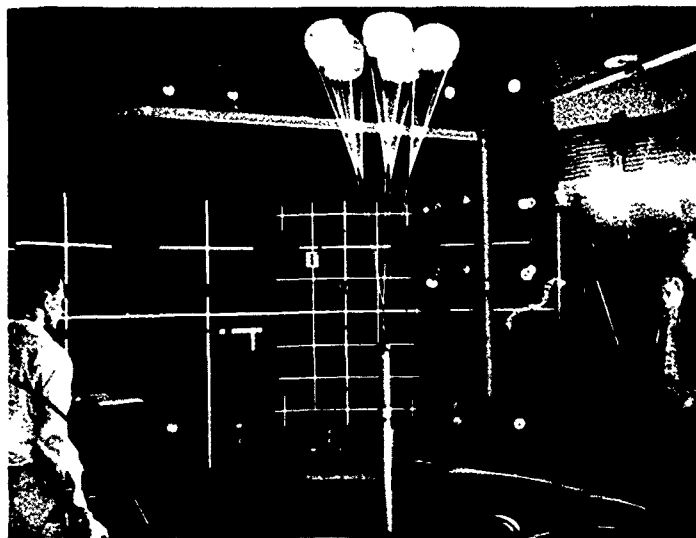


Figure 4. Scene Showing Configuration with Adjustable Suspended Weight for Equilibrium Tests

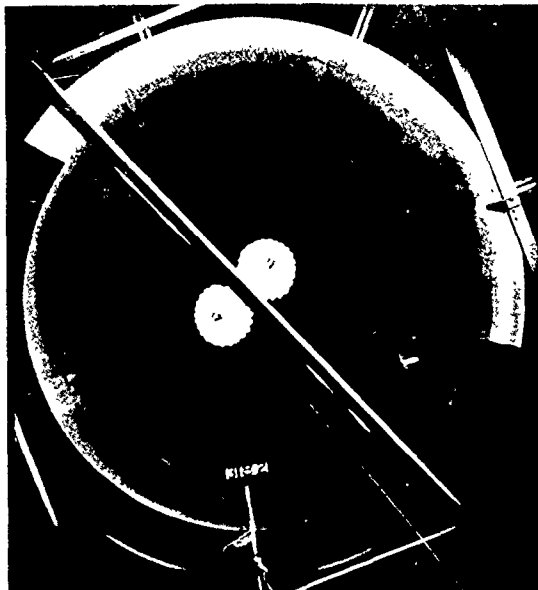
2.2 Sign Convention

The sign convention utilized during this study is shown graphically in Figure 1. This sign convention is a departure from the previously used convention in that a stable system can be defined as exhibiting a negative $dC_M/d\alpha$. Therefore, a stable configuration about zero angle of attack would have a negative pitching moment at positive angles of attack and the opposite at negative angles of attack.

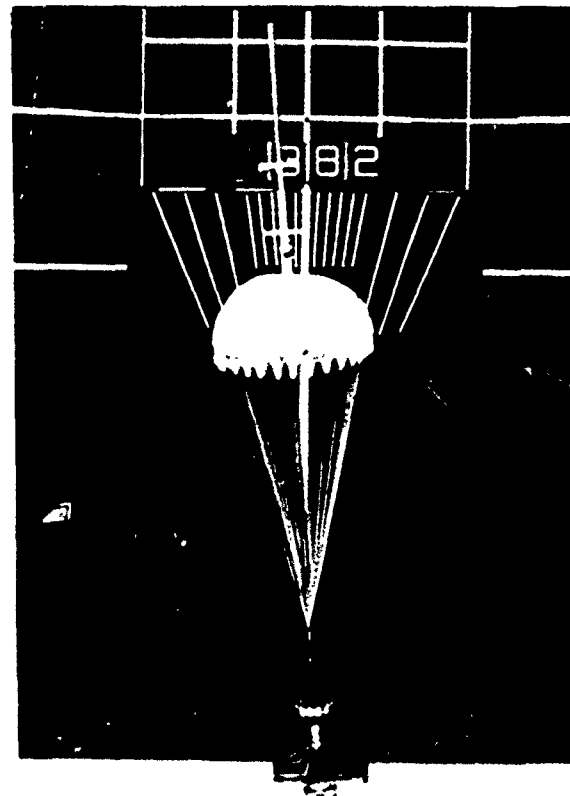
2.3 Model Parachute Canopies

Four types of model parachutes—Flat Circular, Extended Skirt, Ribbon, and Ringslot—were employed in this experimental test program. The Aeronautical Systems Division and Technology Incorporated designed the model canopies specifically for this experimental test program. The canopies were of standard design and based upon data contained in the USAF Parachute Handbook. Fabrication of the model parachutes was accomplished by Irving Airchute, California, under a subcontract. Each canopy had a nominal surface area, S_0 , of approximately 452 square inches. This surface area enabled clusters of up to seven canopies to be tested to an angle of attack from -25 to +25 degrees in the ASD 12-foot Vertical Wind Tunnel. All canopy vent

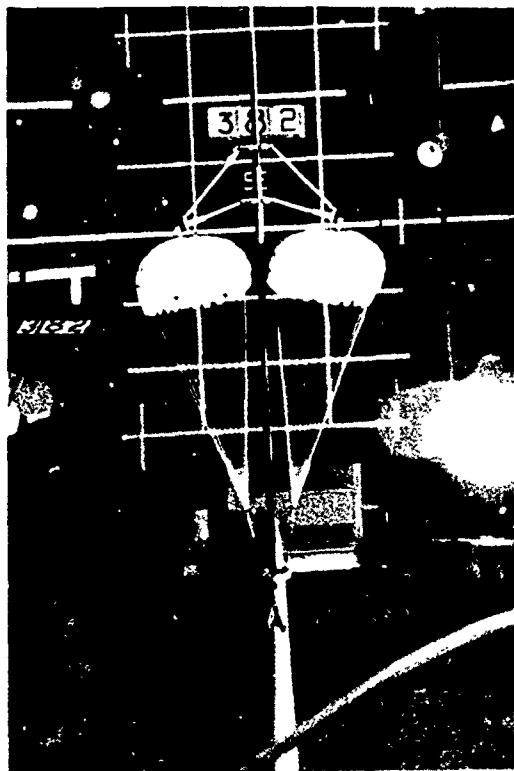
areas were held to approximately one percent of the canopy nominal surface area. Figure 5 shows three orthogonal views of a model parachute cluster arrangement during captive tests.



Direction of Airflow



Perpendicular to Strut



Parallel to Strut

Figure 5. Orthogonal Views of Model Two-Cluster Parachute Arrangement

Cloth permeability or geometric porosity values and the finished nominal surface and vent areas for each canopy tested are presented in Table I. These data were measured or computed directly from the model parachute canopies. All canopies were constructed with 24 gores and 24-inch suspension line lengths. Each canopy bore a number to identify it during the program. Figure 6 illustrates a parachute cluster attached to the two-component balance.

Table I

Model Parachute Description

Chute No	Design	Average Cloth Permeability ($Ft^3/Ft^2 \cdot Min$) @ 1/2 in H_2O	Geometric* Porosity %	Measured Canopy Surface Area (S_0) Sq In	Vent Area Sq In
2	Ringslot	-	16	407	4 4
3		-	17	372	4 0
4		-	15	397	4 9
5		-	16	404	5 2
6		-	17	404	4 9
7		-	17	393	5 4
8		-	18	393	4 9
9		-	14	413	4 4
10	Ribbon	-	17	415	4 4
11		-	17	415	6 8
12		-	20	402	4 4
13		-	16	411	4 4
14	Extended Skirt	116	-	456	4 9
15		110	-	479	4 0
16		115	-	456	4 7
17		118	-	465	4 4
18	Solid Flat	131	-	470	4 7
19		132	-	452	4 4
20		156	-	471	4 9
21		131	-	434	4 9
22		142	-	452	4 9
23		144	-	452	4 9
24		114	-	462	4 9
25	**	-	-	-	-
26	Extended Skirt	122	-	472	4 9

* Vent Area Not Included As Open Area

** Destroyed

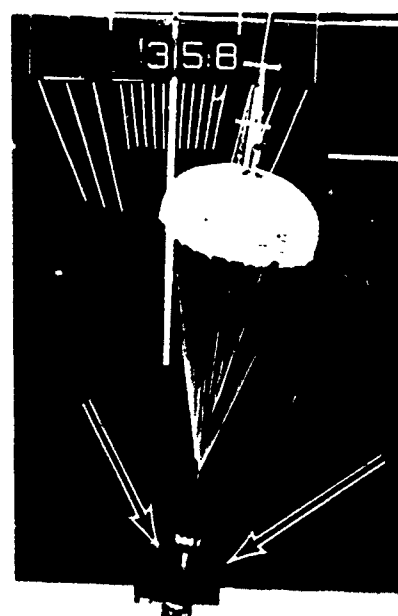


Figure 6.

Two-Component Balance Seen at the Base of the Parachute Cluster Configuration

2.4 Description of the ASD Vertical Wind Tunnel

The Aeronautical Systems Division 12-foot Vertical Wind Tunnel is a closed-return type of tunnel. The open air jet is directly upward out of a 12-foot long nozzle whose cross section is a 16-sided polygon with a 12-foot inscribed diameter circle. The air flows through the test chamber with a velocity ranging from 15 to 135 feet per second, or from 10 to 90 miles per hour, and with a dynamic pressure of approximately 22 pounds per square foot at the maximum test velocity. Presented in Figure 7 is a drawing of the wind tunnel, indicating the direction of air flow.

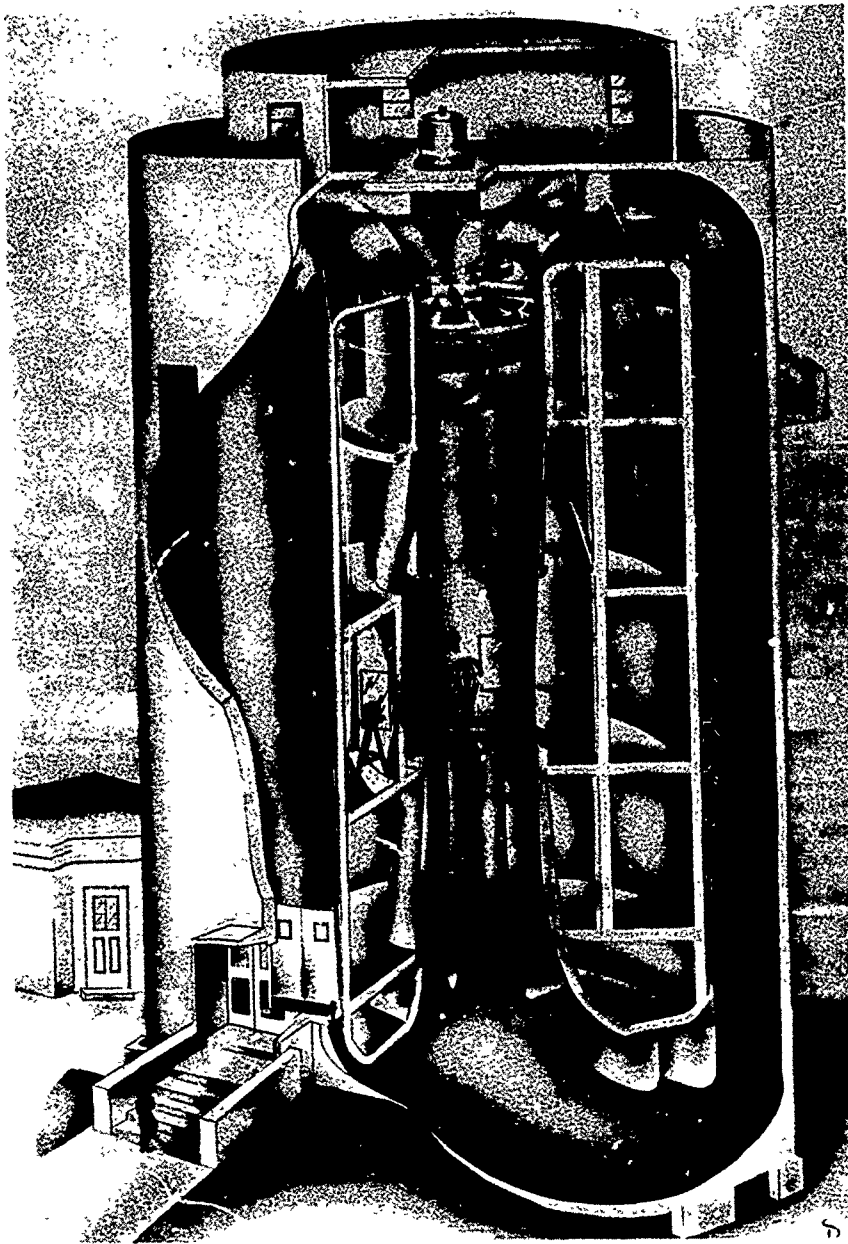


Figure 7. Sectional Drawing of the ASD Vertical Wind Tunnel
Indicating the Air Flow Direction

A four-bladed variable-pitch fan, located near the top of the tunnel and driven by a 1000-hp variable-speed D.C. motor with a maximum controllable speed of 800 rpm, is employed to power the wind tunnel. The D.C. power is furnished by a motor generator set located in the utility room adjacent to the tunnel. The speed is controlled manually by the wind tunnel operator from either of two control consoles, one of which is located in the observation room and the other in the test chamber. The control console in the observation room features an inclined manometer on which the dynamic pressure can be read directly.

2.5 Instrumentation

The instrumentation utilized during the test program consisted of a specially designed two-component strain gage type of balance and associated recording and auxiliary equipment. Appendix II discusses the instrumentation system employed.

2.6 Testing Procedure, Captive Tests

The canopies, in either single or clustered configurations, were positioned very carefully in order that the projected confluence point of the canopy suspension lines, or risers in the case of clusters, would be exactly at the neutral axis of the force sensing element. The canopies were positioned in a cluster so that a 1/2-inch spacing was maintained between adjacent canopies in the inflated state. This was accomplished by means of a mechanical positioner located at the top of the balance sting. When the positioning was completed, the instruments were set at zero and the pretest calibrations were performed. During all tests, the vertical air velocity was held at a constant dynamic pressure equivalent to 2.33 inches of water. The angle of attack was varied from 0 to +25 degrees and from 0 to -25 degrees unless the procedure was ended by canopy collapse. Test points were taken at two-degree increments in the -10 to +10 degree range and 5-degree increments were used in the -10 to -25 and +10 to +25 degree ranges. Since the angle of attack was introduced remotely, the air velocity was held constant during each different angle of attack setting.

The planes which passed through the chosen geometric center of each of the canopy cluster configurations tested and about which the angle of attack was varied are shown in Figure 8. The directional lines indicate the positive and negative angle-of-attack travel during each test sequence. It may be noted that the canopy arrangements utilized were in all cases symmetrical with respect to the geometric center of the configuration.

Data were recorded manually before and during each test sequence. These data consist of time, angle of attack, test number,

dynamic pressure, dry bulb temperature, wet bulb temperature, oscillograph record number, transducer number and sting, canopy type and configuration, number of canopies, and cluster orientation.

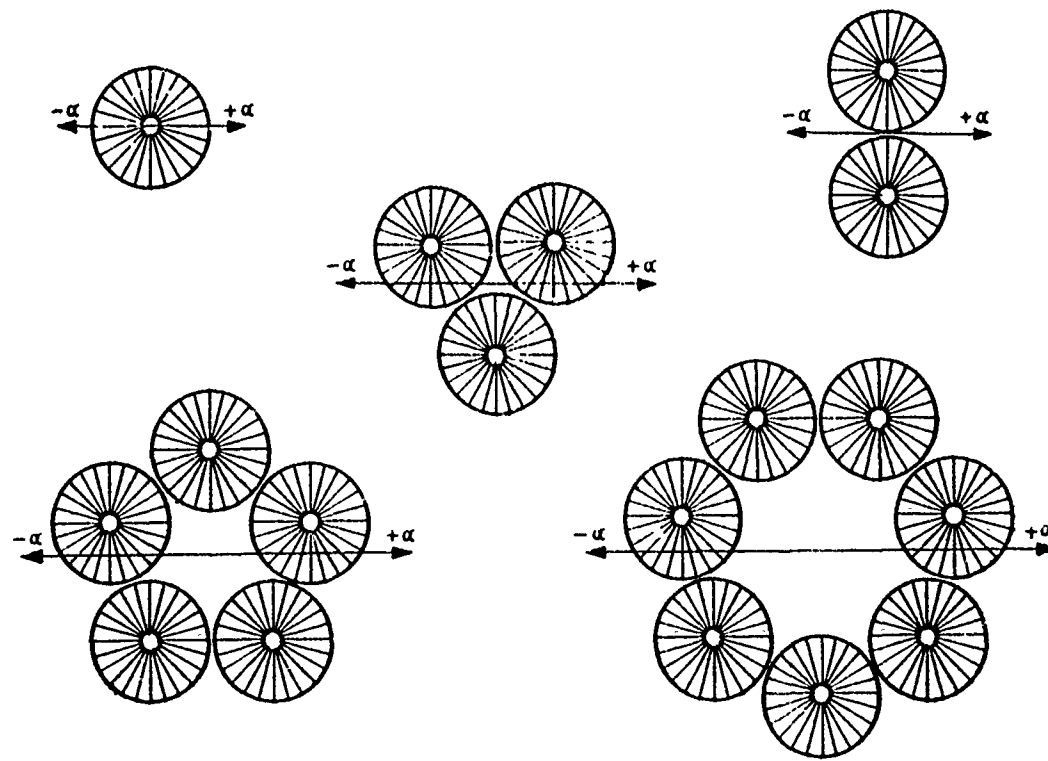


Figure 8. Drawings Depicting Arrangements of Canopy Clusters with Respect to Strut and Travel Direction

After the tunnel velocity had stabilized for a testing sequence, each parachute or cluster configuration was photographed by one 70-mm still and two 35-mm cameras; and the strain-gage output signals from the force-sensing elements were recorded on a C. E. C. oscillograph. All operations were performed simultaneously.

To obtain maximum sensitivity in measuring the tangential force and pitching moment of the various cluster configurations, four easily interchangeable, force-sensing elements of different maximum capacity were employed.

The need for a test point or sequence rerun was determined when a plot of either tangential or moment coefficient versus angle of attack did not follow the general trend of the test data. Also, reruns were made when the system had obviously malfunctioned.

2.7 Testing Procedure, Equilibrium Tests

To obtain data for comparison with the captive test results and to determine the drag coefficient for configurations which did

not inflate properly on the sting balance, equilibrium tests were conducted by using the following testing arrangement: a known weight was suspended from the canopy configurations and the wind tunnel air velocity was adjusted until the configuration floated freely. During these equilibrium tests the weight suspended from the configurations was adjusted by varying the amount of a lead shot filling contained in the cylinder so that all the equilibrium tests could be conducted at approximately the same dynamic pressure and air velocity as those prevailing during the captive tests.

The main advantage of the equilibrium tests is that these tests can simulate actual parachute operation more accurately than the captive tests since all restraints are removed in conducting the former type of tests. In the equilibrium test arrangement, the parachute canopies are free to assume their actual positions in the cluster and are not disturbed by the sting or the mechanical positioning unit. Although the drag coefficients obtained from the two types of tests exhibited no discernible differences in most cases, those derived from the equilibrium tests were considered more accurate because of the reasons mentioned above. However, those areas in the wind tunnel with severe local dynamic pressure variations had to be avoided assiduously.

2.8 Pressure Survey Before and After the Two-Component Balance Installation

A pressure survey was conducted before and after the installation of the two-component balance in the wind tunnel, utilizing a pressure rake, consisting of 25 pitot-static pressure tubes spaced 6 inches on center. Pressure rake measurements were taken at every six inches across the wind tunnel nozzle and at the levels 3 feet, 5 feet, 7 feet, and 9 feet above the moment center.

The 25 static pressures and 25 total pressures were measured by a well type of manometer board and recorded on photographic film. Supplementary data were manually recorded during each pressure-survey condition. These data consisted of the dry bulb temperature, wet bulb temperature, barometric pressure, and any other information pertinent to the survey.

Figures 9 and 10 present the dynamic pressure survey of the Vertical Wind Tunnel before and after installation of the two-component balance. As is evident, there are severe variations in dynamic pressure across the cross-section of the tunnel. To counteract this variation and reduce the resultant scatter in the data attributable to it, dynamic pressure corrections were applied during the computation of the final data. This was accomplished by obtaining the average dynamic pressure over the projected parachute cluster area at

its location in the tunnel. In this manner, the dynamic pressure was calculated for each different cluster configuration and angle of attack. This averaged dynamic pressure was then used in the calculations for C_{T_0} and C_{M_0} .

2.9 Aerodynamic Tare Determination

The aerodynamic tare was determined by permitting the balance sting and the mechanical parachute positioner without the parachutes to be positioned in five-degree increments through an angle of attack from -25 to +25 degrees while the wind tunnel was at test velocity. This positioning resulted in the induction of both the tangential and the moment forces into the force-sensing element. At each five-degree increment, the induced forces were recorded on the oscillograph. These tare runs were performed for the two stings utilized and for all riser lengths and cluster configurations employed during the experimental testing program. All tare corrections were incorporated into the data reduction by adding the induced forces algebraically to the test data.

2.10 Data Reduction

The information acquired during the wind tunnel test program comprises two types of data: (1) the test data recorded automatically by the two 35-mm cameras, the 70-mm camera, and the C. E. C. oscillograph, and (2) the wind tunnel operation data recorded manually.

The wind tunnel operation data was utilized to correlate the camera and the oscillograph data and to determine the dynamic pressure; these data also include observations made during each test sequence.

The 35-mm cameras provided side views of the cluster configurations during tests. From these photographs angle-of-attack values for each test point were obtained. A Recordak film reader was used to extract the data from the photographs.

A pretest calibration, conducted before each test sequence to condition the force-sensing transducer, produced data for calibrating curves. The tangential and moment forces were derived from these curves. The oscillograph recorded the strain-gage output signals and pretest calibration data.

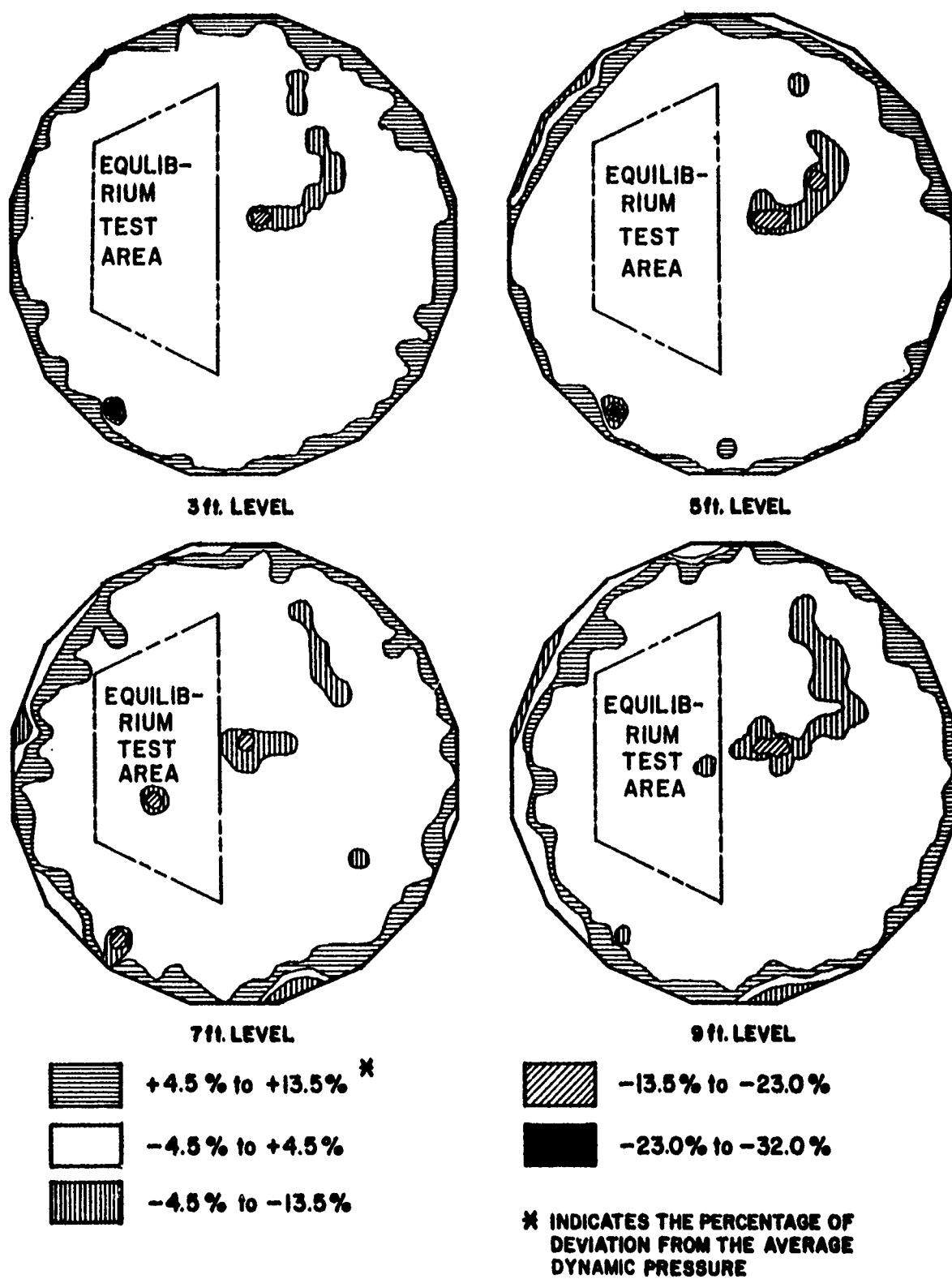


Figure 9. Dynamic Pressure Survey of the ASD Vertical Wind Tunnel before Installation of Two-Component Balance

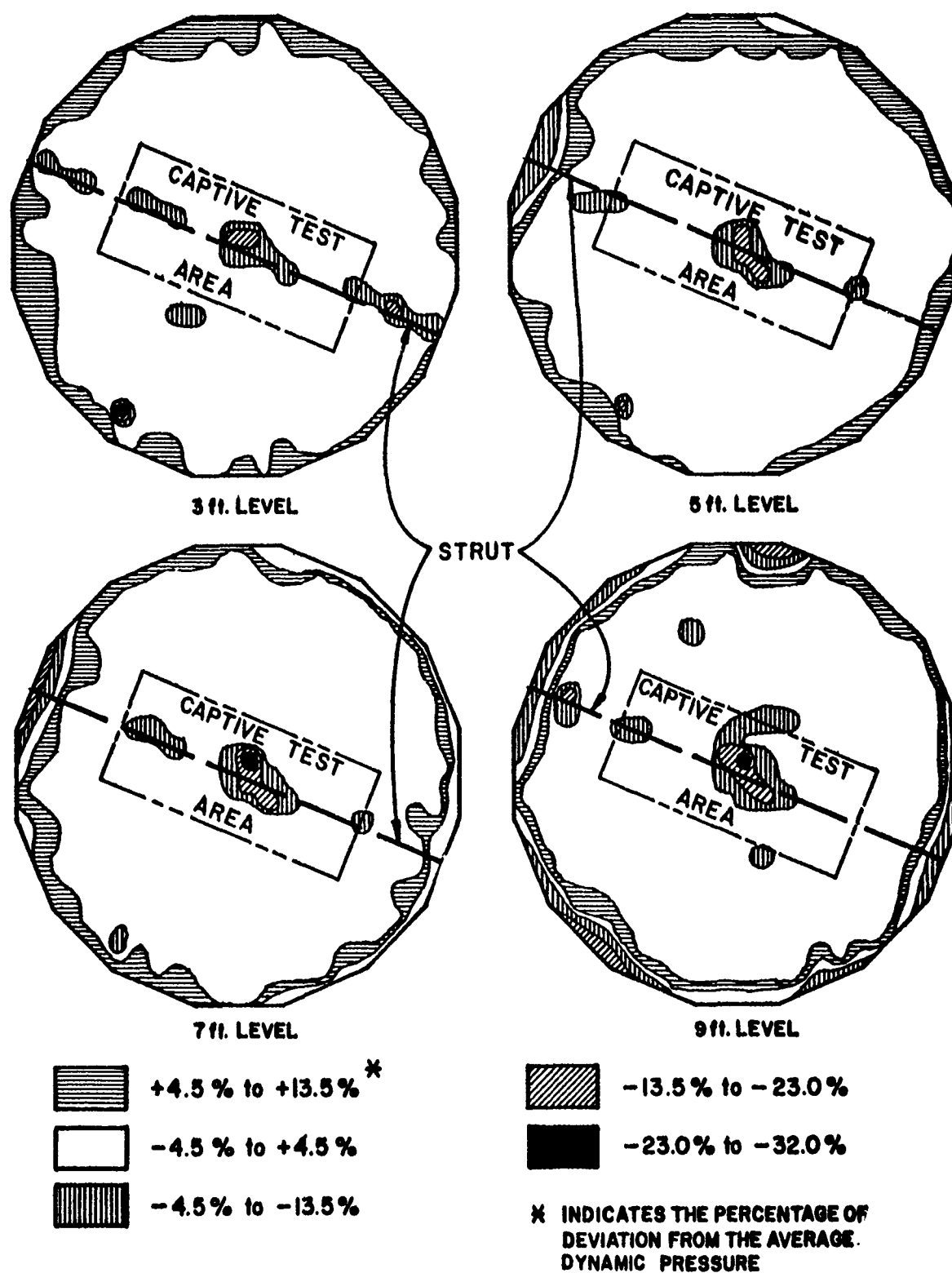


Figure 10. Dynamic Pressure Survey of the ASD Vertical Wind Tunnel after Installation of Two-Component Balance

Reduction of the data to coefficient form involved the following: First, the raw test data for each test condition were acquired by reading the galvanometer deflections on the oscillograms and the angle-of-attack values on the 35-mm photographs. Next, the corrected tangential and moment coefficients were computed by utilizing the following expressions:

$$C_{T_o} = \frac{F_T}{q \left(\sum_{i=1}^n S_{o_i} \right)} \quad (1)$$

and

$$C_{M_o} = \frac{M}{nq \left(\sum_{i=1}^n S_{o_i} \right) \left(\sum_{i=1}^n D_{o_i} \right)} \quad (2)$$

where n = number of canopies.

For the equilibrium tests the drag coefficient was computed from the relationship:

$$C_{D_o} = \frac{W}{q \left(\sum_{i=1}^n S_{o_i} \right)} \quad (3)$$

Plots of coefficients versus angle of attack, prepared manually, are presented in Section 3.

SECTION 3

RESULTS

3.1 General

As indicated previously, two types of tests, captive and equilibrium, were performed during the wind tunnel test program. Approximately 130 different parachute configurations utilizing the sting and two-component balance were tested in a captive state to determine the aerodynamic coefficients, C_{T_o} and C_{M_o} , at various angles of attack. When it was found that the canopies with a reefing ratio of 0.2 would not inflate properly while attached to the sting, a series of equilibrium tests were conducted to determine the drag coefficients for this reefing ratio and to verify the results obtained from the previous tests at other reefing ratios. Approximately 200 different equilibrium tests were performed.

The test results in the form of tangential force coefficient, C_{T_o} , and moment coefficient, C_{M_o} , versus angle of attack, α , of each configuration are presented in Figures 12 through 89. Every test point has been plotted. When the points did not follow a pattern delineating an obvious trend, either no curve was traced or an estimated curve formed by dashes was drawn. The vertical lines in

dash form at the extremities of the C_{T_0} curve indicate the angle of attack at which individual canopies in a cluster started to exhibit the tendency to collapse. Figure 11 shows the canopies in cluster just before collapse.

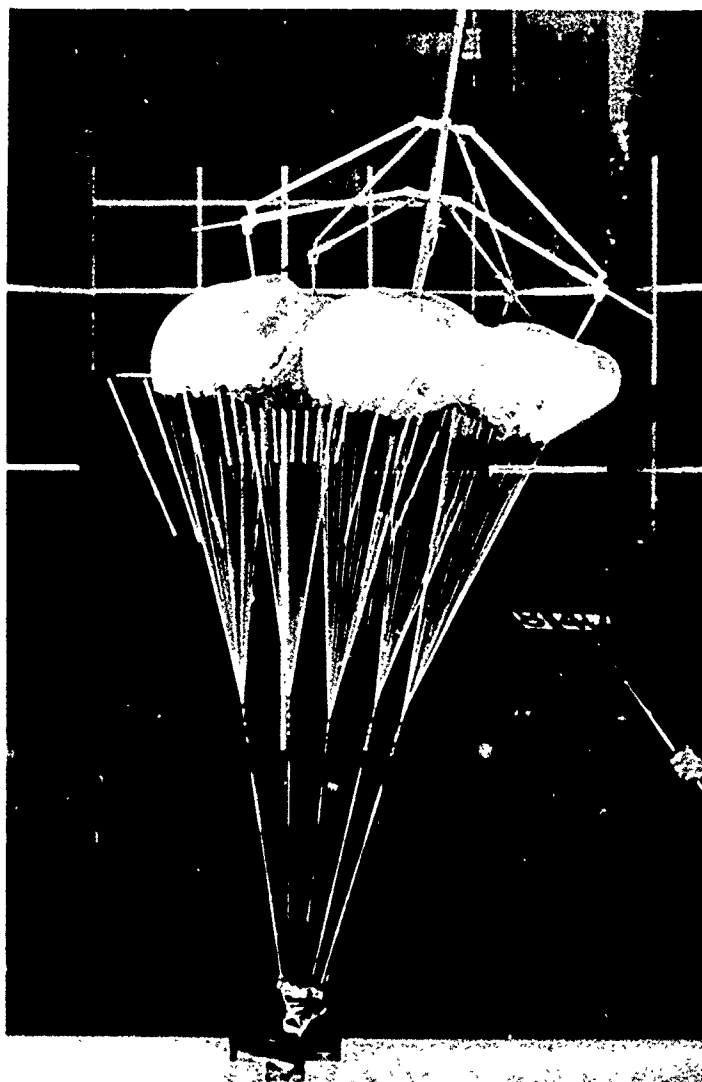


Figure 11.

View of Five Extended Skirt Canopies Illustrating Onset of Collapse

Figures 90 to 109 present the results of the equilibrium tests in the form of drag coefficient, C_{D_0} , versus reefing ratio. All test points are shown; however, no curves were plotted.

3.2 Order of Results Presentation

Tables II through V synopsize the parachute cluster configurations for both types of testing. An "X" in these tables indicates that the configuration was tested in a captive state over an angle-of-attack range, and an "O" indicates that the configuration was subjected to equilibrium tests. As noted, both equilibrium and captive tests on certain configurations were made for comparison purposes.

Table II

Summary of Captive and
Equilibrium Tests on Flat
Circular Type of Canopies

No. of Canopies							Reeving Ratio - D_r/D_o	Riser Length - l_r/D_o
1	2	3	4	5	6	7		
		X		X		X	Full Open (No Reeving)	1.5
	X	X		X		X		1.0
X		X		X		X		0.5
								0
		X		X		X	0.5	1.5
	X0	X		X		X	0.5	1.0
X	0			X			0.5	0.5
							0.5	0
0		X	0	X		X	0.3	1.5
0	X	X	0	X			0.3	1.0
X0	0	0	0				0.3	0.5
							0.3	0
	0	0	0				0.2	1.5
0	0	0	0				0.2	1.0
0	0	0	0				0.2	0.5
X0	0	0	0				0.2	0

X Captive test
0 Equilibrium Test

Table III

Summary of Captive and
Equilibrium Tests on Extended
Skirt Type of Canopies

No. of Canopies							Reeving Ratio - D_r/D_o	Riser Length - l_r/D_o
1	2	3	4	5	6	7		
		X		X			Full Open (No Reeving)	1.5
	X	X		X				1.0
X		X		X				0.5
								0
		X		X			0.5	1.5
0	X0	X		X			0.5	1.0
X				X			0.5	0.5
							0.5	0
		X		X			0.3	1.5
0	X0	X0		X			0.3	1.0
X							0.3	0.5
							0.3	0
	0	0	0				0.2	1.5
0	0	0	0				0.2	1.0
0	0	0	0				0.2	0.5
X0	0	0	0				0.2	0

X Captive Test
0 Equilibrium Test

Table IV

Summary of Captive and
Equilibrium Tests on Ribbon
Type of Canopies

No. of Canopies							Reeving Ratio - D_r/D_o	Riser Length - l_r/D_o
1	2	3	4	5	6	7		
		X		X			Full Open (No Reeving)	1.5
	X	X		X				1.0
X		X		X				0.5
								0
	0	0	0	X0			0.5	1.5
	0	X0	0	X0			0.5	1.0
X0	0	X0	0	0			0.5	0.5
	0	0	0	0			0.5	0
	0	0	0	0			0.3	1.5
	0	0	0	0			0.3	1.0
	0	0	0	0			0.3	0.5
X0	0	0	0	0			0.3	0
	0	0	0	0			0.2	1.5
0	0	0	0	0			0.2	1.0
0	0	0	0	0			0.2	0.5
X0	0	0	0	0			0.2	0

X Captive Test
0 Equilibrium Test

Table V

Summary of Captive and
Equilibrium Tests on Ringslot
Type of Canopies

No. of Canopies							Reeving Ratio - D_r/D_o	Riser Length - l_r/D_o
1	2	3	4	5	6	7		
		X		X			Full Open (No Reeving)	1.5
	X	X		X				1.0
X		X		X				0.5
								0
	0	0					0.5	1.5
	0	X0					0.5	1.0
0	0	X0					0.5	0.5
X	0	0					0.5	0
	0	0	0	0			0.3	1.5
	0	X0	0	0			0.3	1.0
	0	X0	0	0			0.3	0.5
X0	0	0	0	0			0.3	0
	0	0	0	0	0	0	0.2	1.5
	0	0	0	0	0	0	0.2	1.0
0	0	0	0	0	0	0	0.2	0.5
X0	0	0	0	0	0	0	0.2	0

X Captive Test
0 Equilibrium Test

The results of the captive tests (sting-balance tests) are presented before those of the equilibrium tests. The order of presentation for both types of testing is first, Flat Circular type of canopy configurations; second, Extended Skirt type of canopy configurations; third, Ribbon type of canopy configurations; and fourth, Ringslot type of canopy configurations. The reefing ratios and riser lengths related to canopies in a cluster are presented in the order of increasing number of canopies per cluster.

3.3 Constant Dynamic Pressure as Opposed to Constant Velocity

All captive testing was conducted at a constant dynamic pressure of 11.00 pounds per square foot, which corresponded to a velocity of 100 ± 2 feet per second, depending upon ambient air conditions. As it was impossible to test at both constant dynamic pressure and constant velocity, it was decided to let velocity vary since its effect was considered to be less than that of dynamic pressure.

During the equilibrium tests, the suspended weight was varied so that the dynamic pressure would be approximately the same. The variation in dynamic pressure was held to ± 0.15 inch of water. To decrease this variation would have been too time consuming since a weight change required stopping the tunnel operation.

3.4 Parachute Cluster Orientation

As noted previously, during the captive tests the parachute canopies were spaced in clustered configurations so that a 1/2-inch separation between adjacent canopies was maintained when the canopies were inflated.

During the equilibrium tests it was found that the separation between the canopies varied from zero to about six inches, depending upon riser length, number of parachutes, and reefing ratio. However, the 1/2-inch separation was a compromise since the large separations were evidenced mainly in the cluster configurations with long riser lengths and small reefing ratios.

It also became evident that the assumption of symmetrical canopy positioning for the seven canopy clusters was incorrect, for during the equilibrium tests one of the seven canopies always centered itself while the others spaced themselves evenly about it.

A similar canopy positioning was observed in the performance of the six canopy clusters. However, the configurations for five or less canopies in a cluster, as shown in Figure 8, proved to be correct.

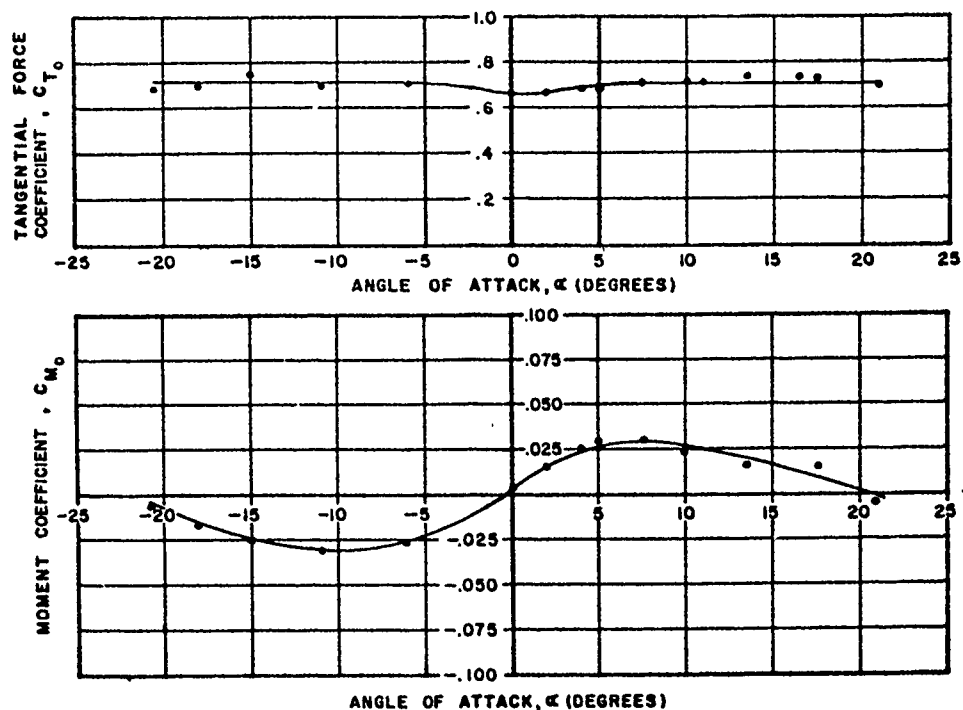


Figure 12. Variation of Tangential Force and Moment Coefficients with Angle-of-Attack: Canopy Type - Flat Circular; Cluster - one; Reefing Ratio - none; Riser Length - $0 D_0$

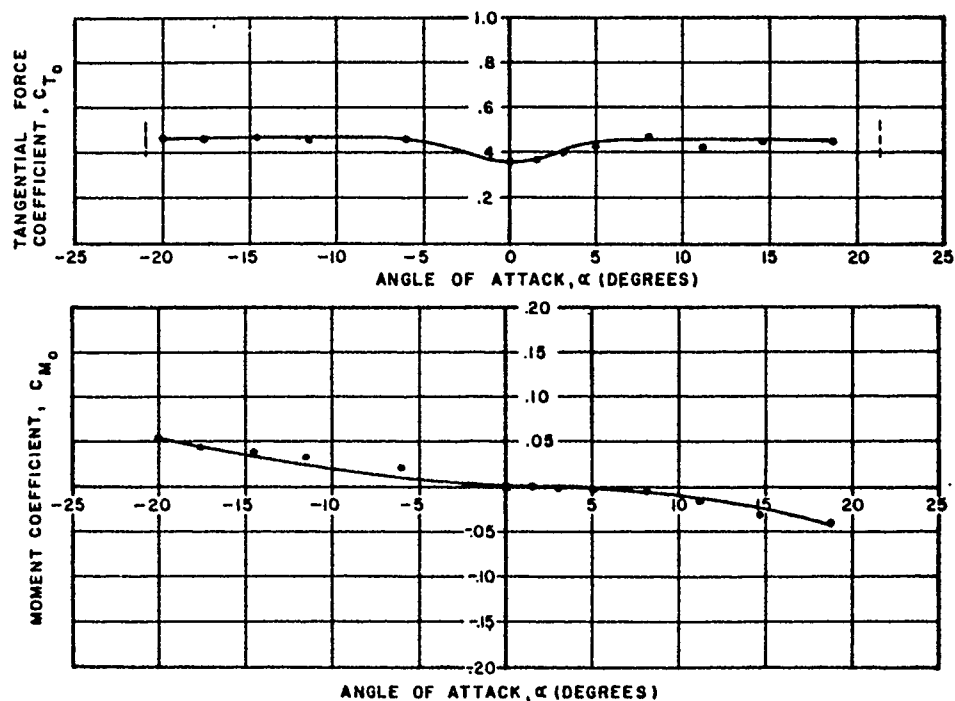


Figure 13. Variation of Tangential Force and Moment Coefficients with Angle-of-Attack: Canopy Type - Flat Circular; Cluster - one; Reefing Ratio - 0.5; Riser Length - $0 D_0$

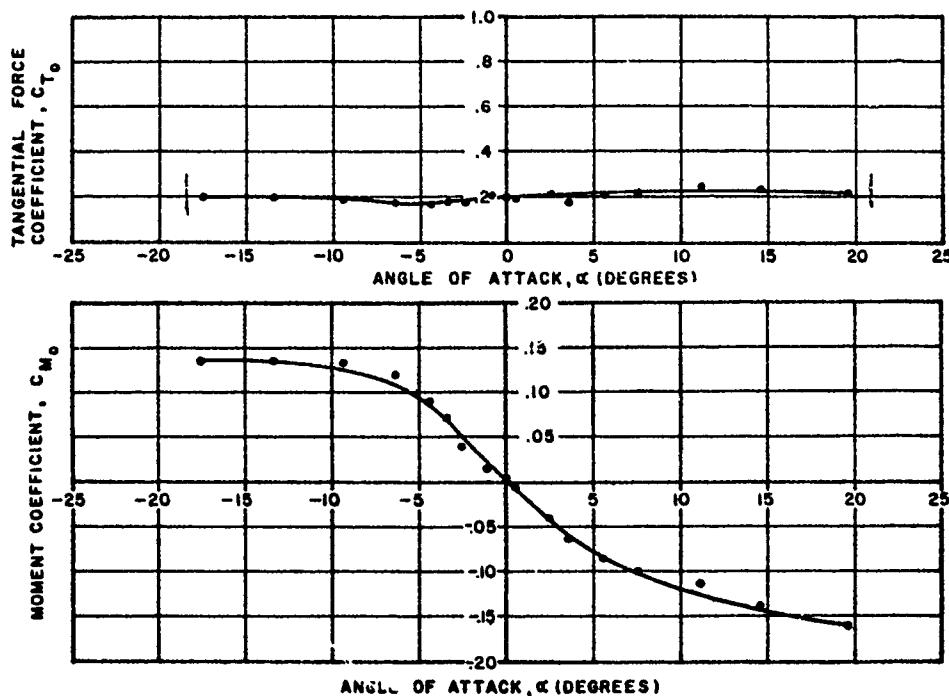


Figure 14. Variation of Tangential Force and Moment Coefficients with Angle-of-Attack: Canopy Type - Flat Circular; Cluster - one; Reefing Ratio - 0.3; Riser Length - $0 D_0$

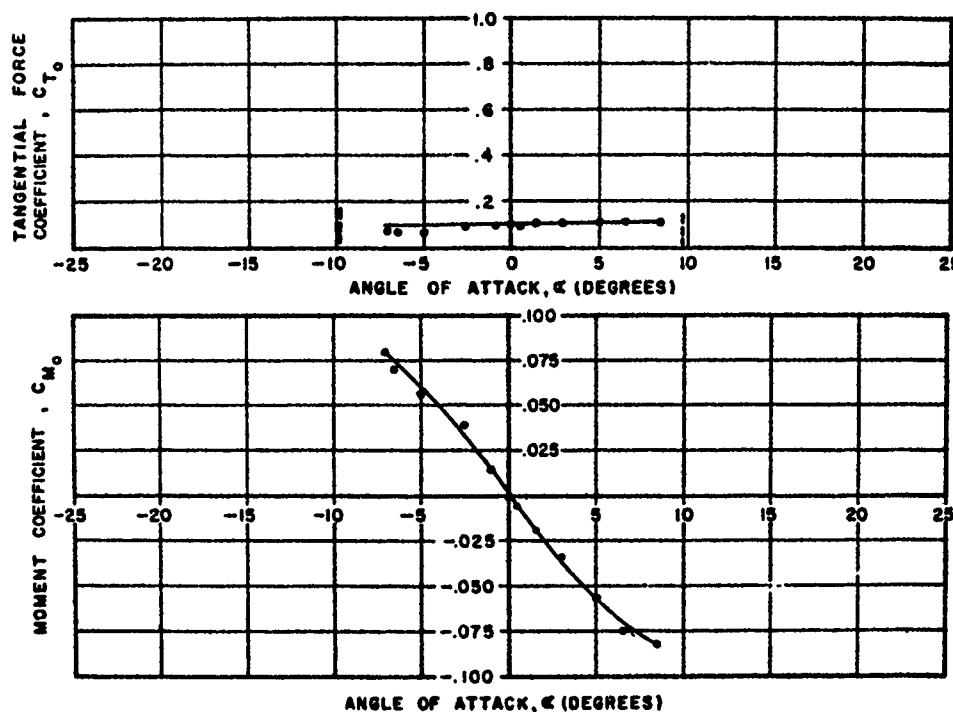


Figure 15. Variation of Tangential Force and Moment Coefficients with Angle-of-Attack: Canopy Type - Flat Circular; Cluster - one; Reefing Ratio - 0.2; Riser Length - $0 D_0$

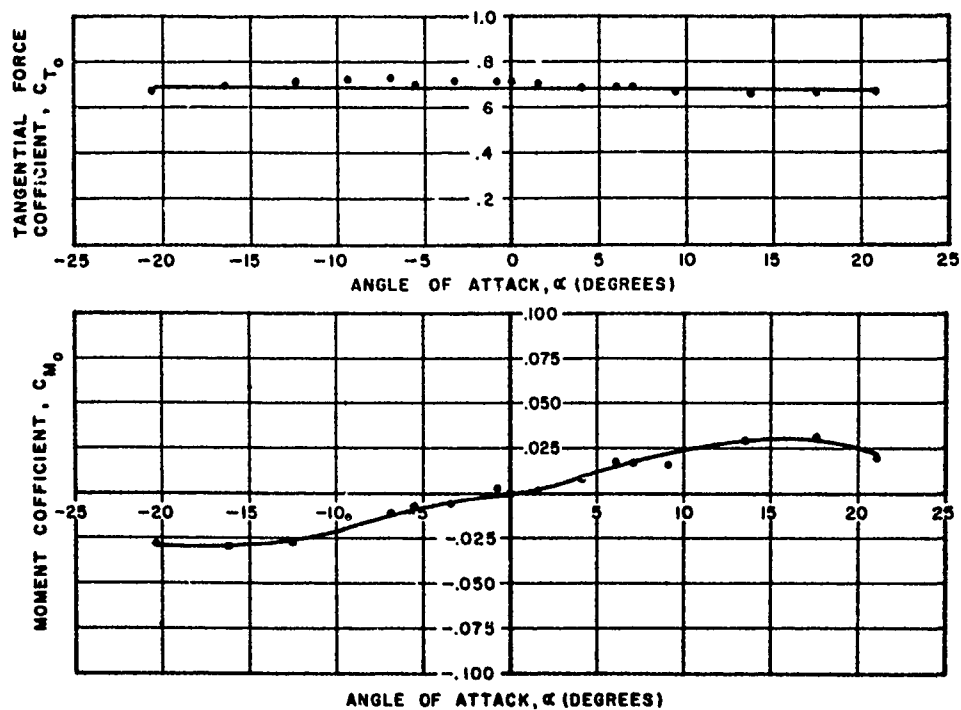


Figure 16. Variation of Tangential Force and Moment Coefficients with Angle-of-Attack: Canopy Type - Flat Circular; Cluster - two; Reefing Ratio - none; Riser Length - $0.5 D_0$

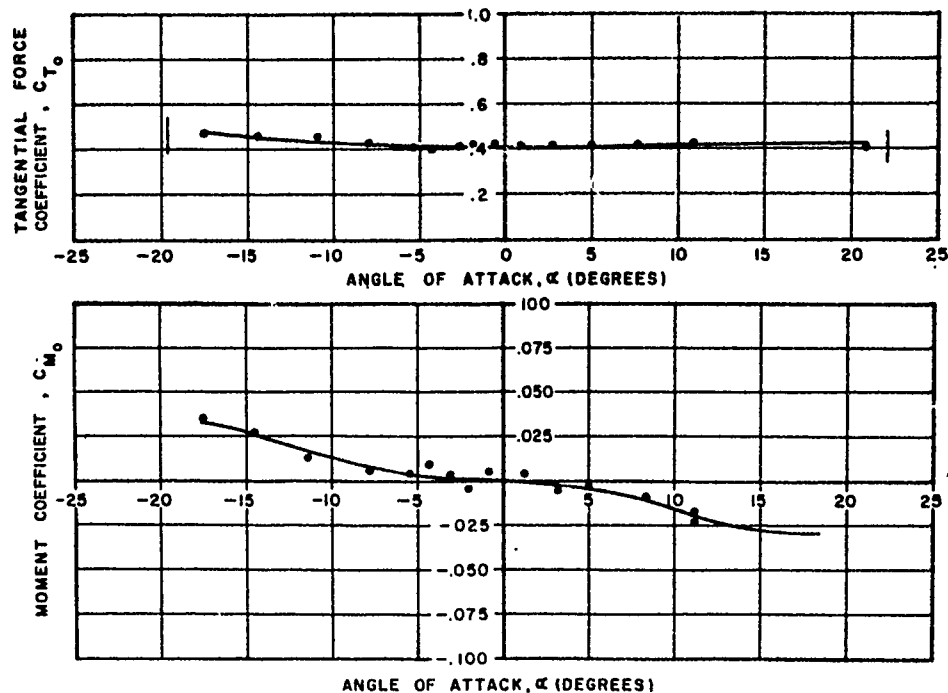


Figure 17. Variation of Tangential Force and Moment Coefficients with Angle-of-Attack: Canopy Type - Flat Circular; Cluster - two; Reefing Ratio - 0.5; Riser Length - $0.5 D_0$

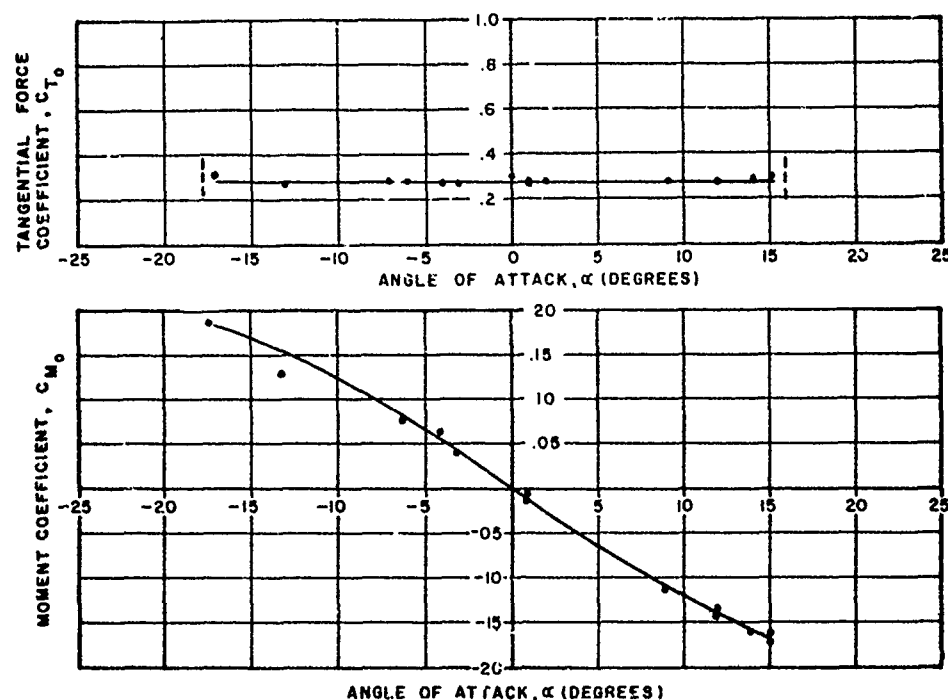


Figure 18. Variation of Tangential Force and Moment Coefficients with Angle-of-Attack: Canopy Type - Flat Circular; Cluster - two; Reefing Ratio - 0.3; Riser Length - $0.5 D_0$

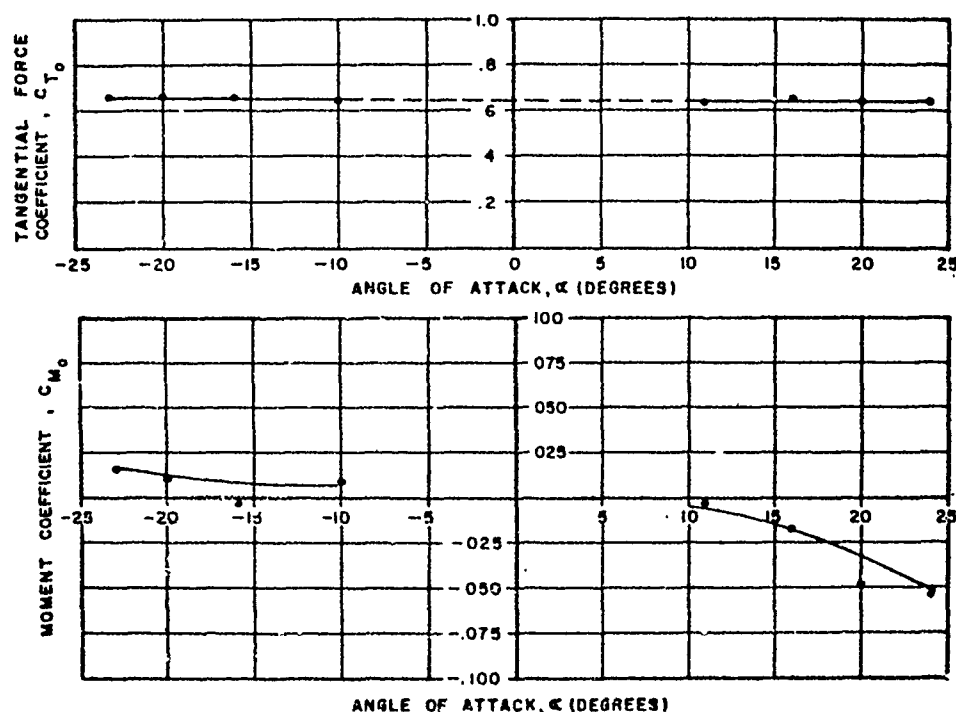


Figure 19. Variation of Tangential Force and Moment Coefficients with Angle-of-Attack: Canopy Type - Flat Circular; Cluster - three; Reefing Ratio - none; Riser Length - $1.0 D_0$

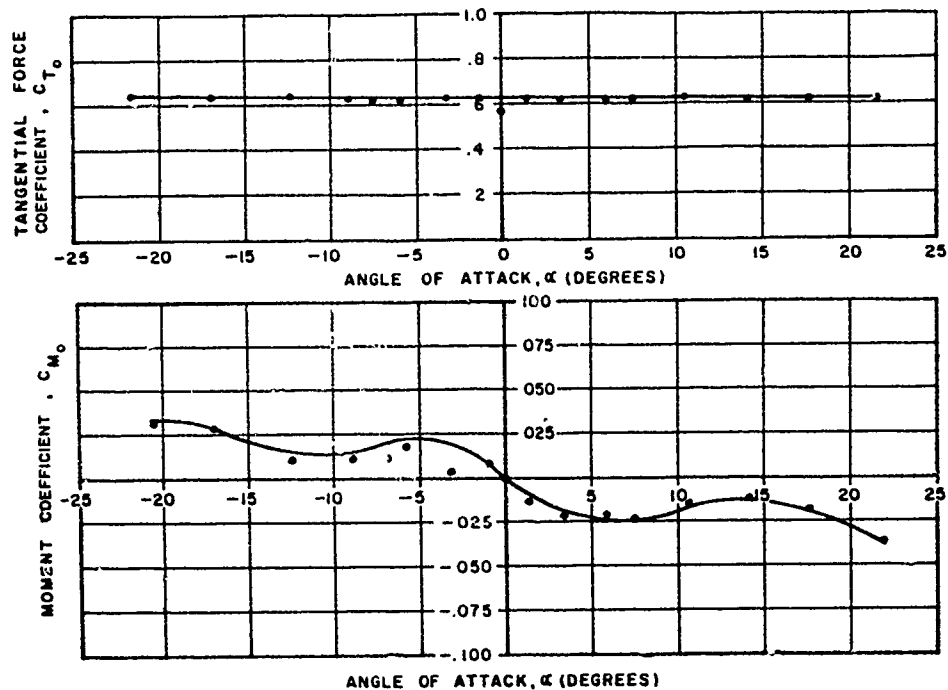


Figure 20. Variation of Tangential Force and Moment Coefficients with Angle-of-Attack: Canopy Type - Flat Circular; Cluster - three; Reefing Ratio - none; Riser Length - $0.5 D_0$

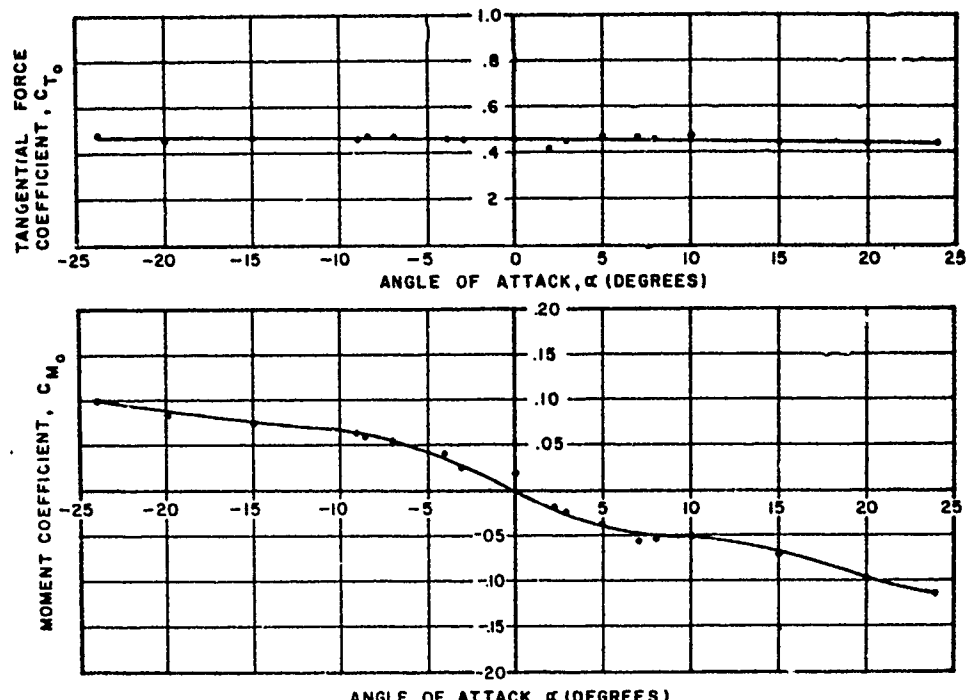


Figure 21. Variation of Tangential Force and Moment Coefficients with Angle-of-Attack: Canopy Type - Flat Circular; Cluster - three; Reefing Ratio - 0.5; Riser Length - $1.0 D_0$

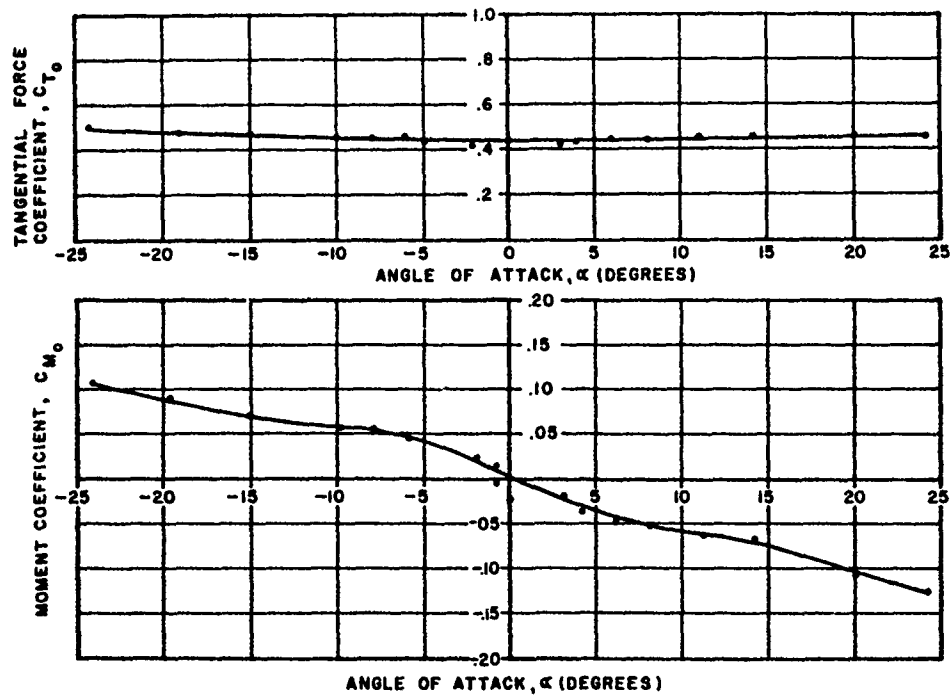


Figure 22. Variation of Tangential Force and Moment Coefficients with Angle-of-Attack: Canopy Type - Flat Circular; Cluster - three; Reefing Ratio - 0.5; Riser Length - $0.5 D_0$

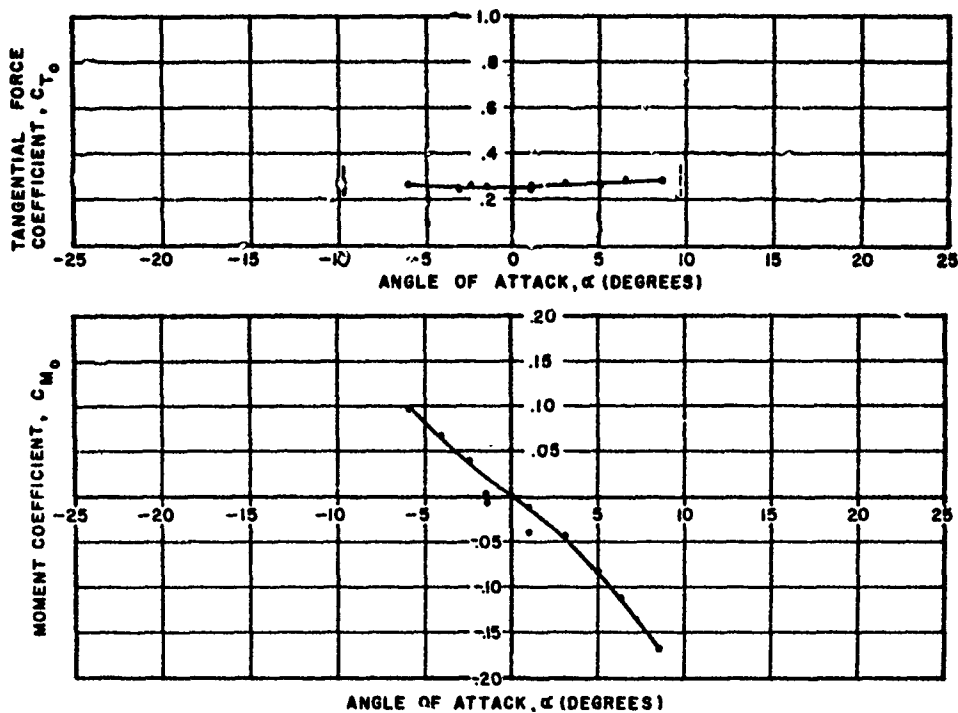


Figure 23. Variation of Tangential Force and Moment Coefficients with Angle-of-Attack: Canopy Type - Flat Circular; Cluster - three; Reefing Ratio - 0.3; Riser Length - $1.0 D_0$

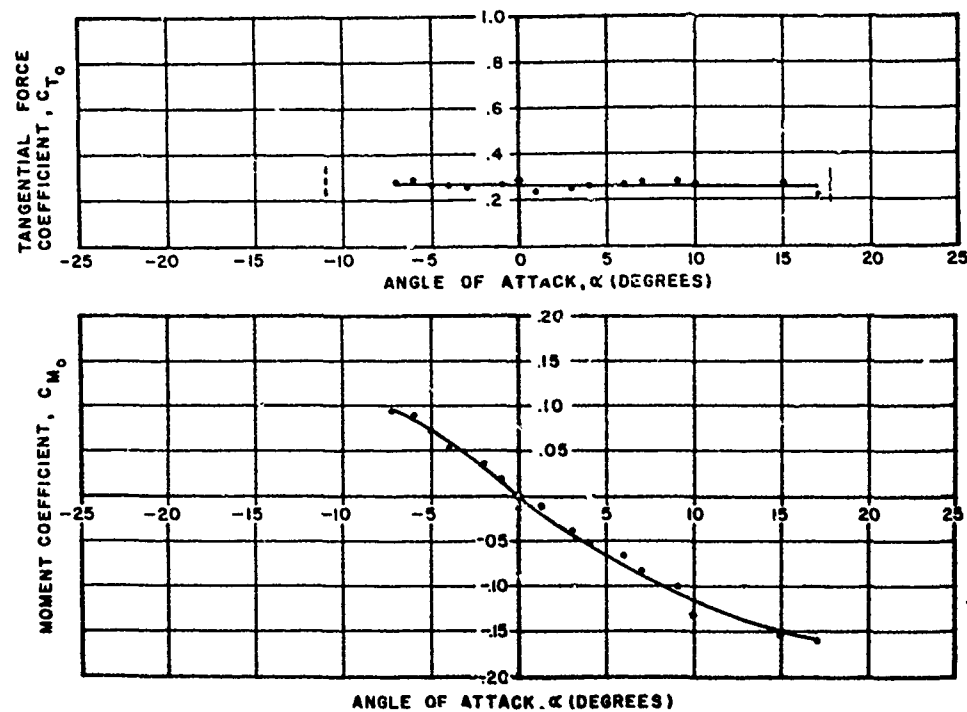


Figure 24. Variation of Tangential Force and Moment Coefficients with Angle-of-Attack: Canopy Type - Flat Circular; Cluster - three; Reefing Ratio - 0.3; Riser Length - $0.5 D_0$

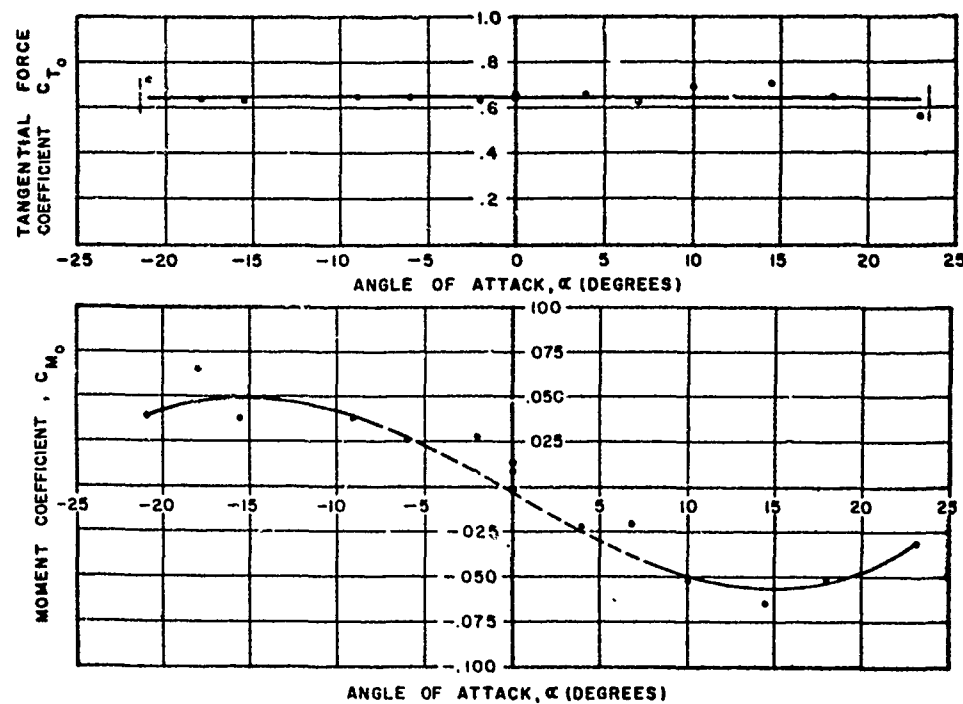


Figure 25. Variation of Tangential Force and Moment Coefficients with Angle-of-Attack: Canopy Type - Flat Circular; Cluster - five; Reefing Ratio - none; Riser Length - $1.5 D_0$

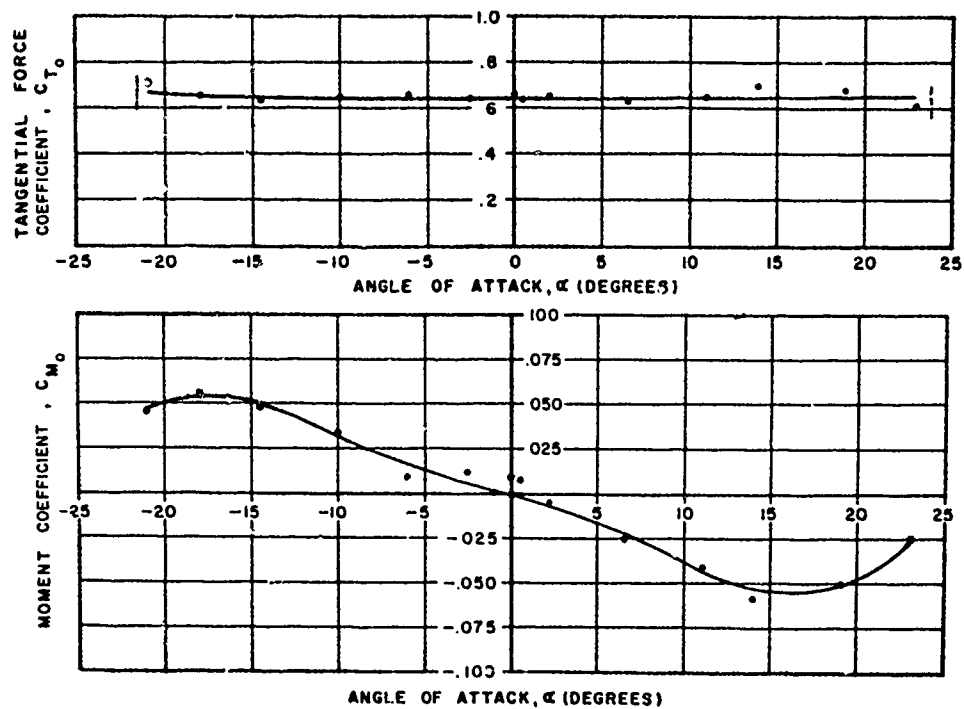


Figure 26. Variation of Tangential Force and Moment Coefficients with Angle-of-Attack: Canopy Type - Flat Circular; Cluster - five; Reefing Ratio - none; Riser Length - $1.0 D_0$

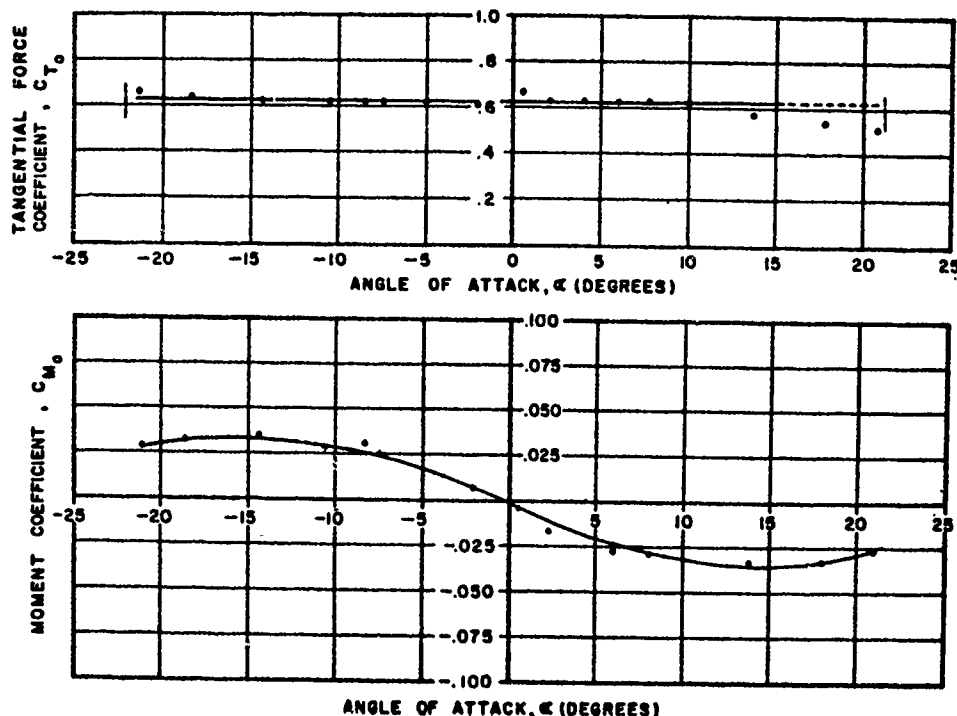


Figure 27. Variation of Tangential Force and Moment Coefficients with Angle-of-Attack: Canopy Type - Flat Circular; Cluster - five; Reefing Ratio - none; Riser Length - $0.5 D_0$

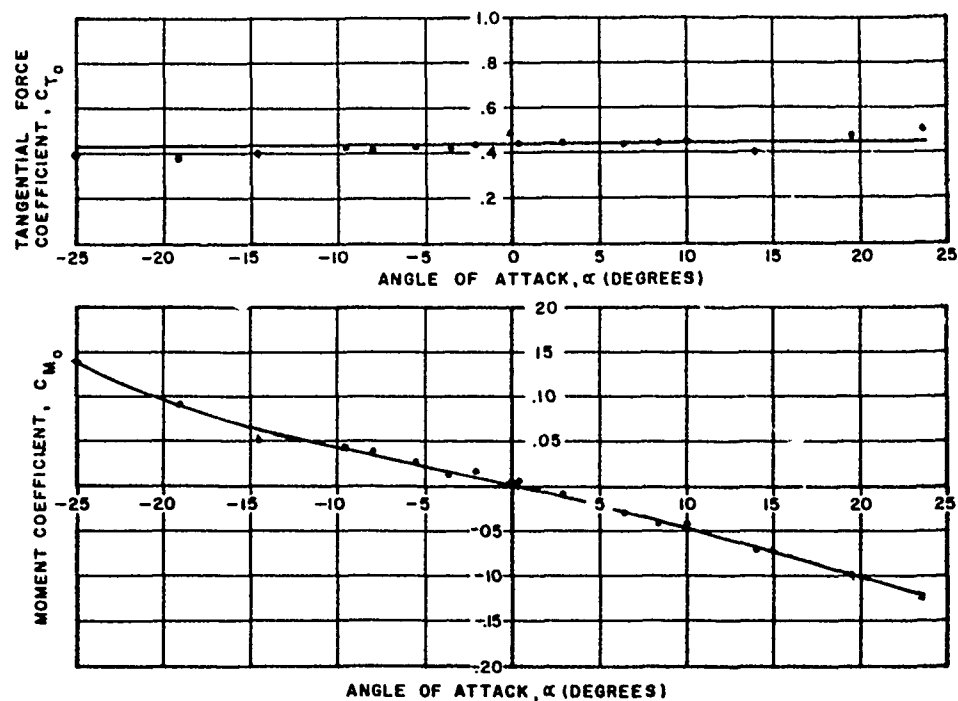


Figure 28. Variation of Tangential Force and Moment Coefficients with Angle-of-Attack: Canopy Type - Flat Circular; Cluster - five; Reefing Ratio - 0.5; Riser Length - $1.5 D_0$

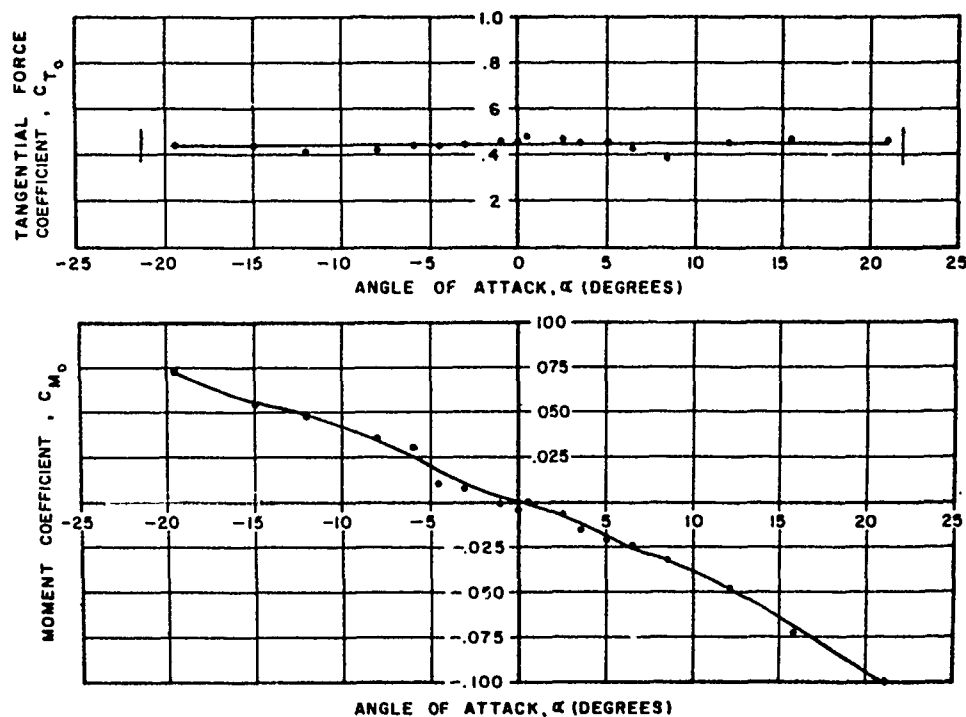


Figure 29. Variation of Tangential Force and Moment Coefficients with Angle-of-Attack: Canopy Type - Flat Circular; Cluster - five; Reefing Ratio - 0.5; Riser Length - $1.0 D_0$

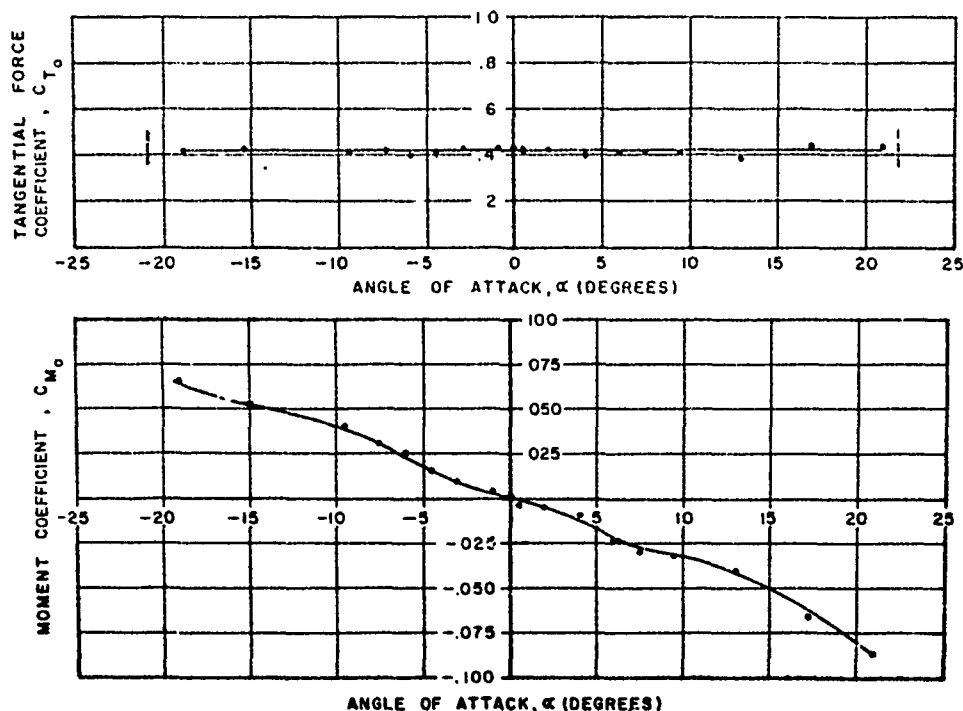


Figure 30. Variation of Tangential Force and Moment Coefficients with Angle-of-Attack: Canopy Type - Flat Circular; Cluster - five; Reefing Ratio - 0.5; Riser Length - $0.5 D_0$

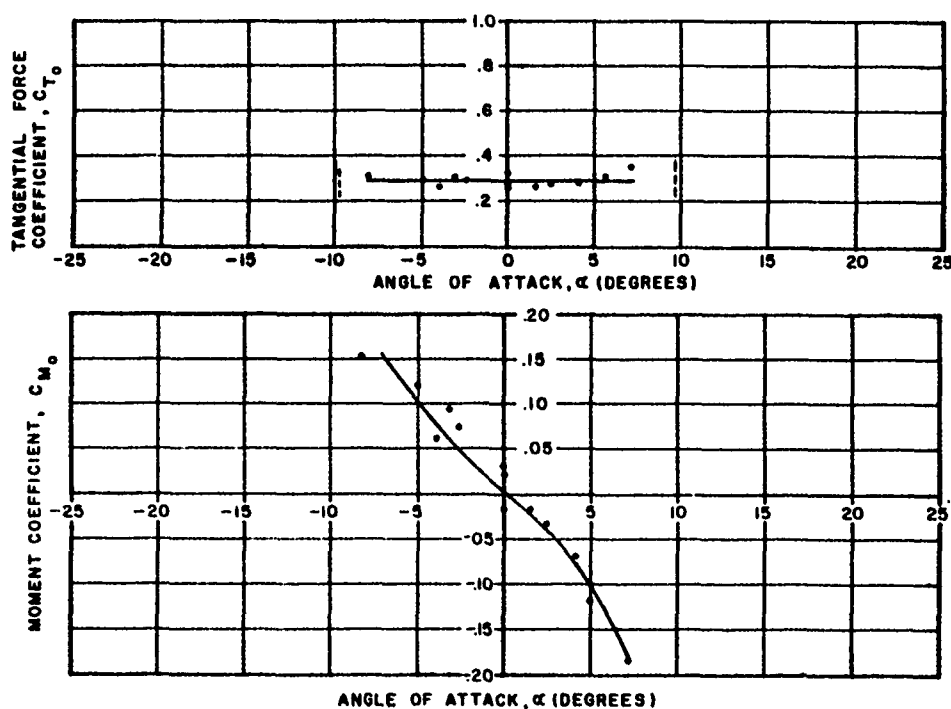


Figure 31. Variation of Tangential Force and Moment Coefficients with Angle-of-Attack: Canopy Type - Flat Circular; Cluster - five; Reefing Ratio - 0.3; Riser Length - $1.5 D_0$

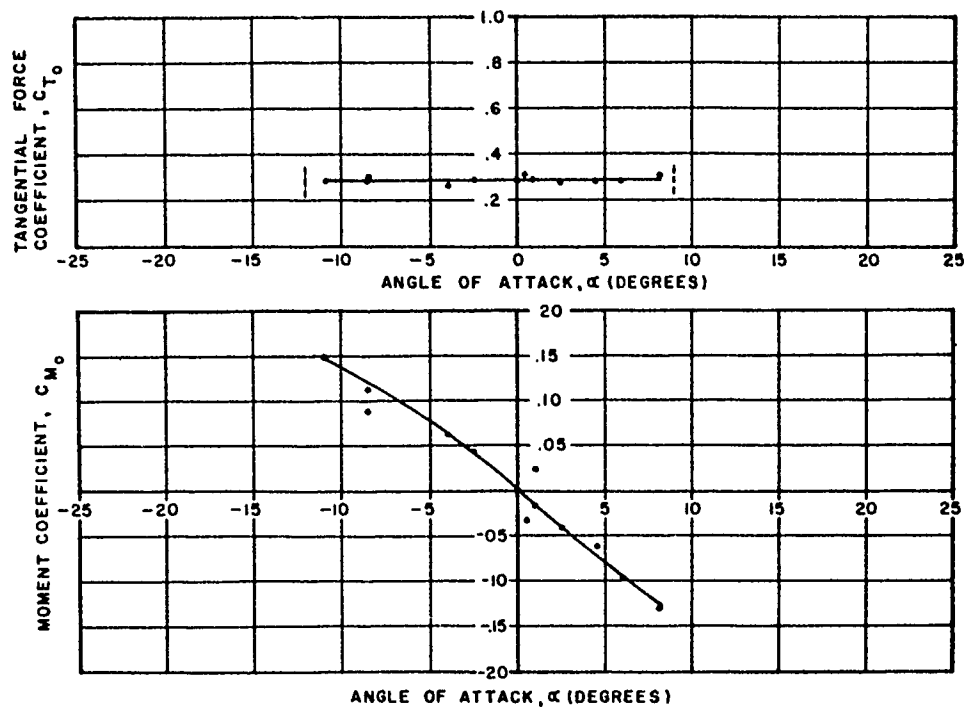


Figure 32. Variation of Tangential Force and Moment Coefficients with Angle-of-Attack: Canopy Type - Flat Circular; Cluster - five; Reefing Ratio - 0.3; Riser Length - $1.0 D_0$

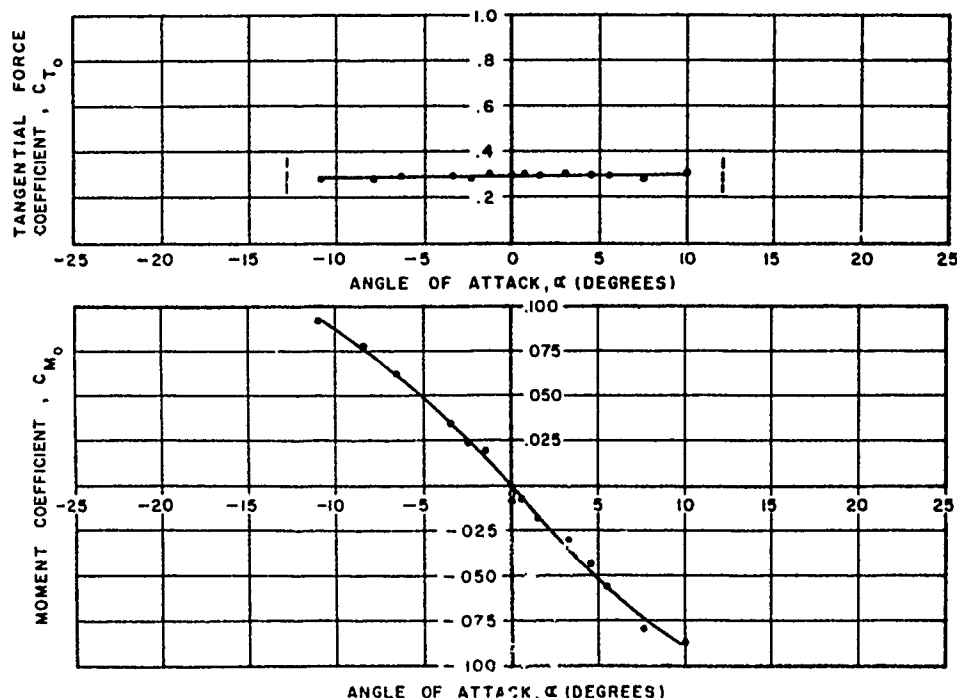


Figure 33. Variation of Tangential Force and Moment Coefficients with Angle-of-Attack: Canopy Type - Flat Circular; Cluster - five; Reefing Ratio - 0.3; Riser Length - $0.5 D_0$

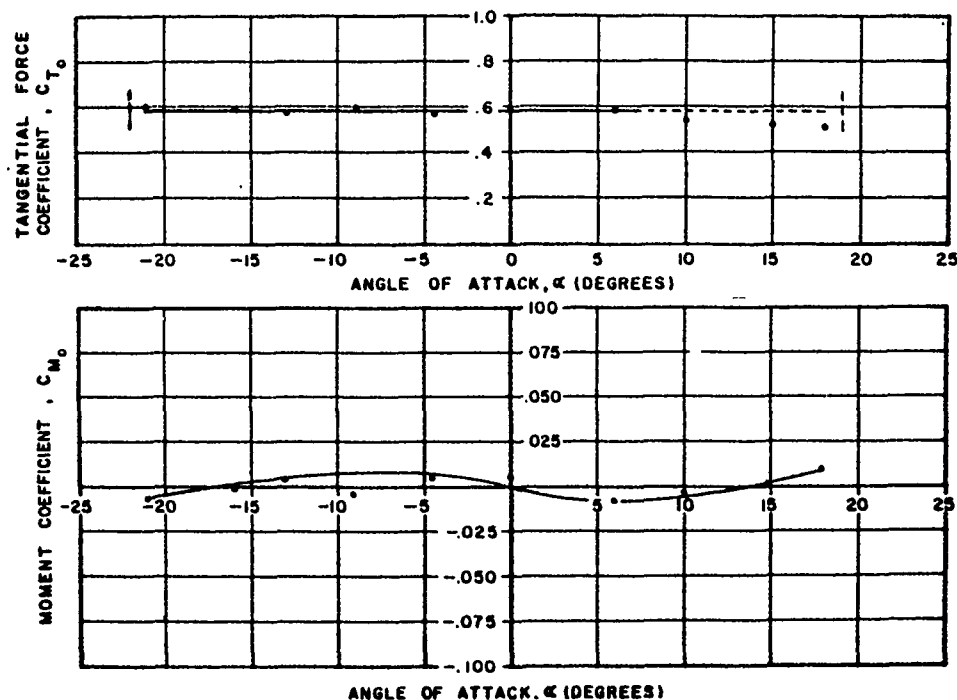


Figure 34. Variation of Tangential Force and Moment Coefficients with Angle-of-Attack: Canopy Type - Flat Circular; Cluster - seven; Reefing Ratio - none; Riser Length - $1.5 D_0$

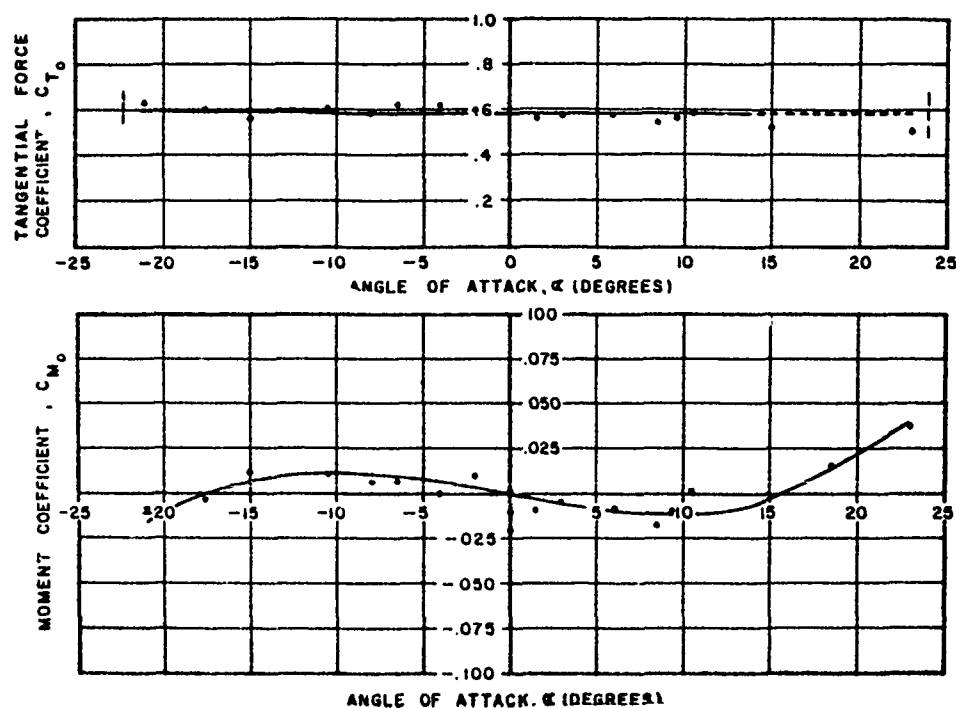


Figure 35. Variation of Tangential Force and Moment Coefficients with Angle-of-Attack: Canopy Type - Flat Circular; Cluster - seven; Reefing Ratio - none; Riser Length - $1.0 D_0$

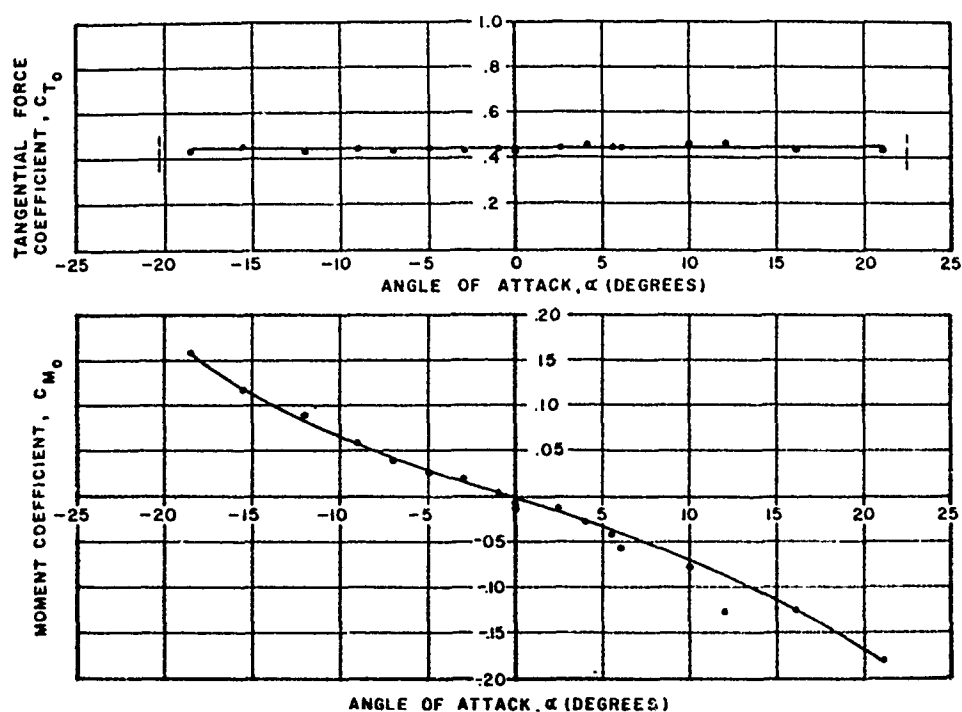


Figure 36. Variation of Tangential Force and Moment Coefficients with Angle-of-Attack: Canopy Type - Flat Circular; Cluster - seven; Reefing Ratio - 0.5; Riser Length - $1.5 D_0$

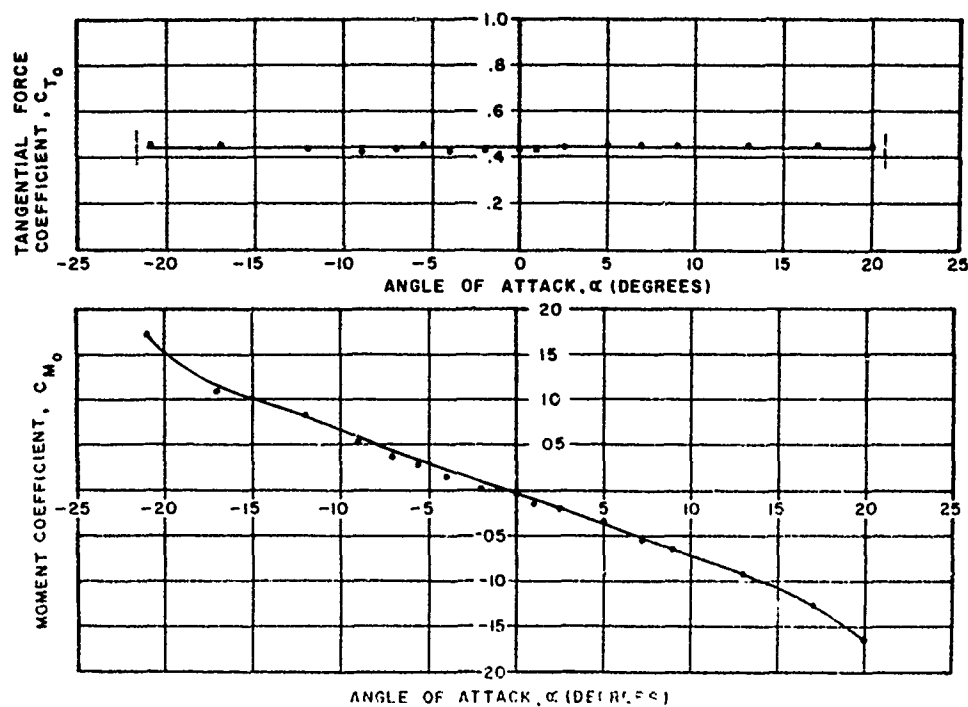


Figure 37. Variation of Tangential Force and Moment Coefficients with Angle-of-Attack: Canopy Type - Flat Circular; Cluster - seven; Reefing Ratio - 0.5; Riser Length - $1.0 D_0$

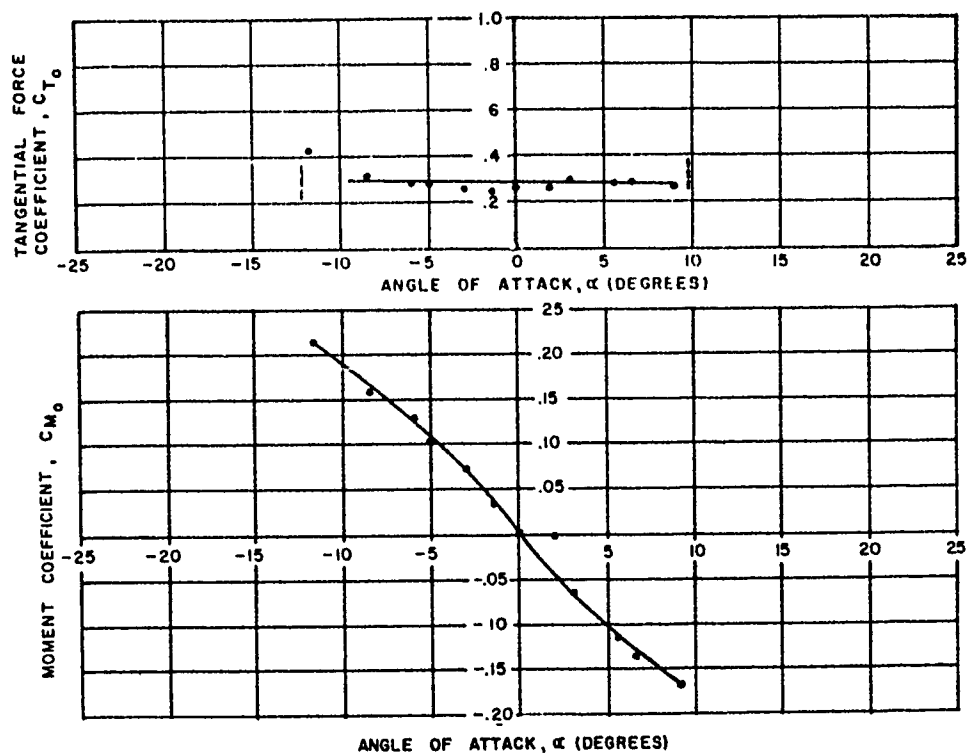


Figure 38. Variation of Tangential Force and Moment Coefficients with Angle-of-Attack: Canopy Type - Flat Circular; Cluster - seven; Reefing Ratio - 0.3; Riser Length - $1.5 D_0$

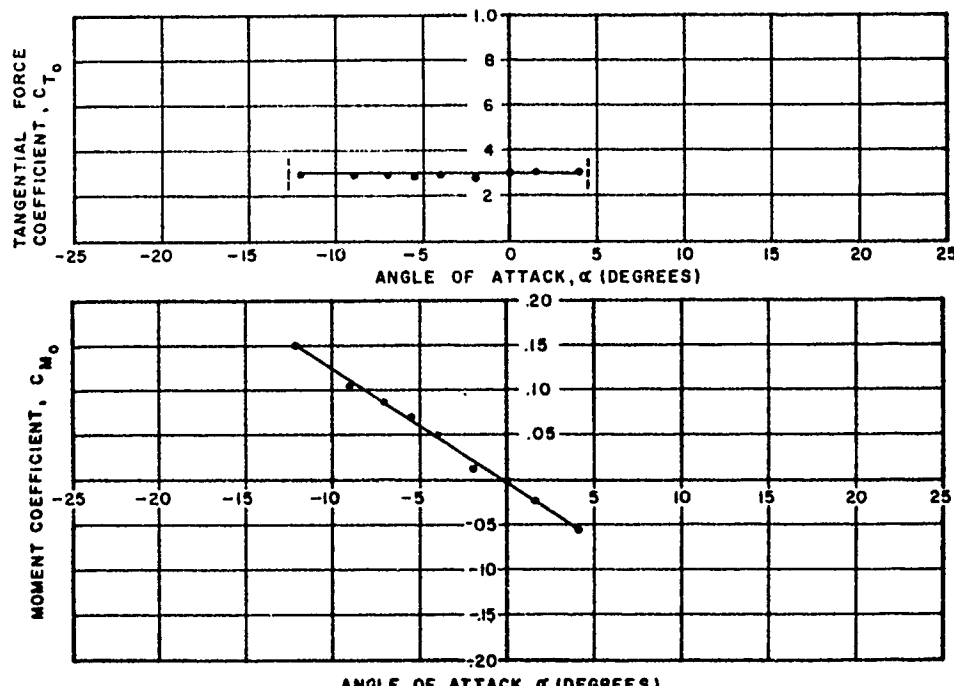


Figure 39. Variation of Tangential Force and Moment Coefficients with Angle-of-Attack: Canopy Type - Flat Circular; Cluster - seven; Reefing Ratio - 0.3; Riser Length - $1.0 D_0$

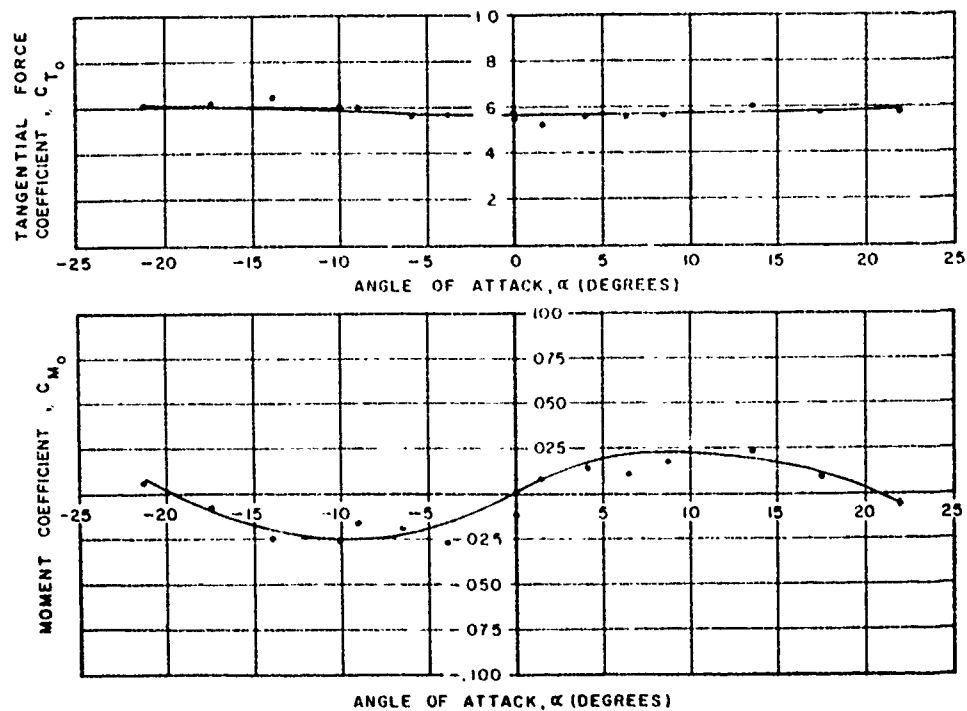


Figure 40. Variation of Tangential Force and Moment Coefficients with Angle-of-Attack: Canopy Type - Extended Skirt; Cluster one; Reefing Ratio - none; Riser Length - $0 D_0$

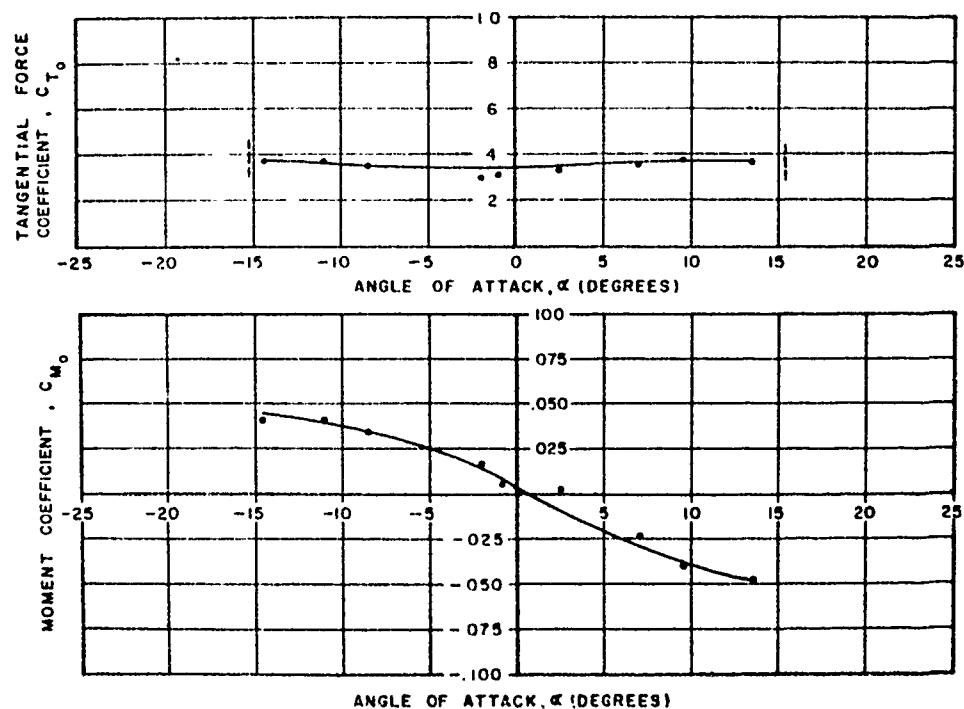


Figure 41. Variation of Tangential Force and Moment Coefficients with Angle-of-Attack: Canopy Type - Extended Skirt; Cluster - one; Reefing Ratio - 0.5; Riser Length - $0 D_0$

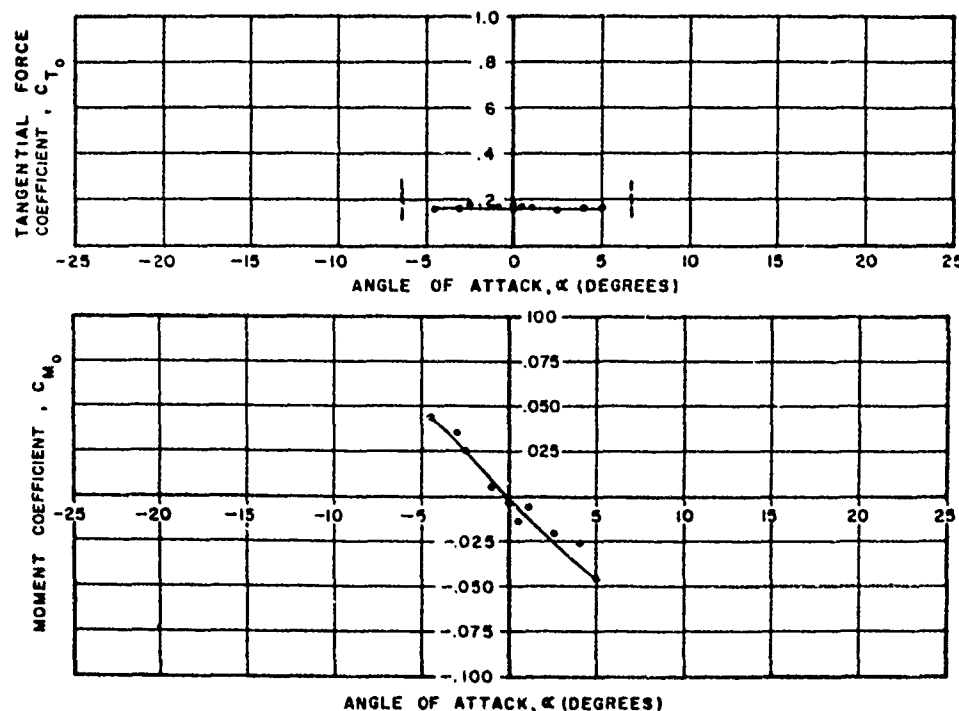


Figure 42. Variation of Tangential Force and Moment Coefficients with Angle-of-Attack: Canopy Type - Extended Skirt; Cluster - one; Reefing Ratio - 0.3; Riser Length - $0 D_0$

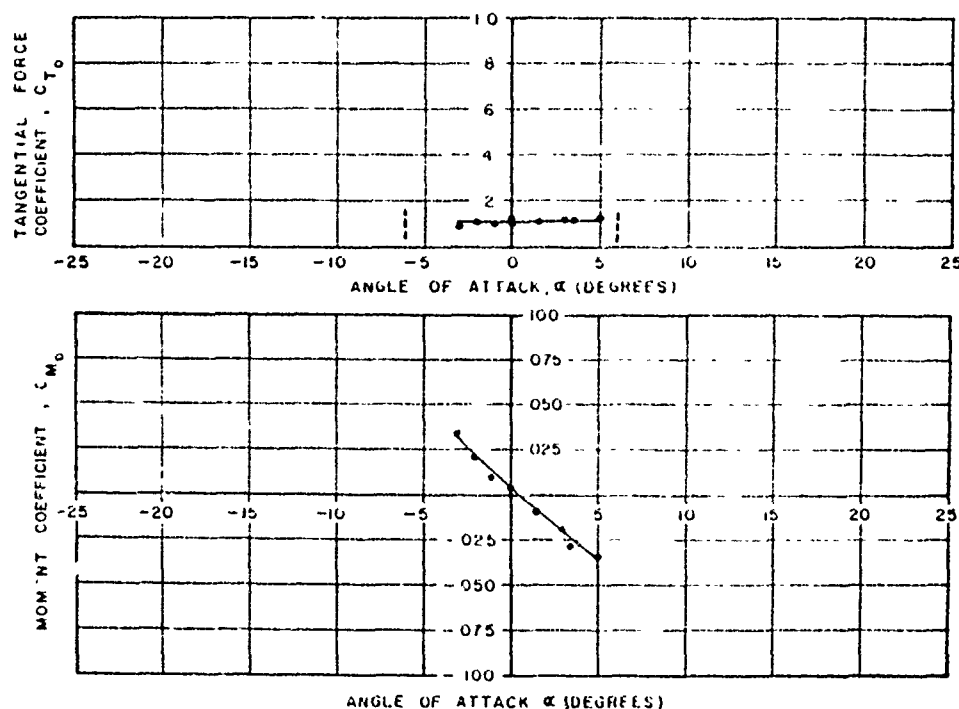


Figure 43. Variation of Tangential Force and Moment Coefficients with Angle-of-Attack: Canopy Type - Extended Skirt; Cluster - one, Reefing Ratio - 0.2; Riser Length - $0 D_0$

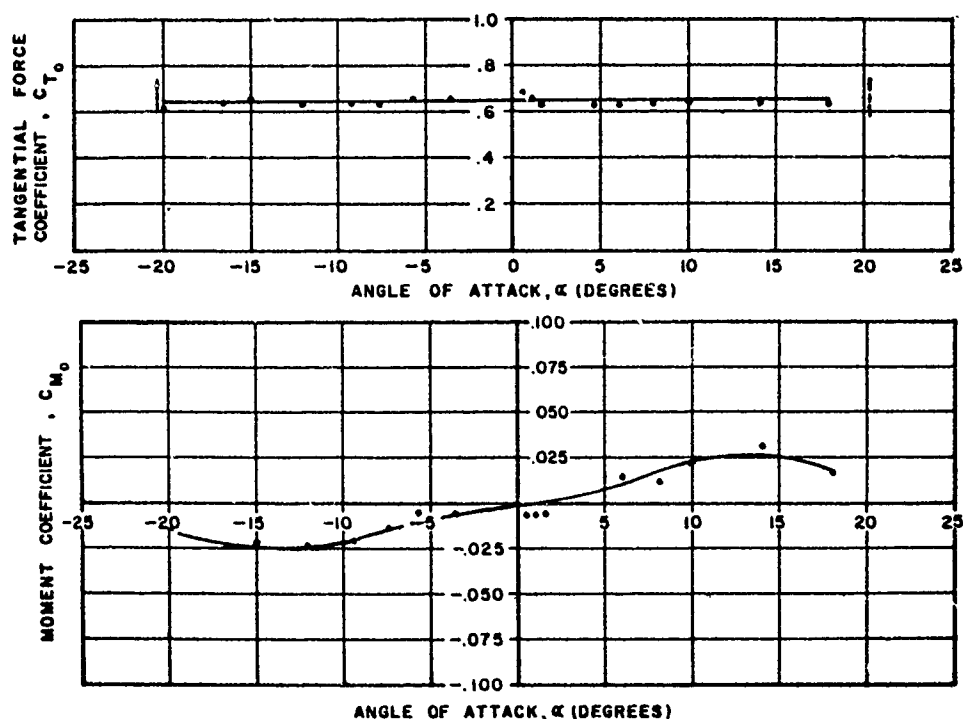


Figure 44. Variation of Tangential Force and Moment Coefficients with Angle-of-Attack: Canopy Type - Extended Skirt; Cluster - two; Reefing Ratio - none; Riser Length - $0.5 D_0$

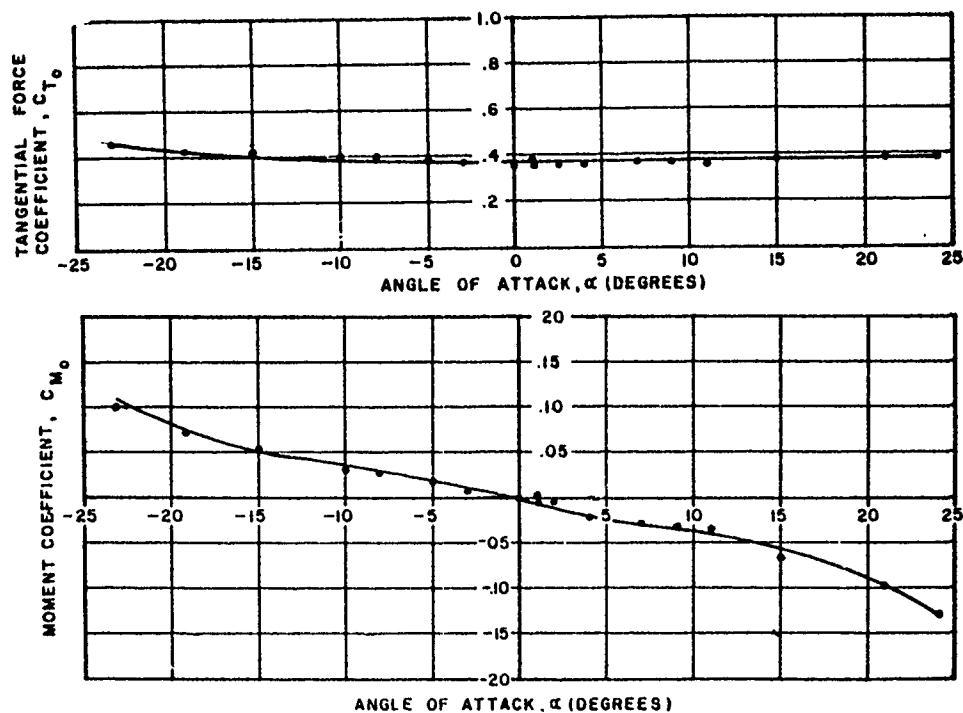


Figure 45. Variation of Tangential Force and Moment Coefficients with Angle-of-Attack: Canopy Type - Extended Skirt; Cluster - two; Reefing Ratio - 0.5; Riser Length - $0.5 D_0$

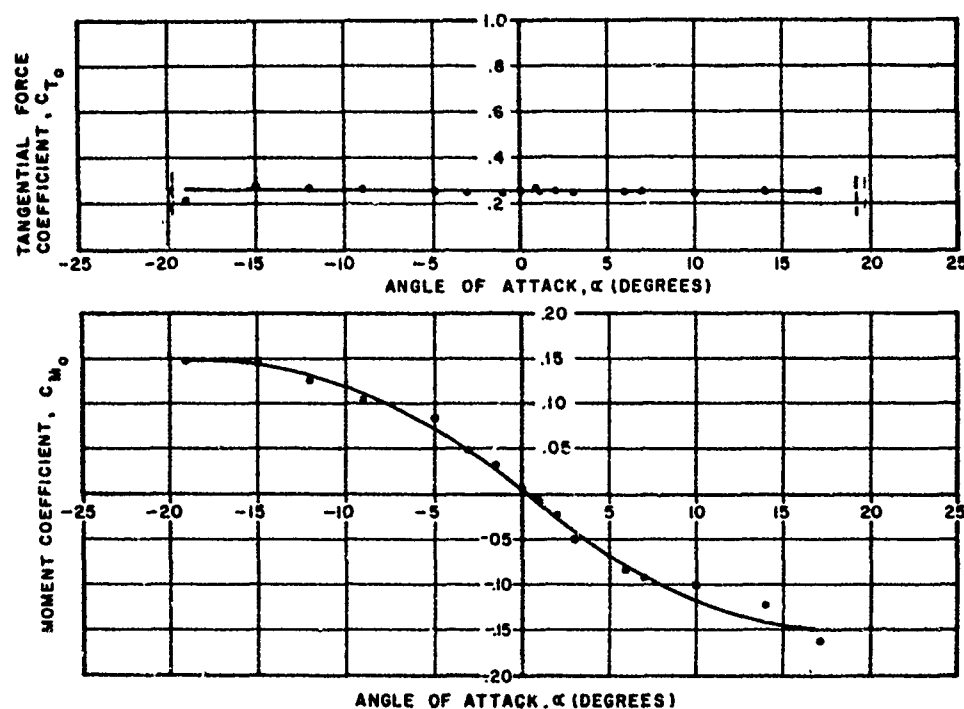


Figure 46. Variation of Tangential Force and Moment Coefficients with Angle-of-Attack: Canopy Type - Extended Skirt; Cluster - two; Reefing Ratio - 0.3; Riser Length - $0.5 D_0$

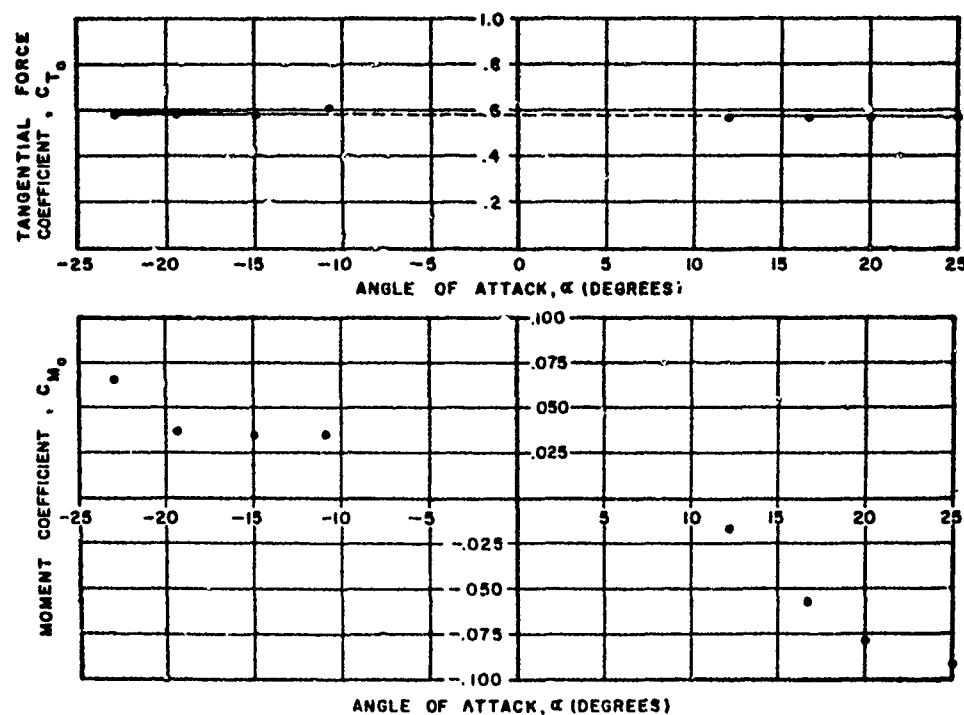


Figure 47. Variation of Tangential Force and Moment Coefficients with Angle-of-Attack: Canopy Type - Extended Skirt; Cluster - three; Reefing Ratio - none; Riser Length - $1.0 D_0$

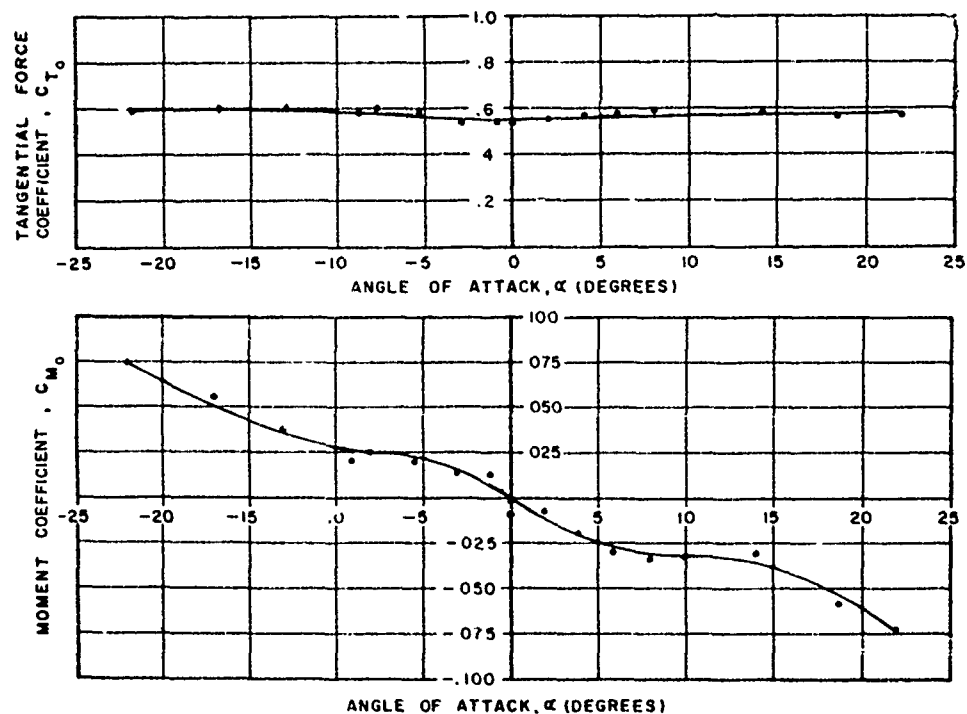


Figure 43. Variation of Tangential Force and Moment Coefficients with Angle-of-Attack: Canopy Type - Extended Skirt; Cluster - three; Reefing Ratio - none; Riser Length - $0.5 D_0$

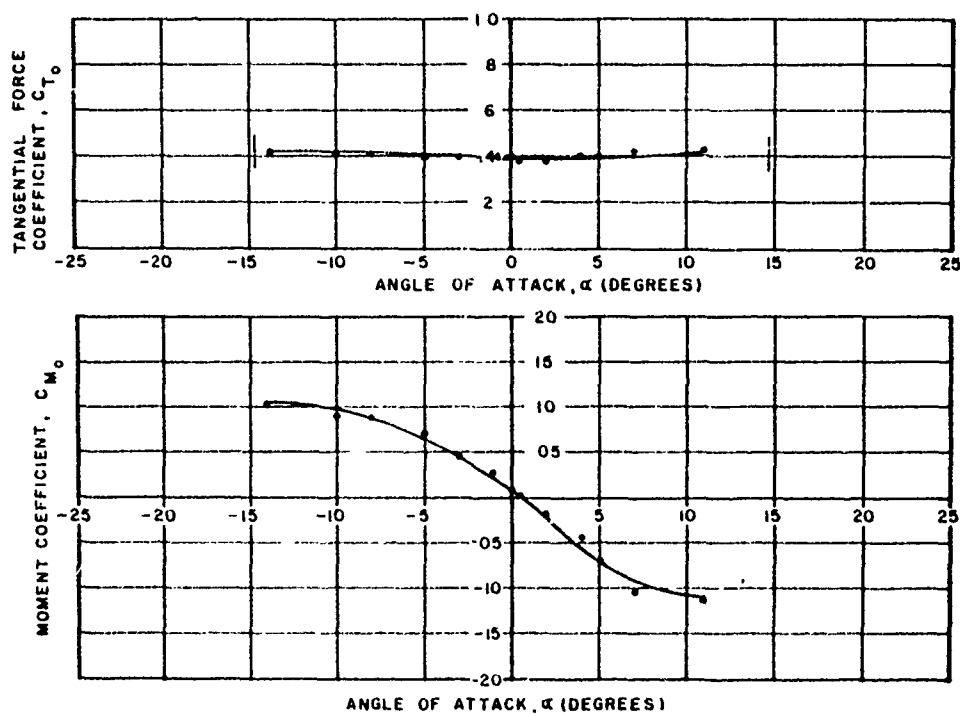


Figure 49. Variation of Tangential Force and Moment Coefficients with Angle-of-Attack: Canopy Type - Extended Skirt; Cluster - three; Reefing Ratio - 0.5; Riser Length - $1.0 D_0$

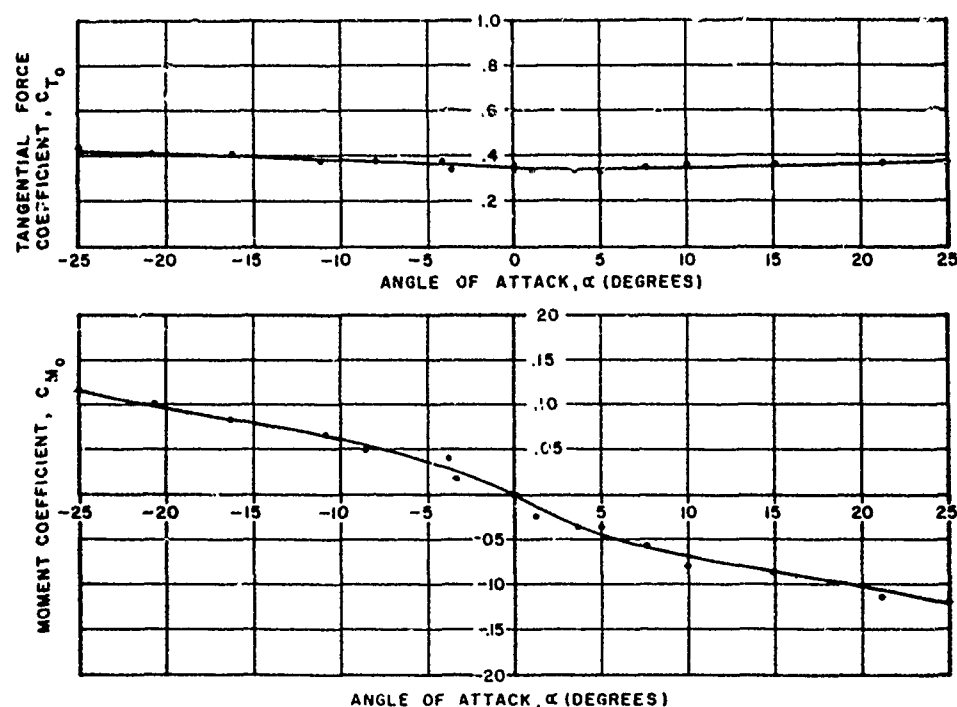


Figure 50. Variation of Tangential Force and Moment Coefficients with Angle-of-Attack: Canopy Type - Extended Skirt; Cluster - three; Reefing Ratio - 0.5; Riser Length - $0.5 D_0$

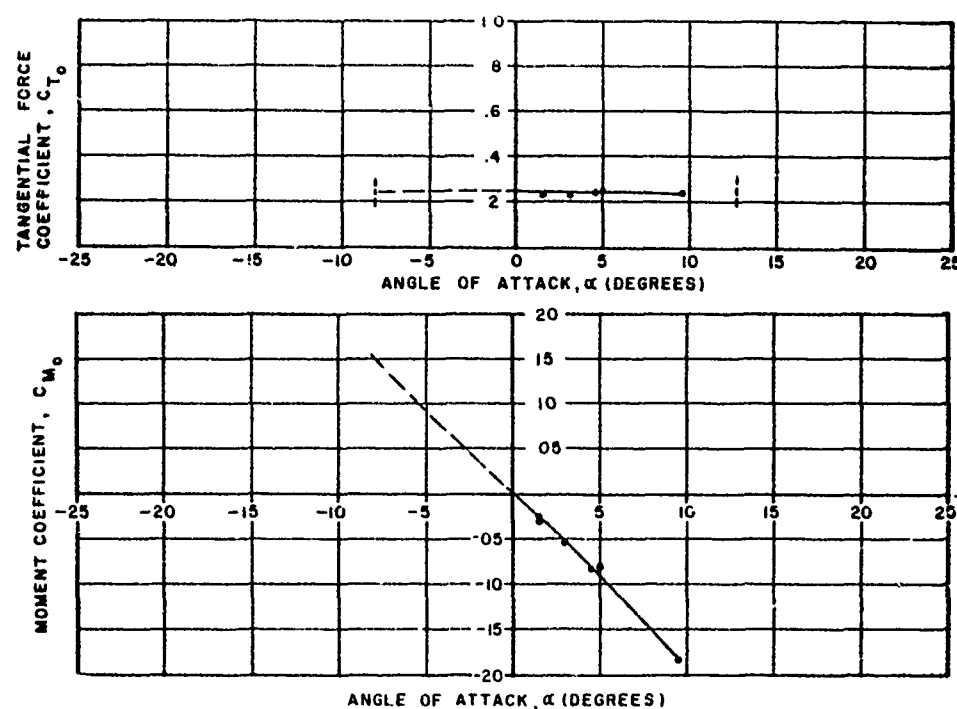


Figure 51. Variation of Tangential force and Moment Coefficients with Angle-of-Attack: Canopy Type - Extended Skirt; Cluster - three; Reefing Ratio - 0.3; Riser Length - $1.0 D_0$

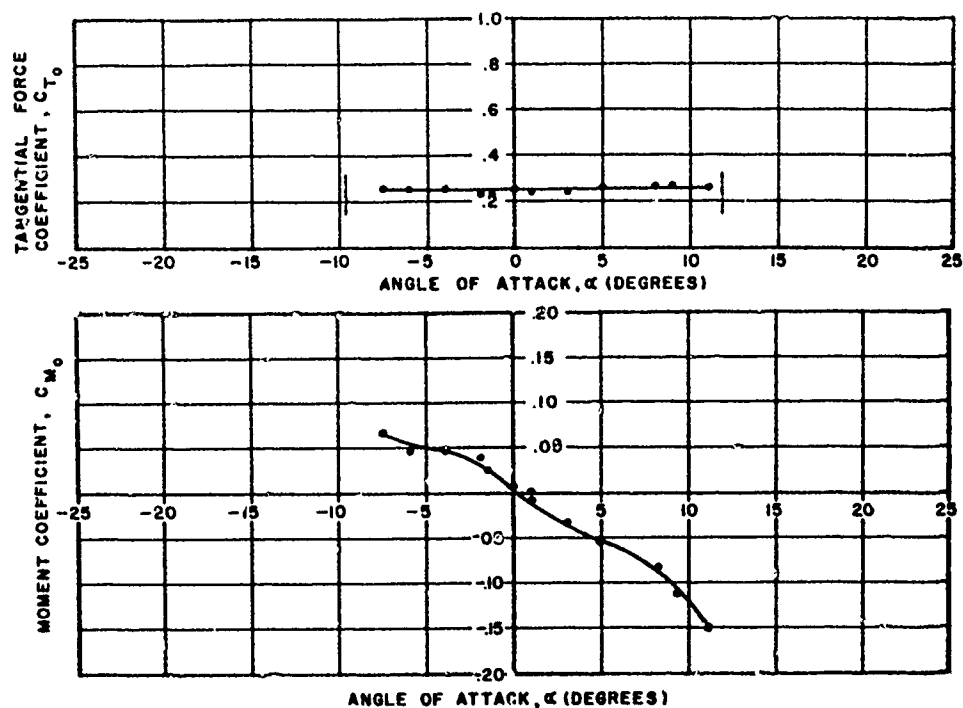


Figure 52. Variation of Tangential Force and Moment Coefficients with Angle-of-Attack: Canopy Type - Extended Skirt, Cluster - three; Reefing Ratio - 0.3; Riser Length - $0.5 D_0$

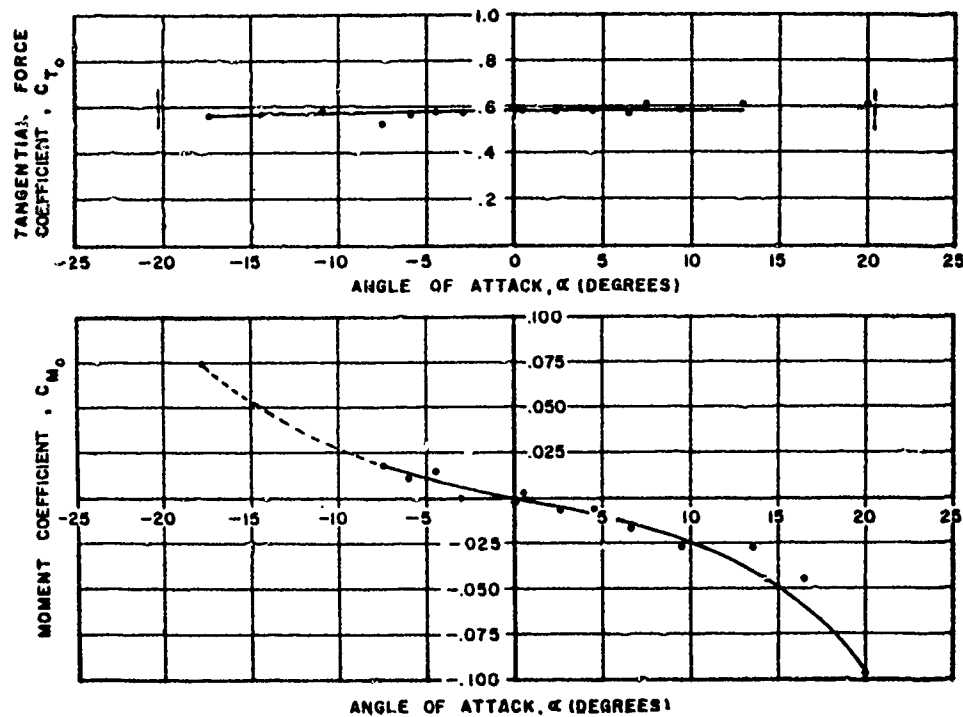


Figure 53. Variation of Tangential Force and Moment Coefficients with Angle-of-Attack: Canopy Type - Extended Skirt; Cluster - five; Reefing Ratio - none; Riser Length - $1.5 D_0$

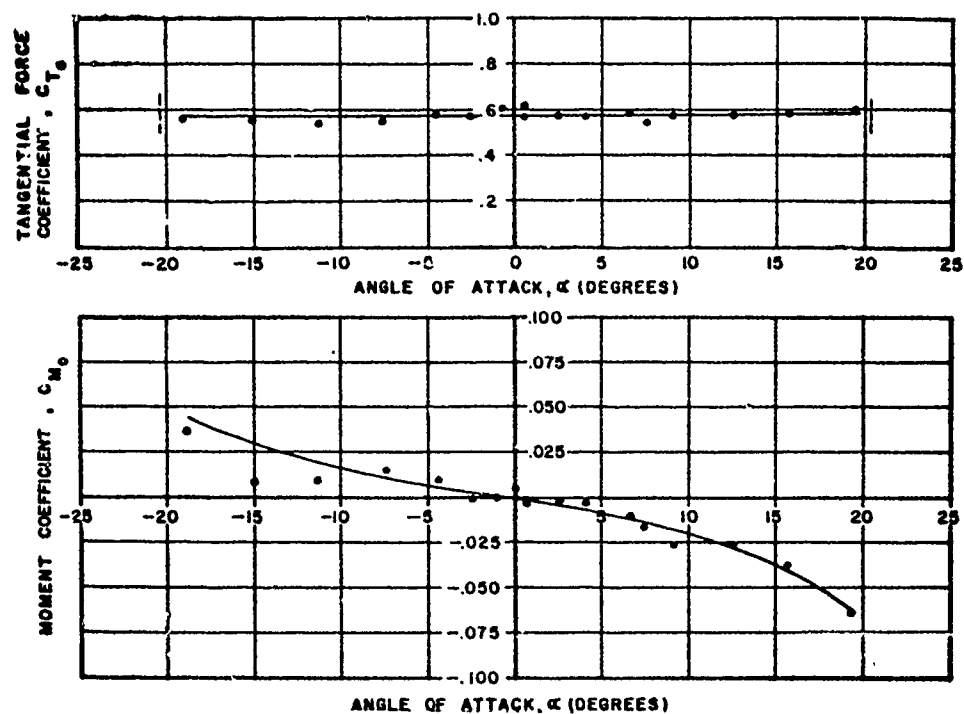


Figure 54. Variation of Tangential Force and Moment Coefficients with Angle-of-Attack: Canopy Type - Extended Skirt; Cluster - five; Reefing Ratio - none; Riser Length - $1.0 D_o$

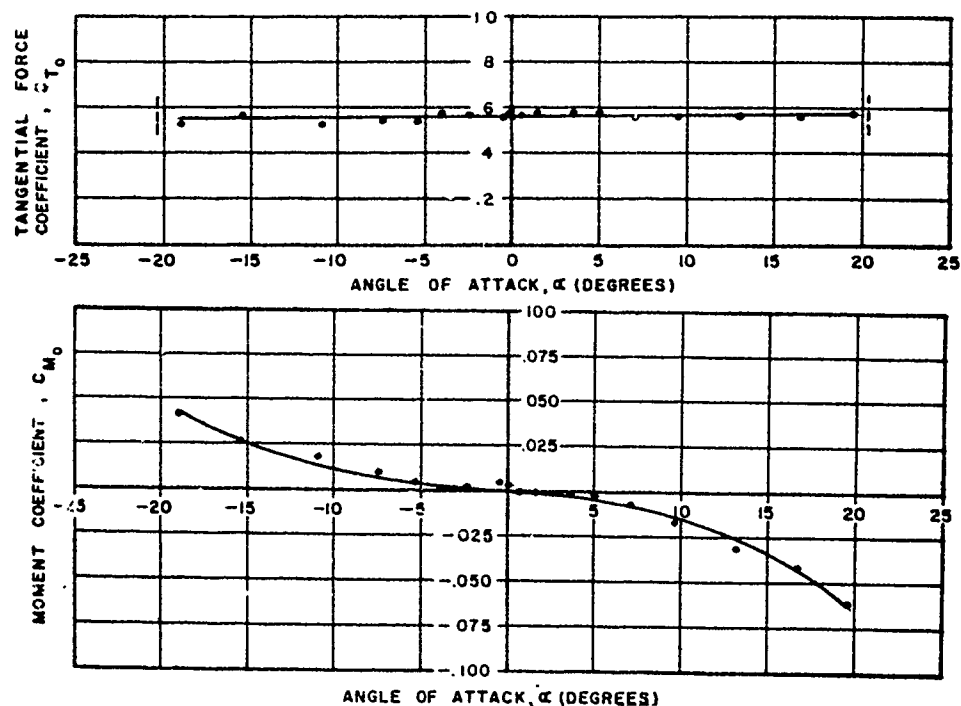


Figure 55 Variation of Tangential Force and Moment Coefficients with Angle-of-Attack: Canopy Type - Extended Skirt; Cluster - five; Reefing Ratio - none; Riser Length - $0.5 D_o$

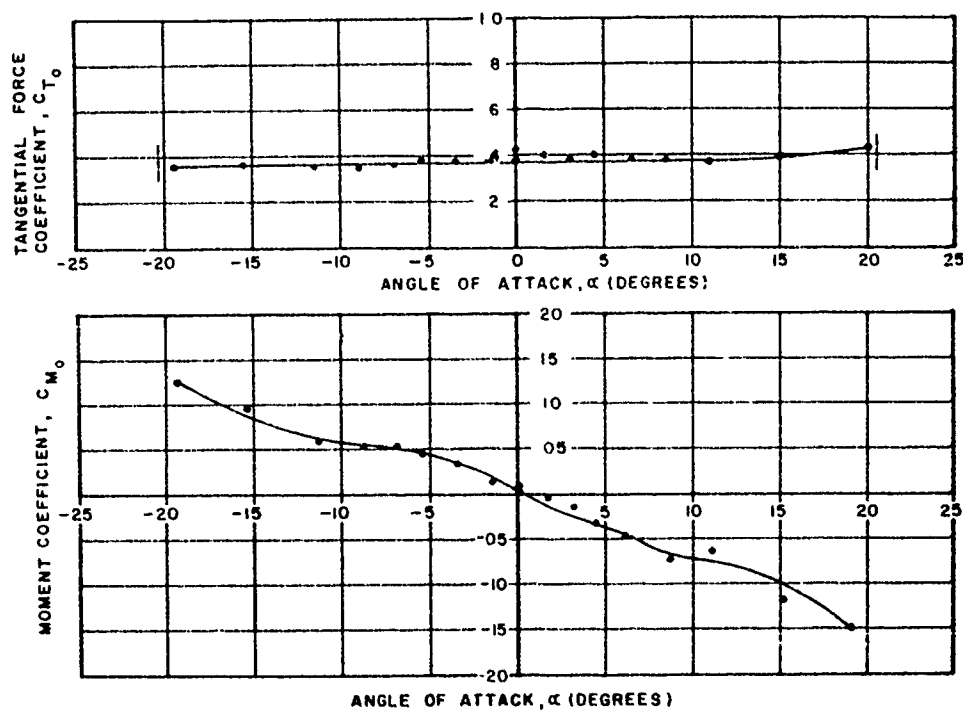


Figure 56. Variation of Tangential Force and Moment Coefficients with Angle-of-Attack: Canopy Type - Extended Skirt; Cluster - five; Reefing Ratio - 0.5; Riser Length - $1.5 D_0$

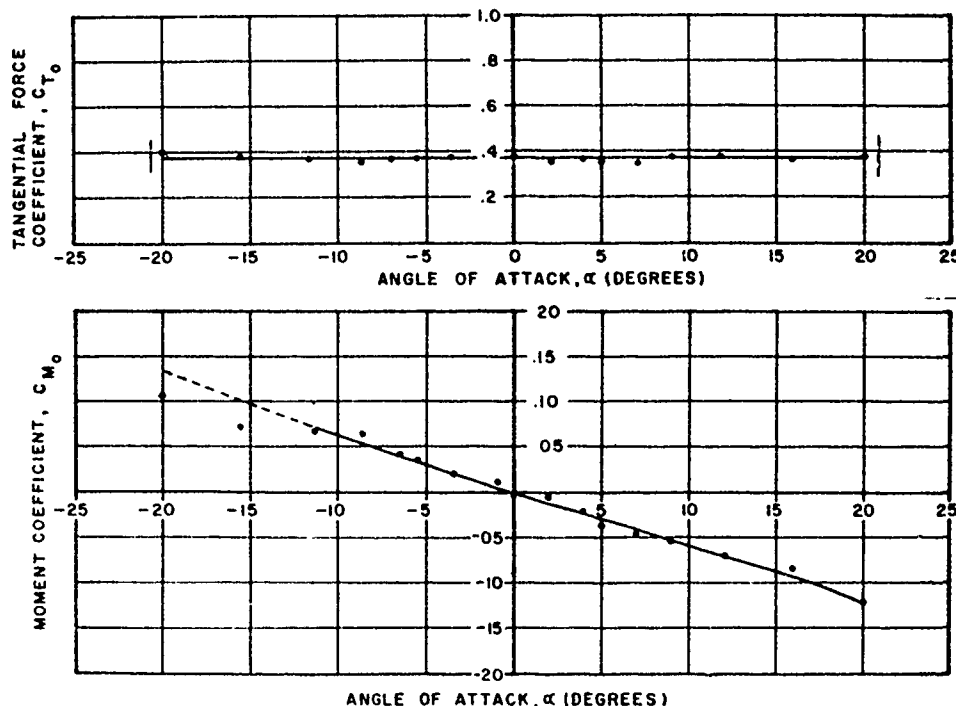


Figure 57. Variation of Tangential Force and Moment Coefficients with Angle-of-Attack: Canopy Type - Extended Skirt; Cluster - five; Reefing Ratio - 0.5; Riser Length - $1.0 D_0$

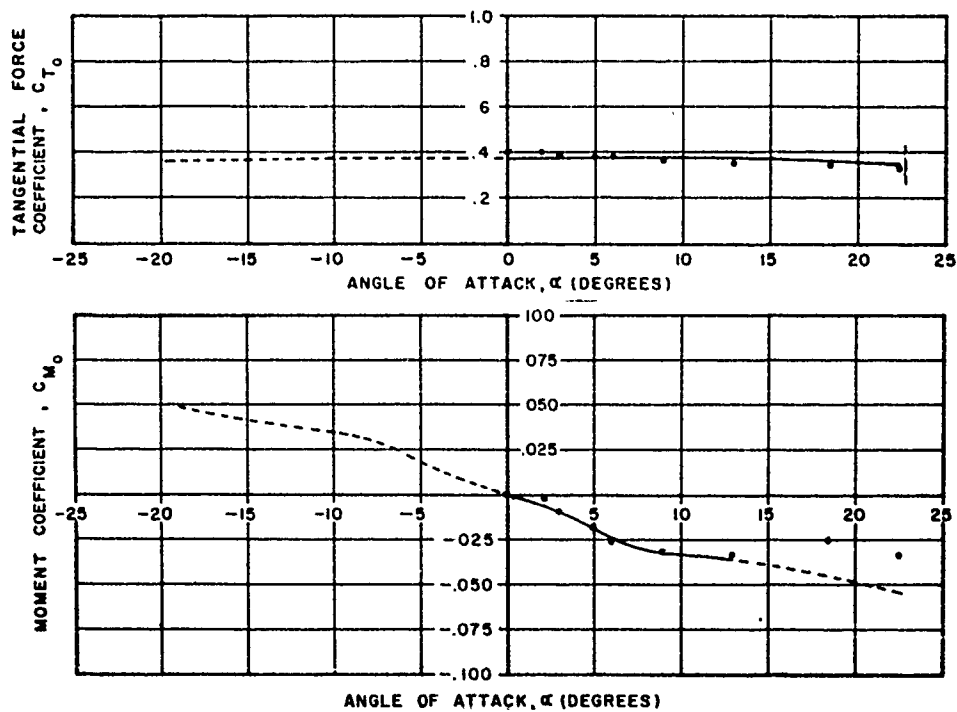


Figure 58. Variation of Tangential Force and Moment Coefficients with Angle-of-Attack: Canopy Type - Extended Skirt; Cluster - five; Reefing Ratio - 0.5; Riser Length - $0.5 D_0$

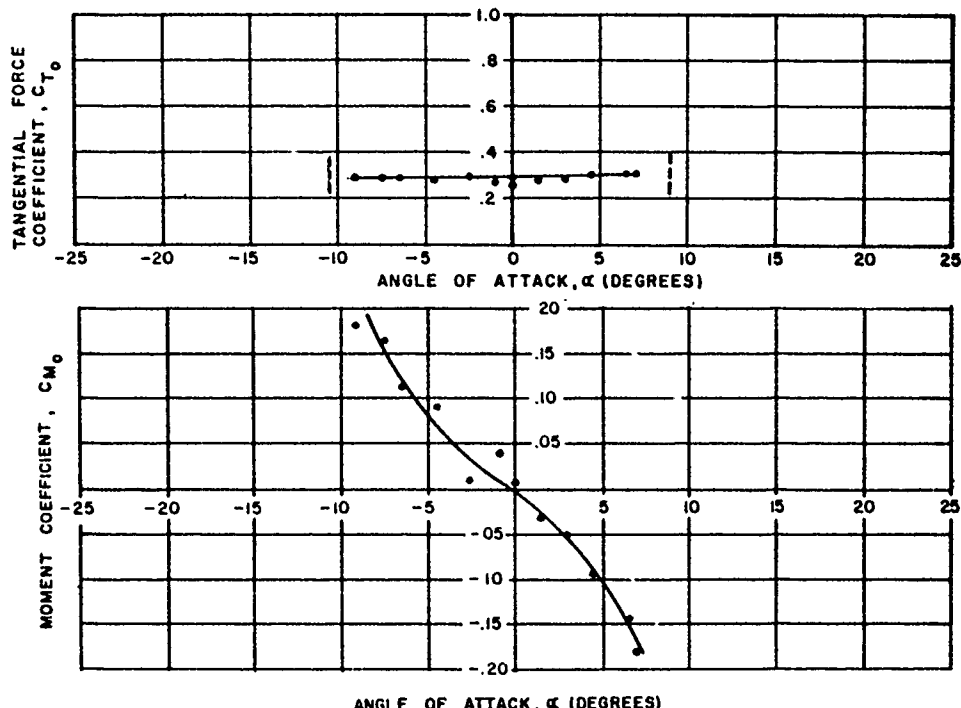


Figure 59. Variation of Tangential Force and Moment Coefficients with Angle-of-Attack: Canopy Type - Extended Skirt; Cluster - five; Reefing Ratio - 0.3; Riser Length - $1.5 D_0$

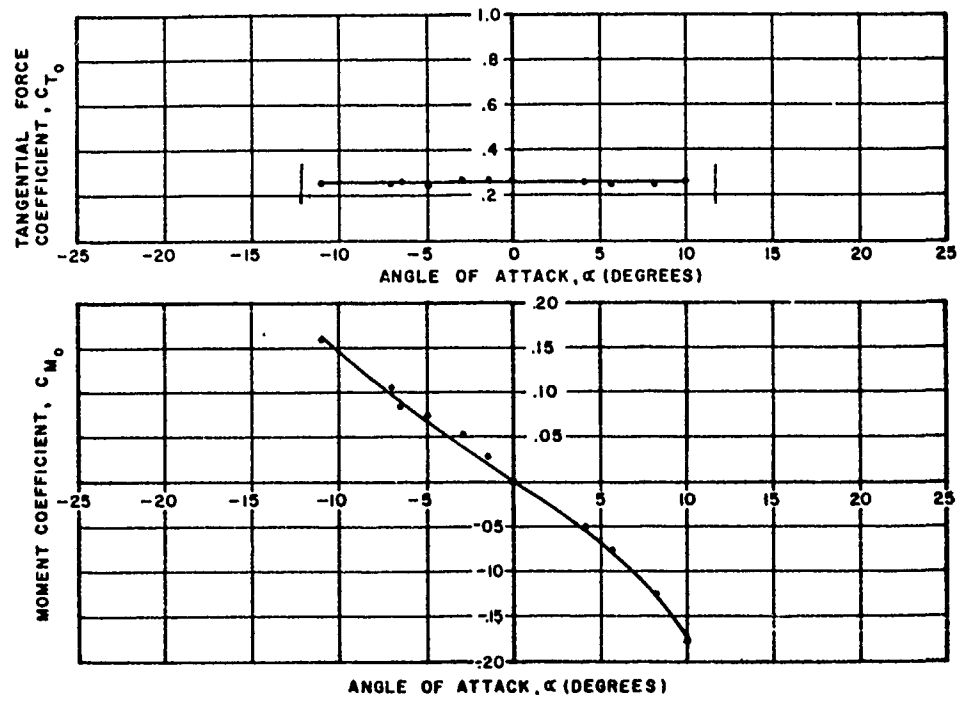


Figure 60. Variation of Tangential Force and Moment Coefficients with Angle-of-Attack: Canopy Type - Extended Skirt; Cluster - five; Reefing Ratio - 0.3; Riser Length - $1.0 D_O$

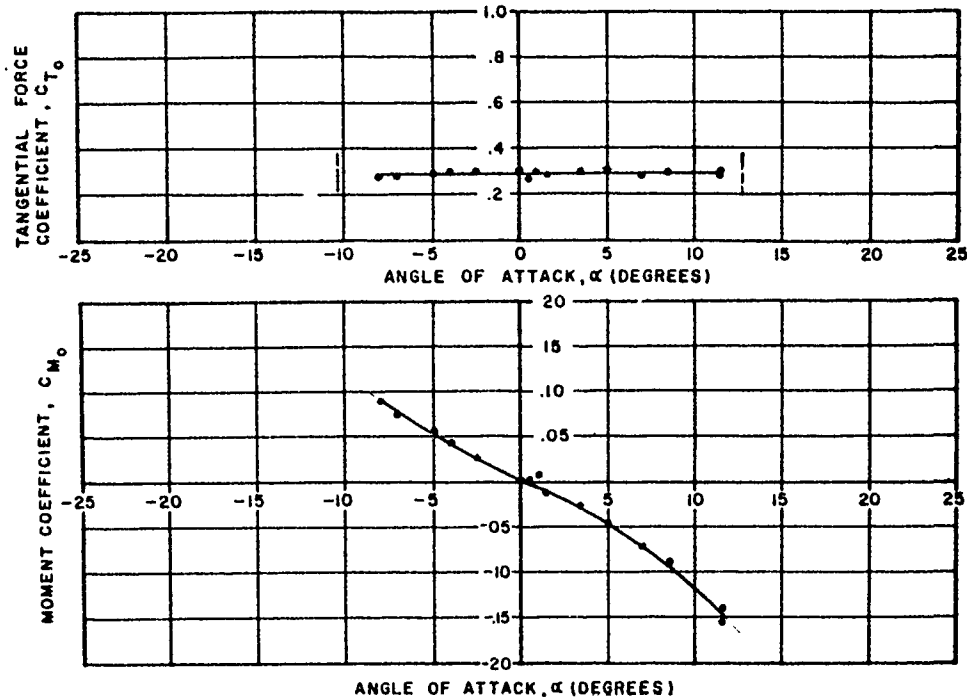


Figure 61. Variation of Tangential Force and Moment Coefficients with Angle-of-Attack: Canopy Type - Extended Skirt; Cluster - five; Reefing Ratio - 0.3; Riser Length - $0.5 D_O$

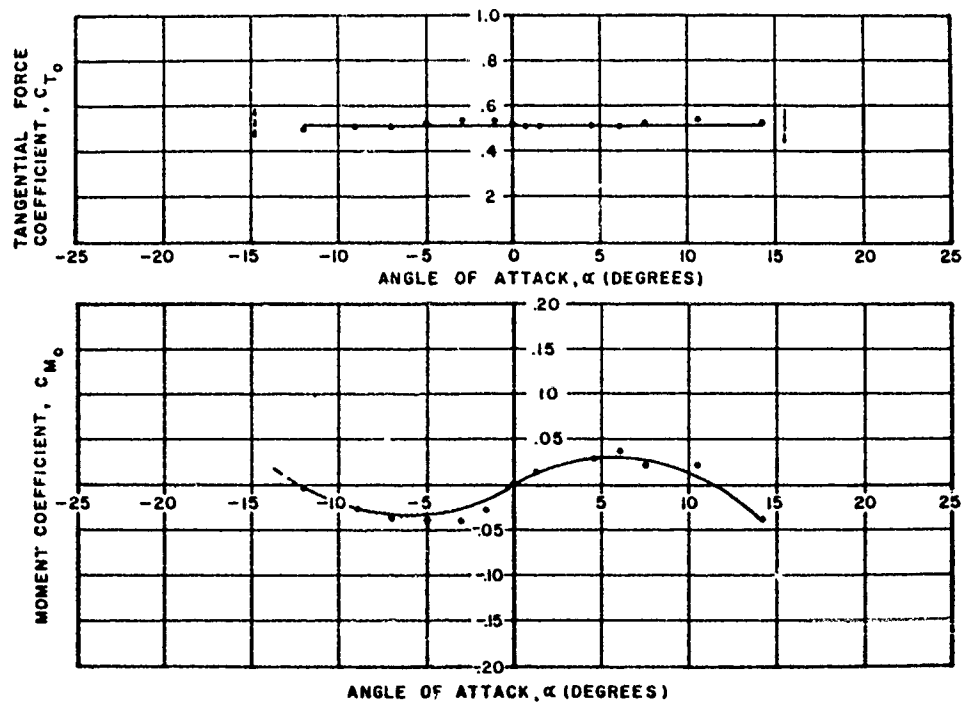


Figure 62. Variation of Tangential Force and Moment Coefficients with Angle-of-Attack: Canopy Type - Ribbon; Cluster - one; Reefing Ratio - none; Riser Length - 0 D_0

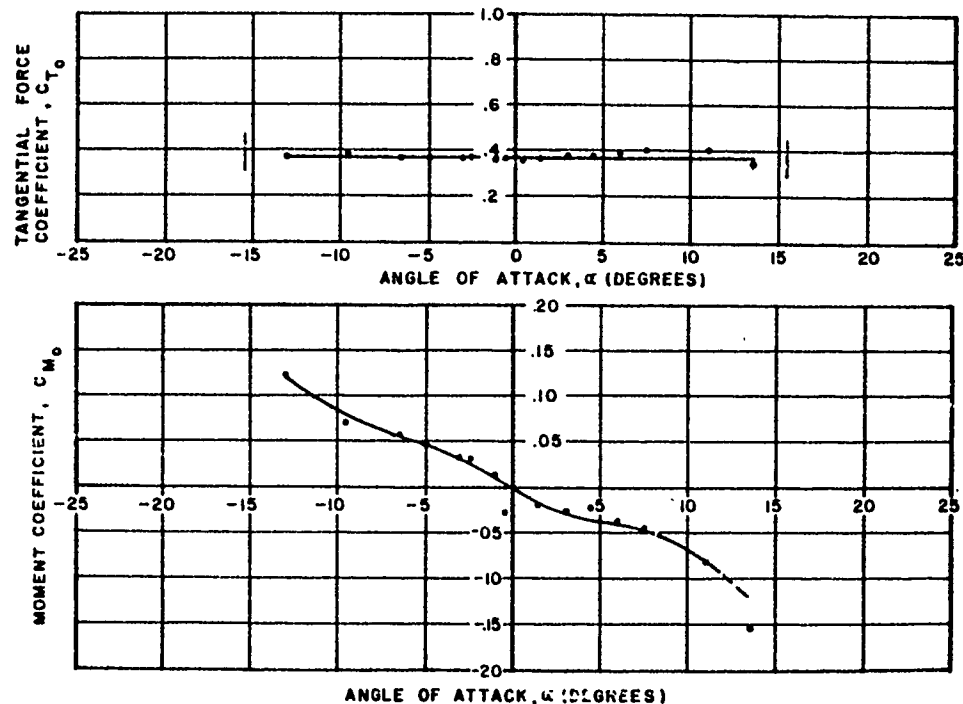


Figure 63. Variation of Tangential Force and Moment Coefficients with Angle-of-Attack: Canopy Type - Ribbon; Cluster - one; Reefing Ratio - 0.5; Riser Length - 0 D_0

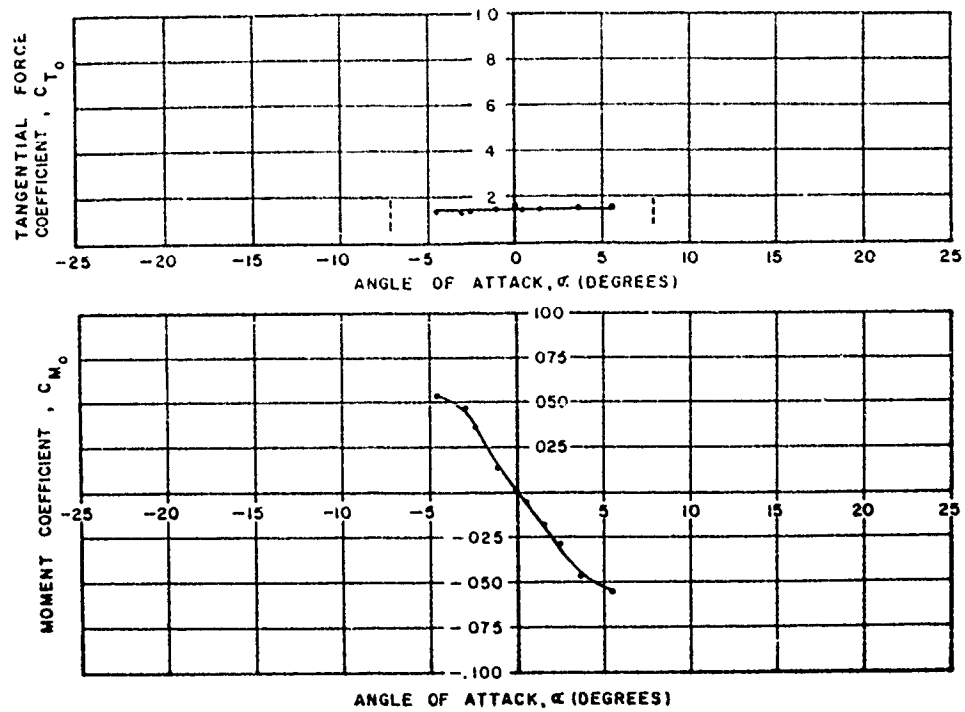


Figure 64. Variation of Tangential Force and Moment Coefficients with Angle-of-Attack: Canopy Type - Ribbon; Cluster - one; Reefing Ratio - 0.3; Riser Length - 0 D_0

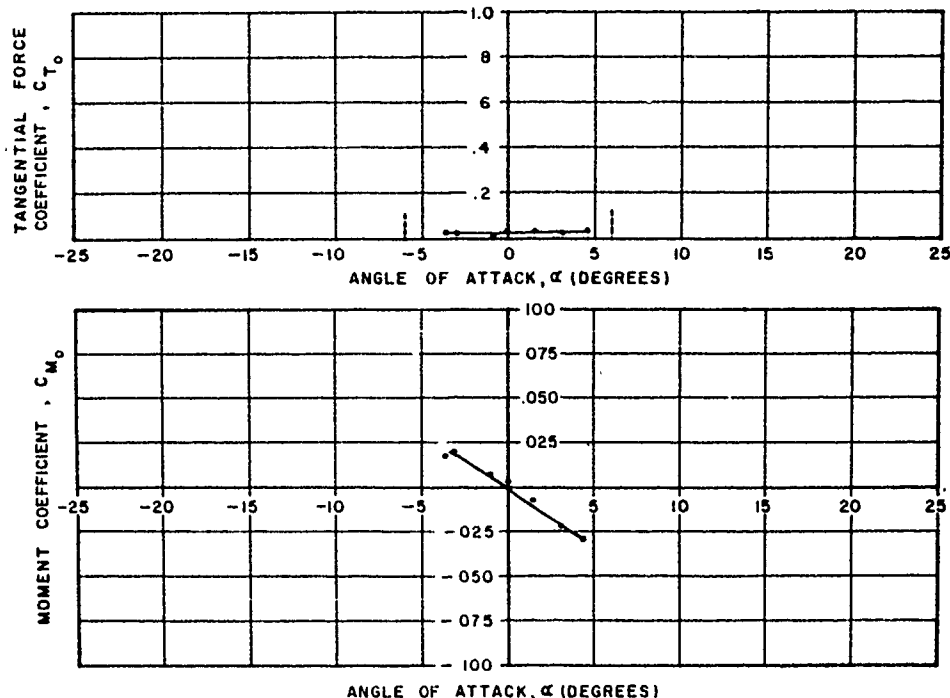


Figure 65. Variation of Tangential Force and Moment Coefficients with Angle-of-Attack: Canopy Type - Ribbon; Cluster - one; Reefing Ratio - 0.2; Riser Length - 0 D_0

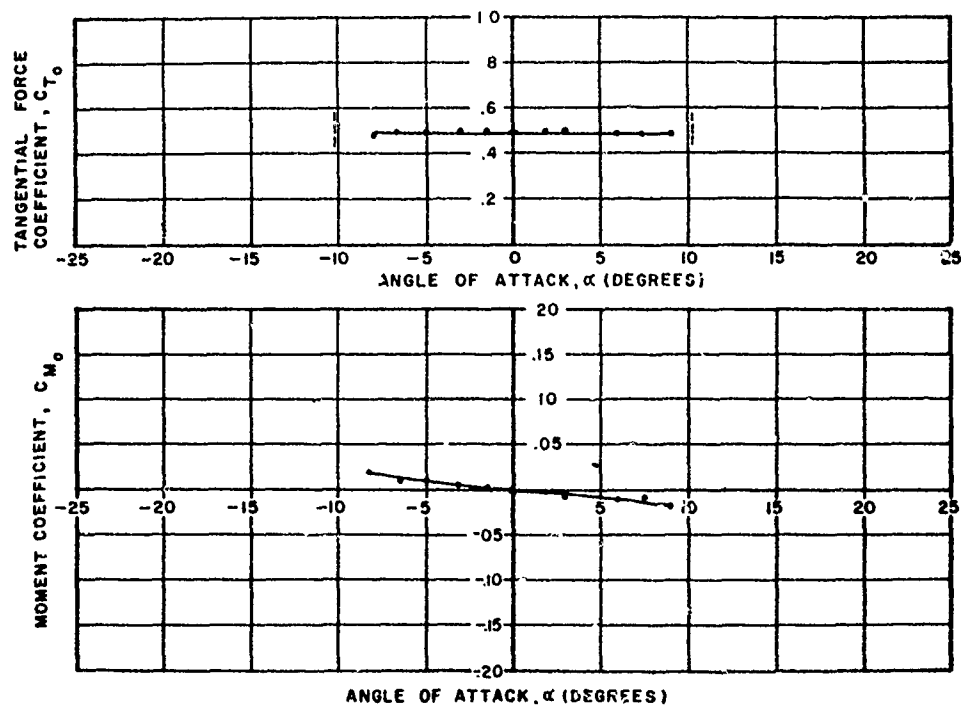


Figure 66. Variation of Tangential Force and Moment Coefficients with Angle-of-Attack: Canopy Type - Ribbon; Cluster - two; Reefing Ratio - none; Riser Length - $0.5 D_0$

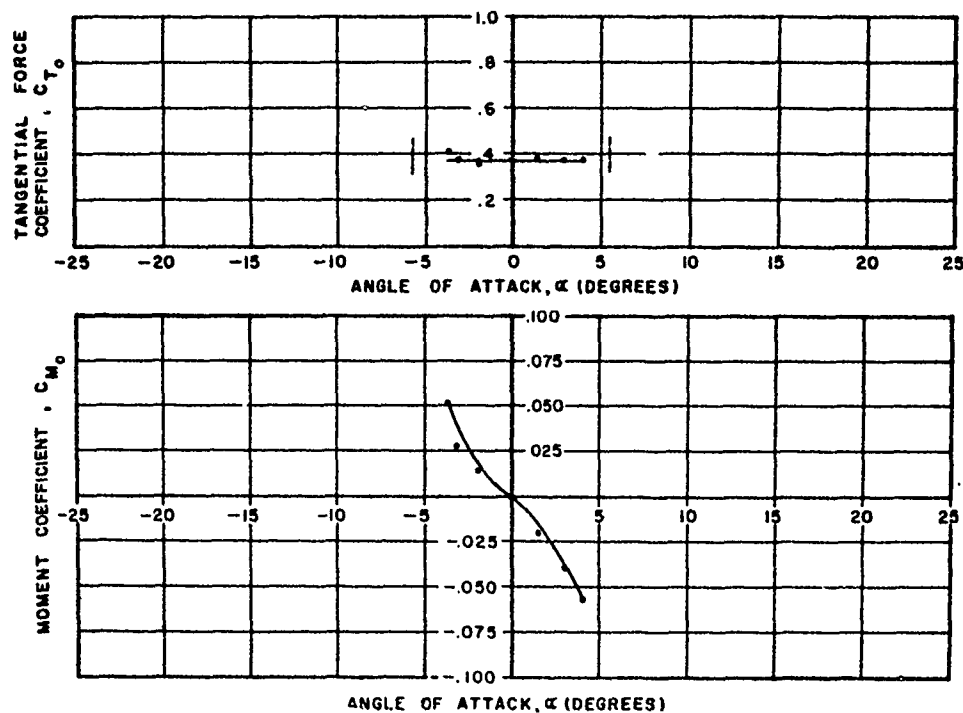


Figure 67. Variation of Tangential Force and Moment Coefficients with Angle-of-Attack: Canopy Type - Ribbon; Cluster - two; Reefing Ratio - 0.5; Riser Length - $0.5 D_0$

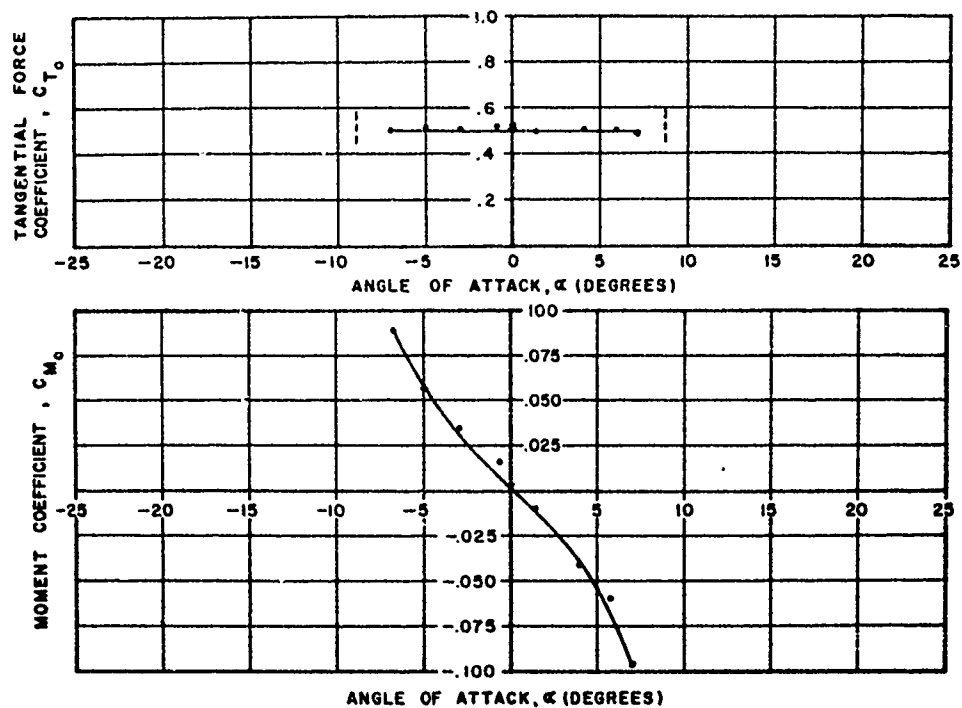


Figure 68. Variation of Tangential Force and Moment Coefficients with Angle-of-Attack: Canopy Type - Ribbon; Cluster - three; Reefing Ratio - none; Riser Length - $1.0 D_0$

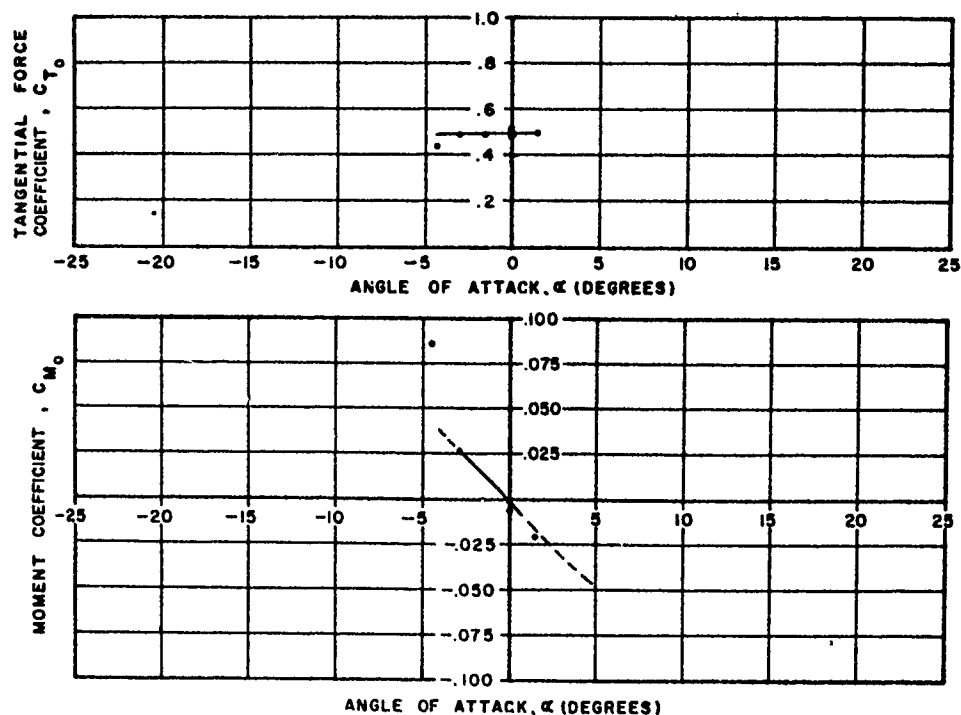


Figure 69. Variation of Tangential Force and Moment Coefficients with Angle-of-Attack: Canopy Type - Ribbon; Cluster - three; Reefing Ratio - none; Riser Length - $0.5 D_0$

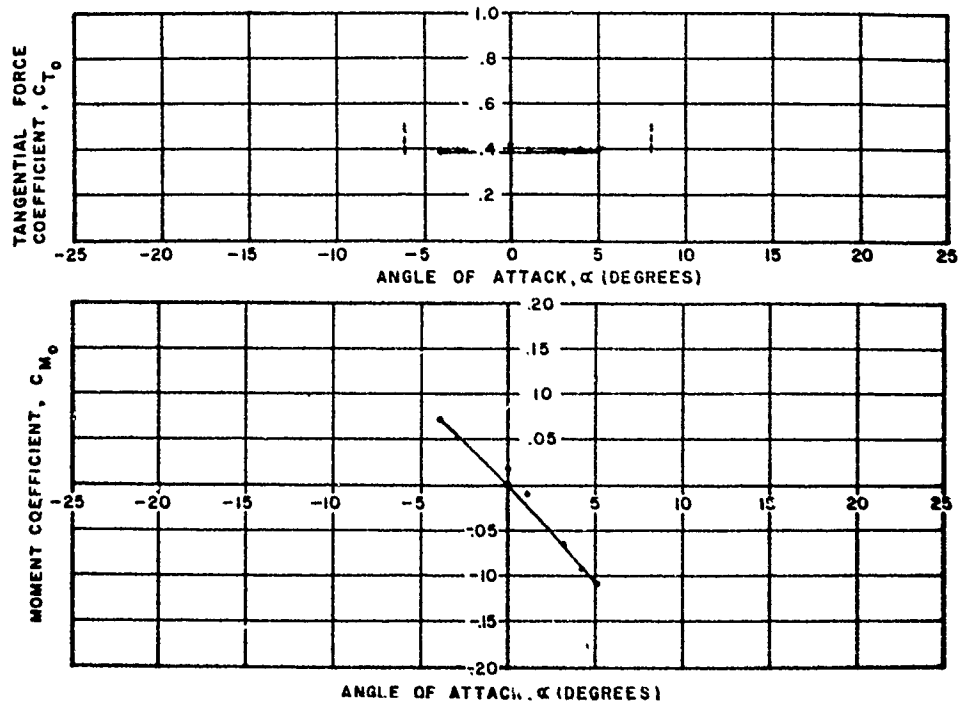


Figure 70. Variation of Tangential Force and Moment Coefficients with Angle-of-Attack: Canopy Type - Ribbon; Cluster - three; Reefing Ratio - 0.5; Riser Length - $1.0 D_0$

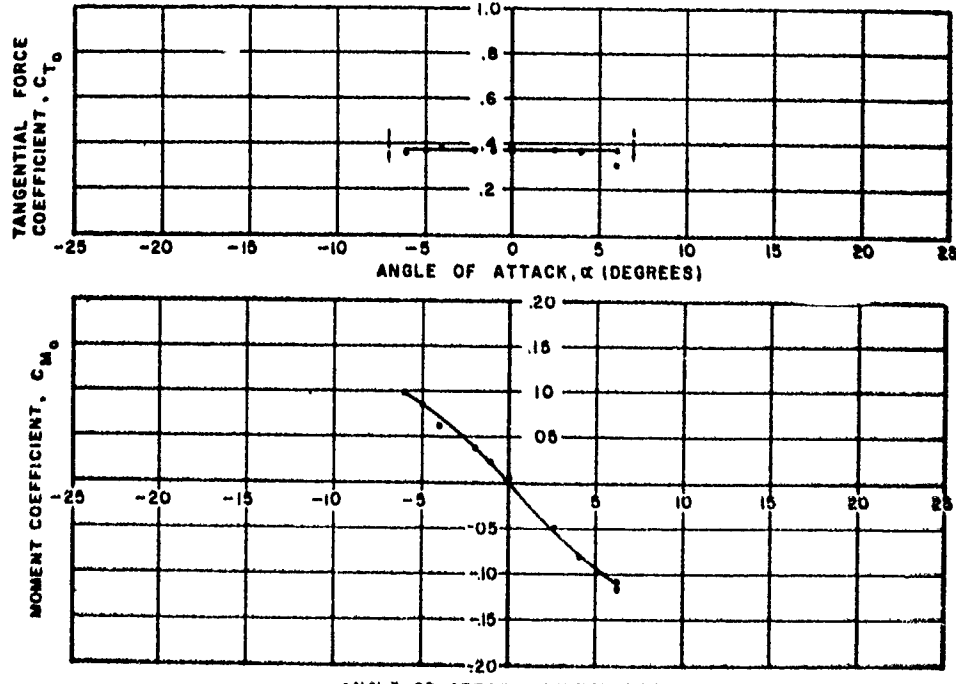


Figure 71. Variation of Tangential Force and Moment Coefficients with Angle-of-Attack: Canopy Type - Ribbon; Cluster - three; Reefing Ratio - 0.5; Riser Length - $0.5 D_0$

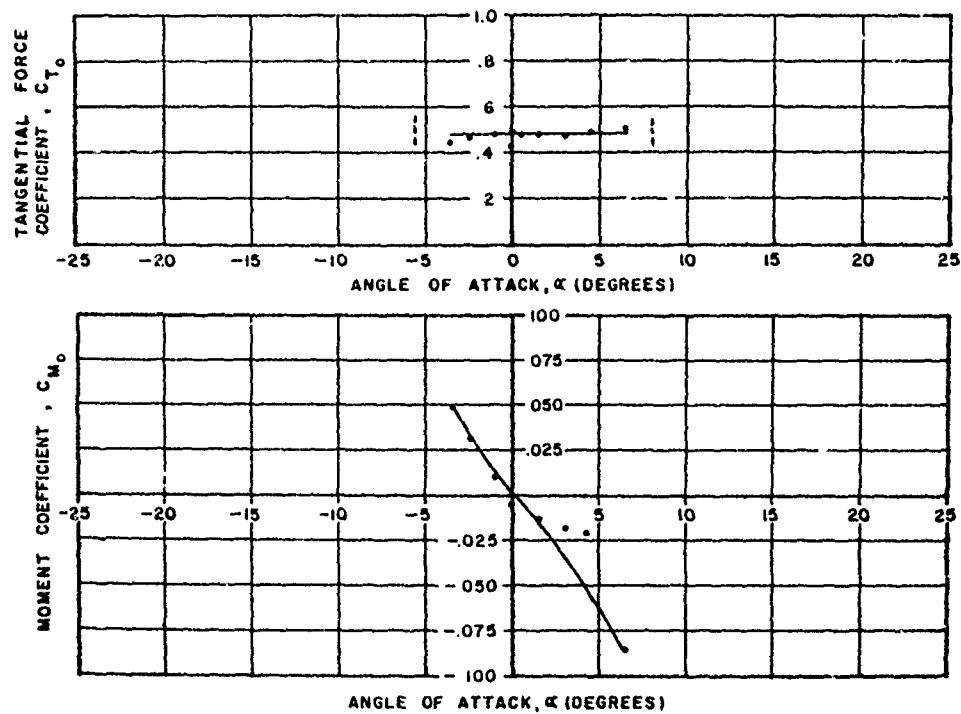


Figure 72. Variation of Tangential Force and Moment Coefficients with Angle-of-Attack: Canopy Type - Ribbon; Cluster - five; Reefing Ratio - none; Riser Length - $1.5 D_0$

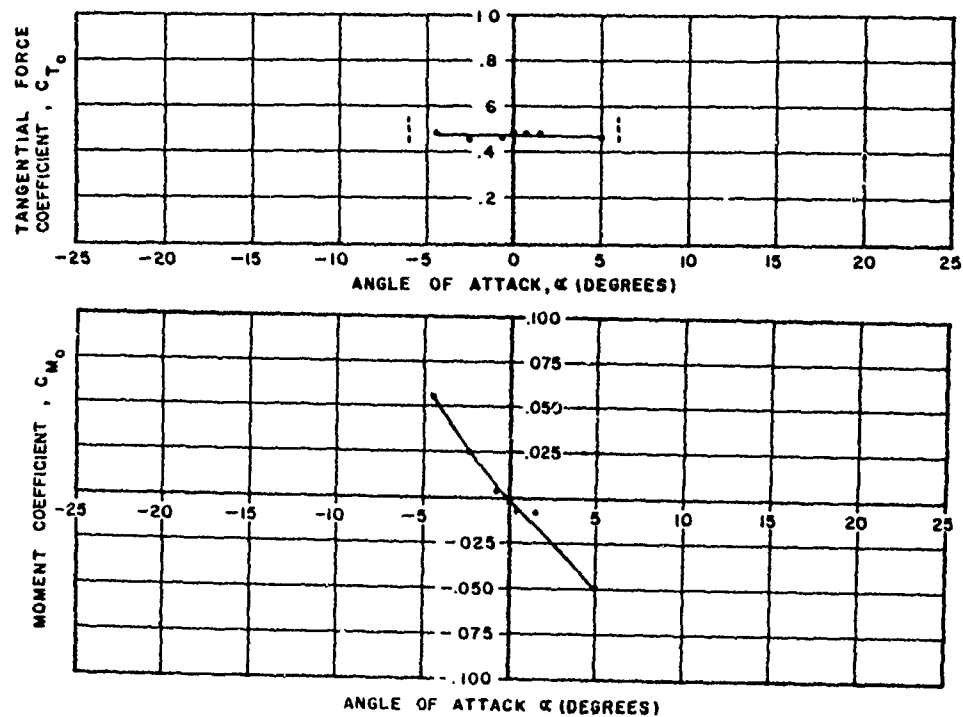


Figure 73. Variation of Tangential Force and Moment Coefficients with Angle-of-Attack: Canopy Type - Ribbon; Cluster - five; Reefing Ratio - none; Riser Length - $1.0 D_0$

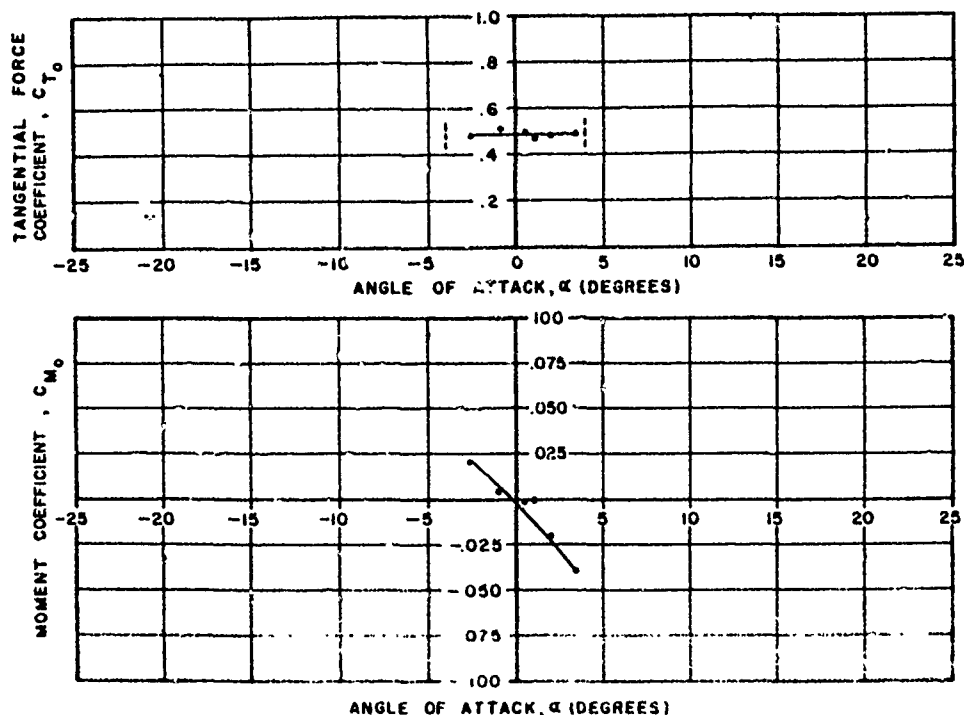


Figure 74. Variation of Tangential Force and Moment Coefficients with Angle-of-Attack: Canopy Type - Ribbon; Cluster - five; Reefing Ratio - none; Riser Length - $0.5 D_0$

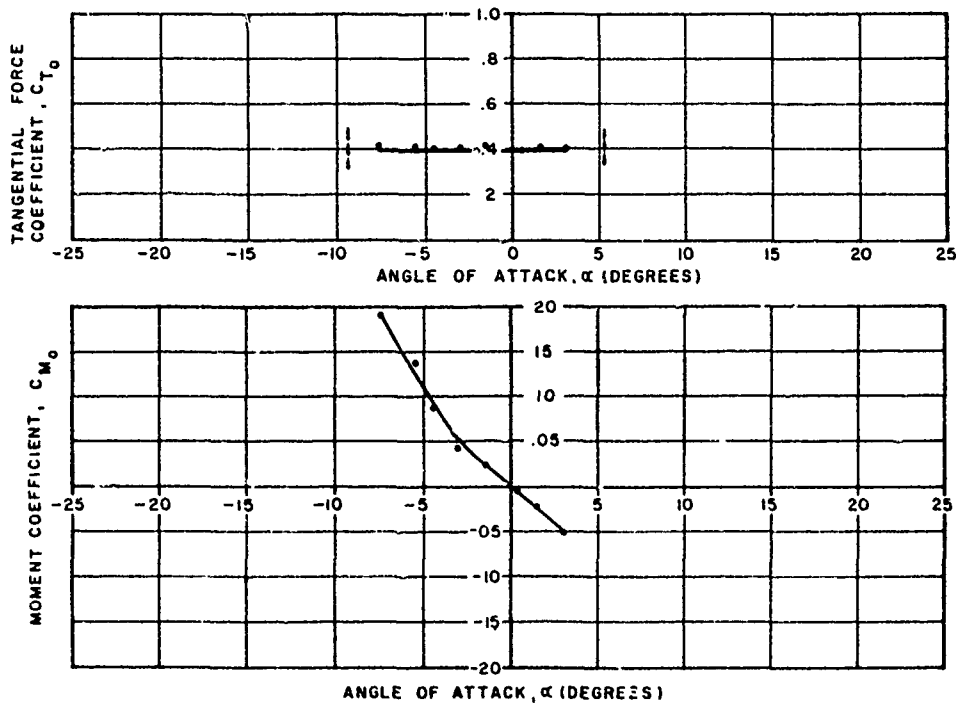


Figure 75. Variation of Tangential Force and Moment Coefficients with Angle-of-Attack: Canopy Type - Ribbon; Cluster - five; Reefing Ratio - 0.5; Riser Length - $1.5 D_0$

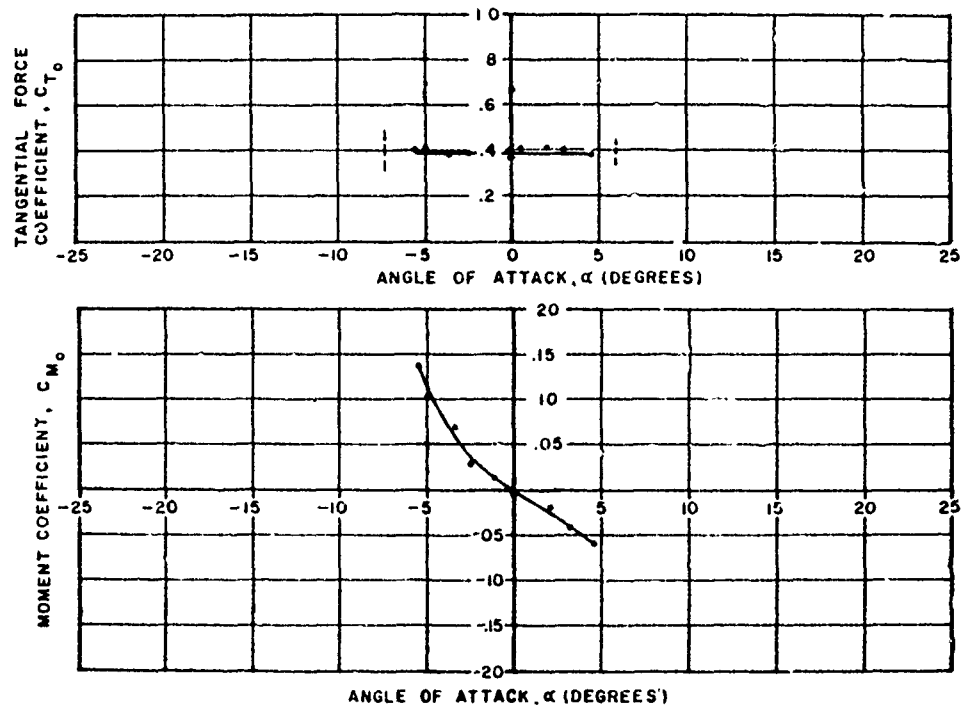


Figure 76. Variation of Tangential Force and Moment Coefficients with Angle-of-Attack: Canopy Type - Ribbon; Cluster - five; Reefing Ratio - 0.5; Riser Length - $1.0 D_0$

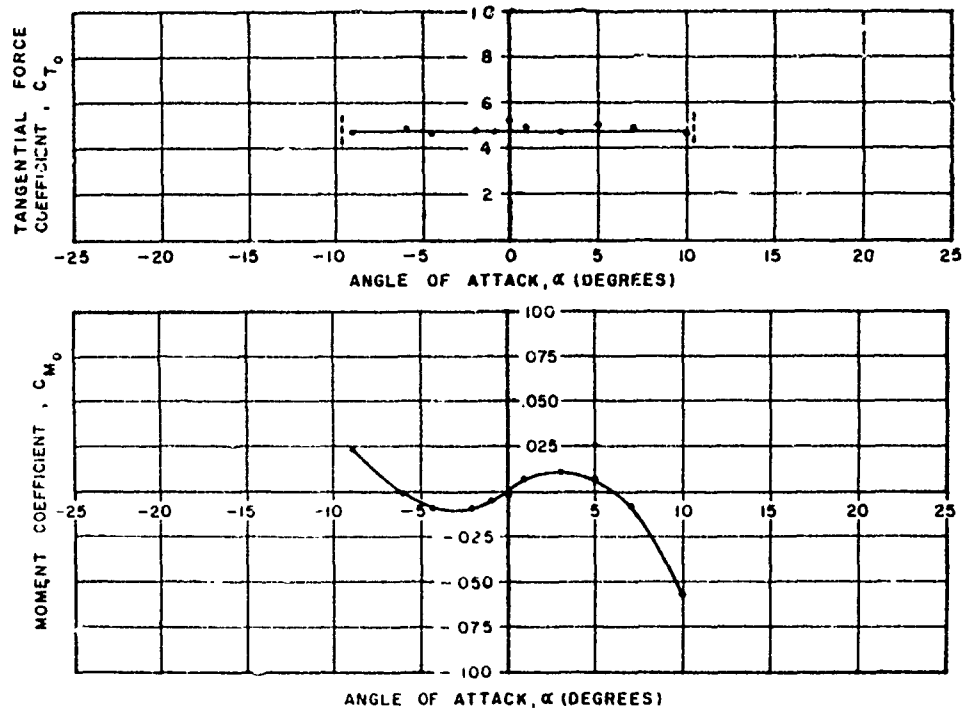


Figure 77. Variation of Tangential Force and Moment Coefficients with Angle-of-Attack: Canopy Type - Ringslot; Cluster - one; Reefing Ratio - none; Riser Length - $0 D_0$

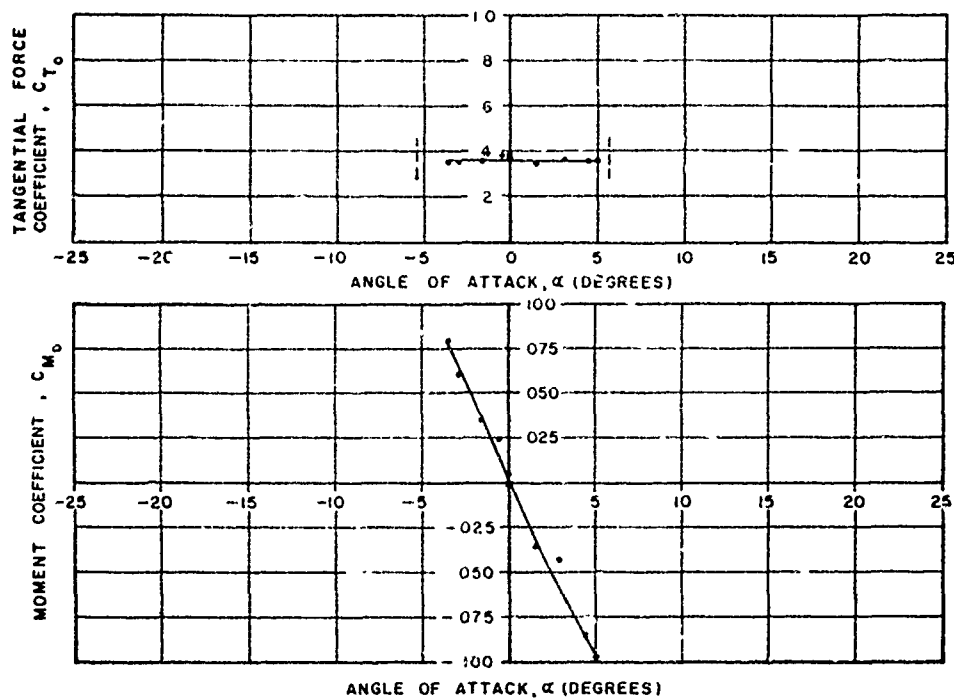


Figure 78. Variation of Tangential Force and Moment Coefficients with Angle-of-Attack: Canopy Type - Ringslot; Cluster - one; Reefing Ratio - 0.5; Riser Length - 0 D_0

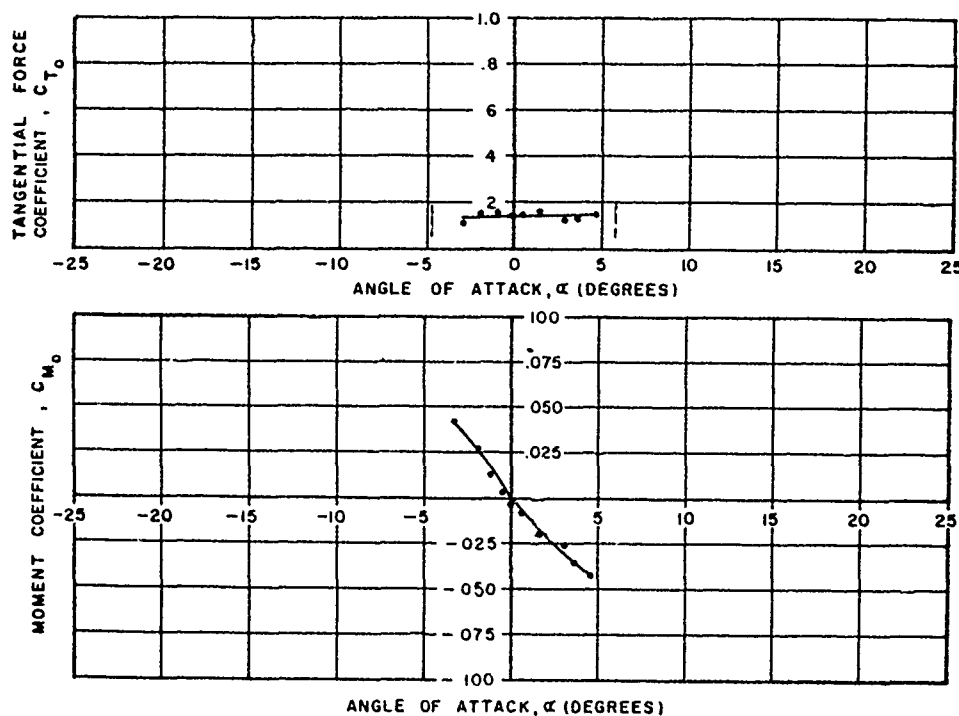


Figure 79. Variation of Tangential Force and Moment Coefficients with Angle-of-Attack: Canopy Type - Ringslot; Cluster - one; Reefing Ratio - 0.3; Riser Length - 0 D_0

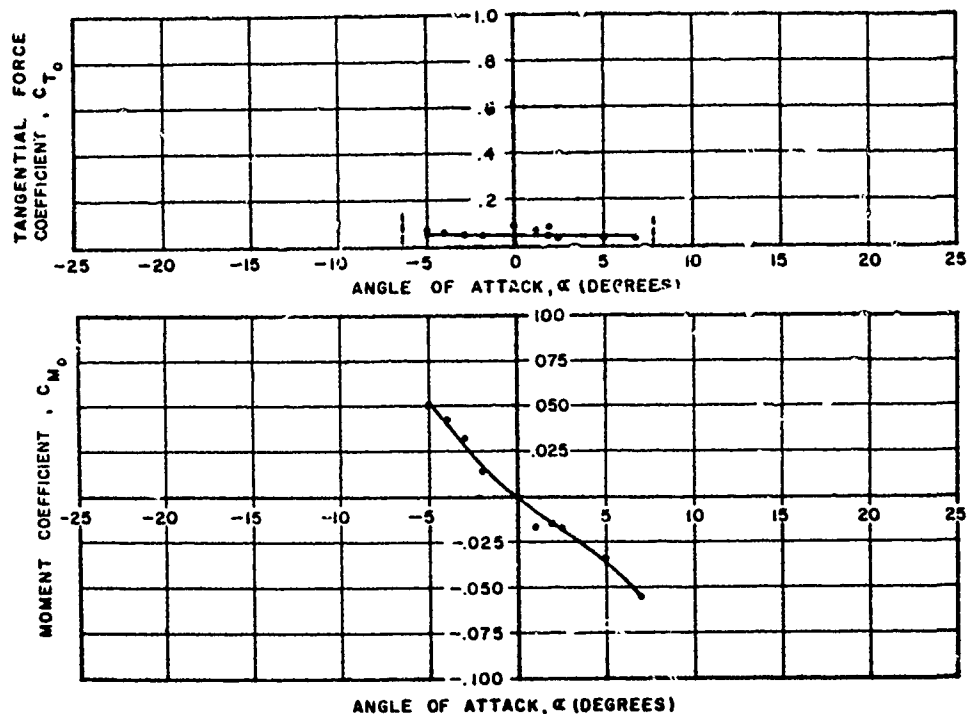


Figure 80. Variation of Tangential Force and Moment Coefficients with Angle-of-Attack: Canopy Type - Ringslot; Cluster - one; Reefing Ratio - 0.2; Riser Length - $0 D_0$

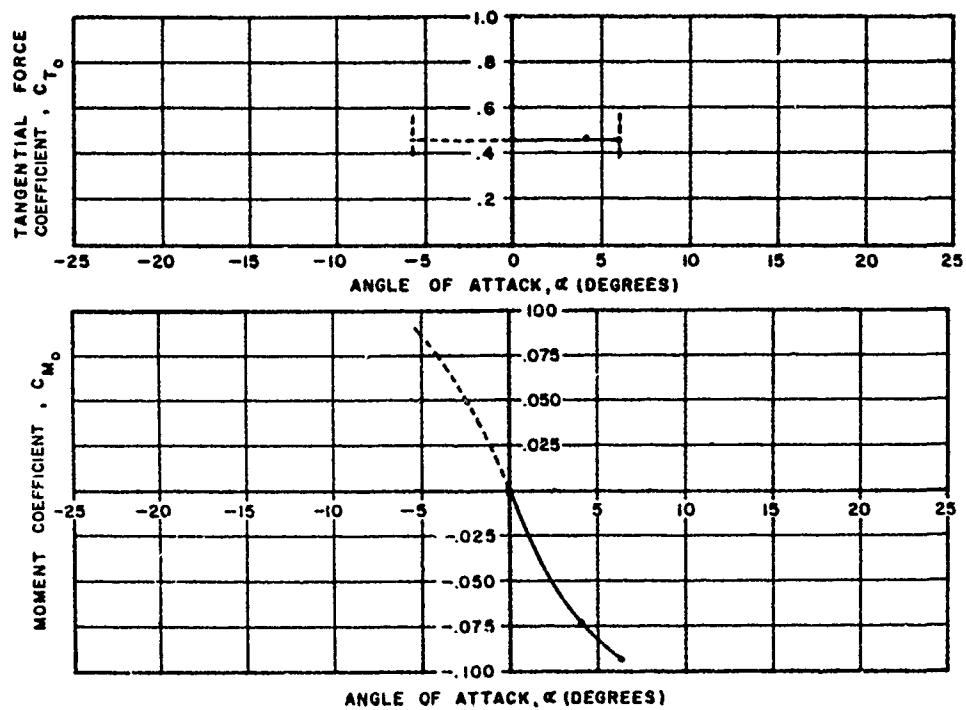


Figure 81. Variation of Tangential Force and Moment Coefficients with Angle-of-Attack: Canopy Type - Ringslot; Cluster - two; Reefing Ratio - none; Riser Length - $0.5 D_0$

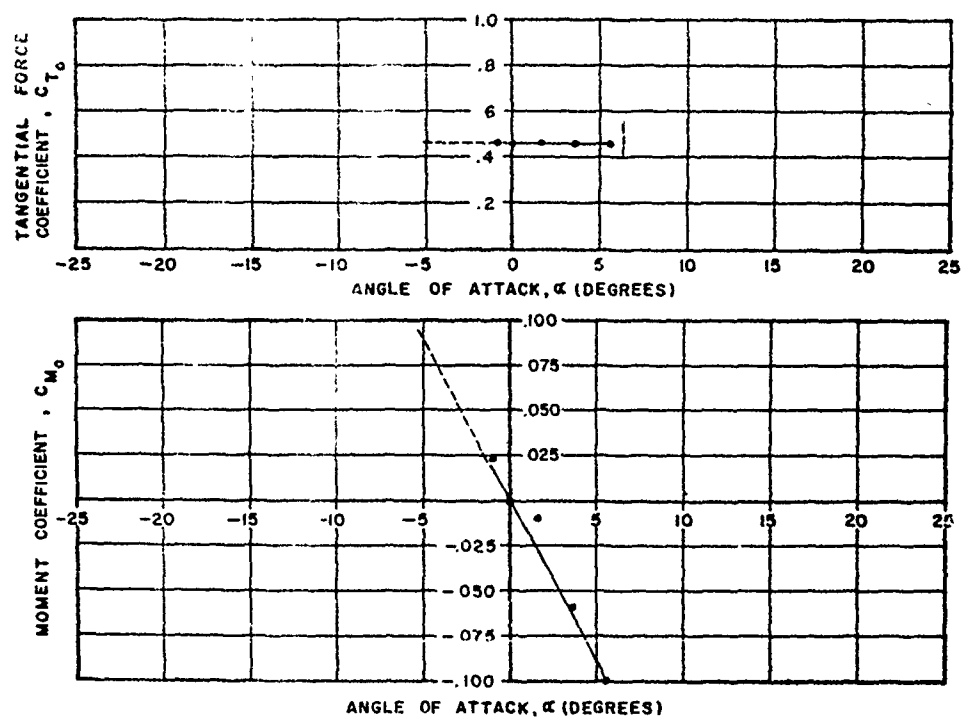


Figure 82. Variation of Tangential Force and Moment Coefficients with Angle-of-Attack: Canopy Type - Ringslot; Cluster - three; Reefing Ratio - none; Riser Length - $1.0 D_0$

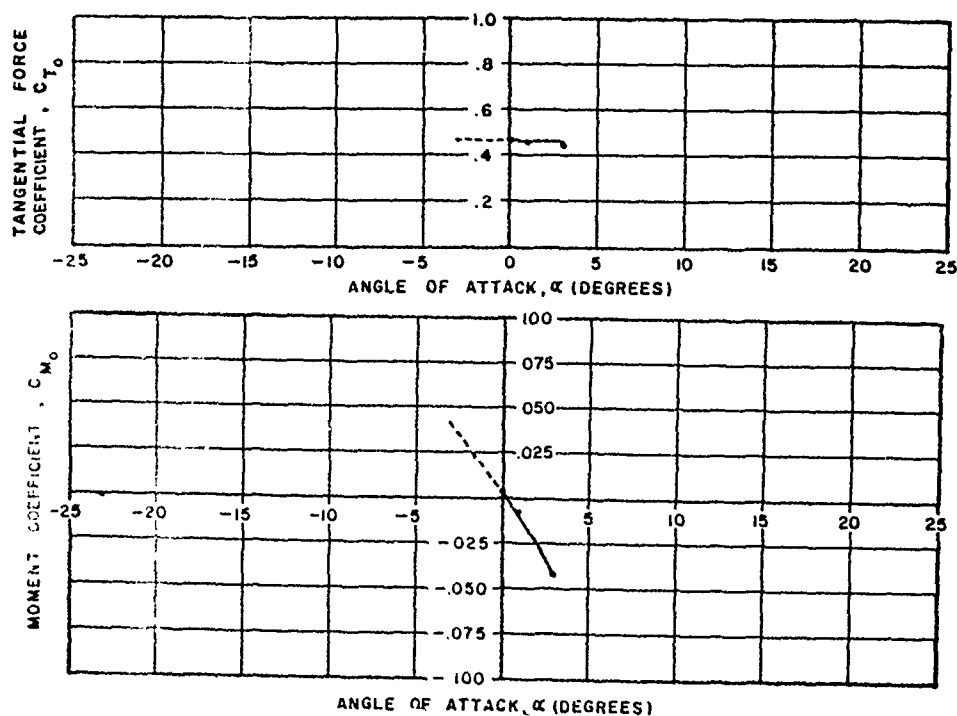


Figure 83. Variation of Tangential Force and Moment Coefficients with Angle-of-Attack: Canopy Type - Ringslot; Cluster - three; Reefing Ratio - none; Riser Length - $0.5 D_0$

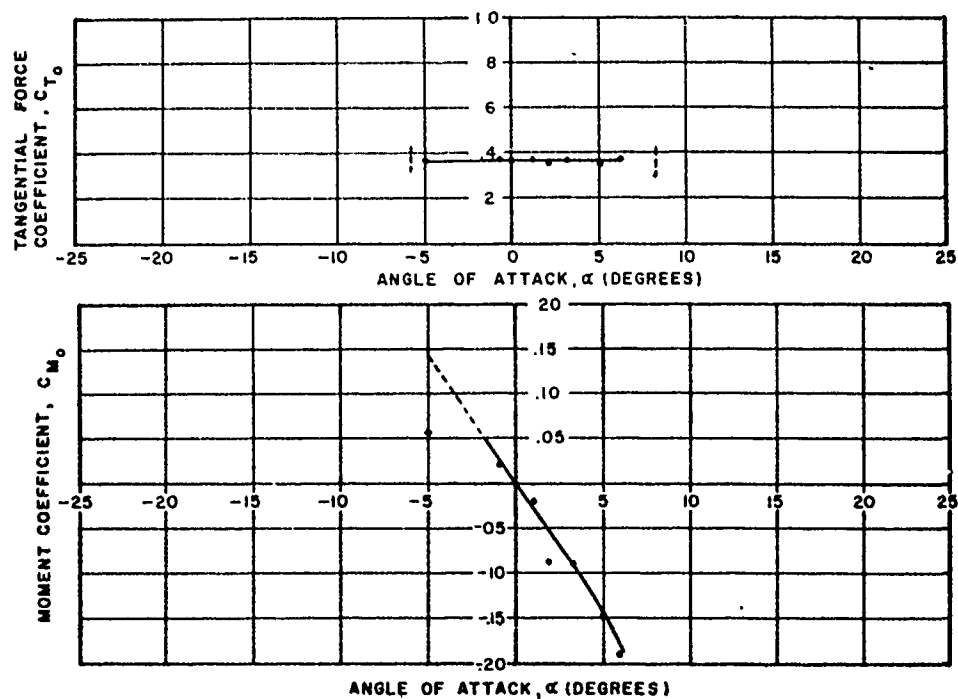


Figure 84. Variation of Tangential Force and Moment Coefficients with Angle-of-Attack: Canopy Type - Ringslot; Cluster - three Reefing Ratio - 0.5; Riser Length - 1.0 D_0

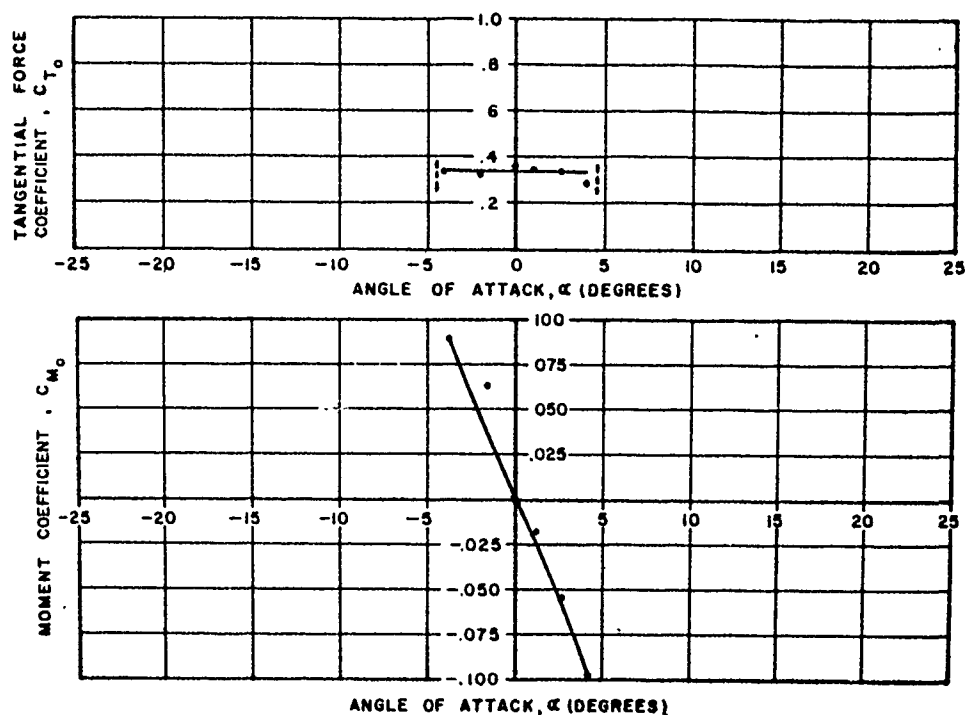


Figure 85. Variation of Tangential Force and Moment Coefficients with Angle-of-Attack: Canopy Type - Ringslot; Cluster - three; Reefing Ratio - 0.5; Riser Length - 0.5 D_0

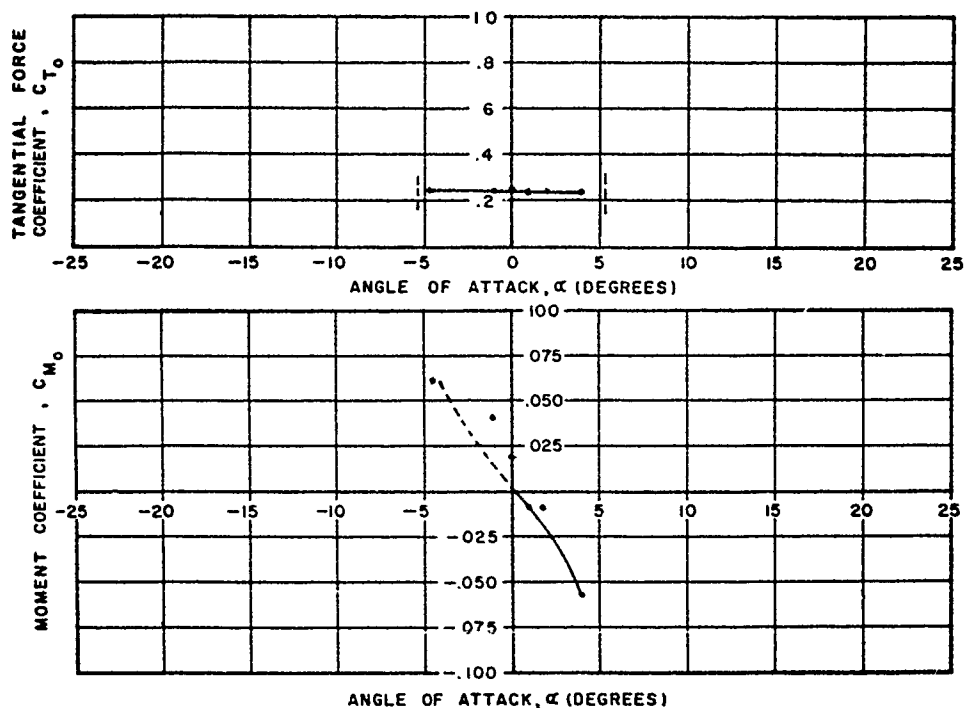


Figure 86. Variation of Tangential Force and Moment Coefficients with Angle-of-Attack: Canopy Type - Ringslot; Cluster - three; Reefing Ratio - 0.3; Riser Length - 1.0 D_0

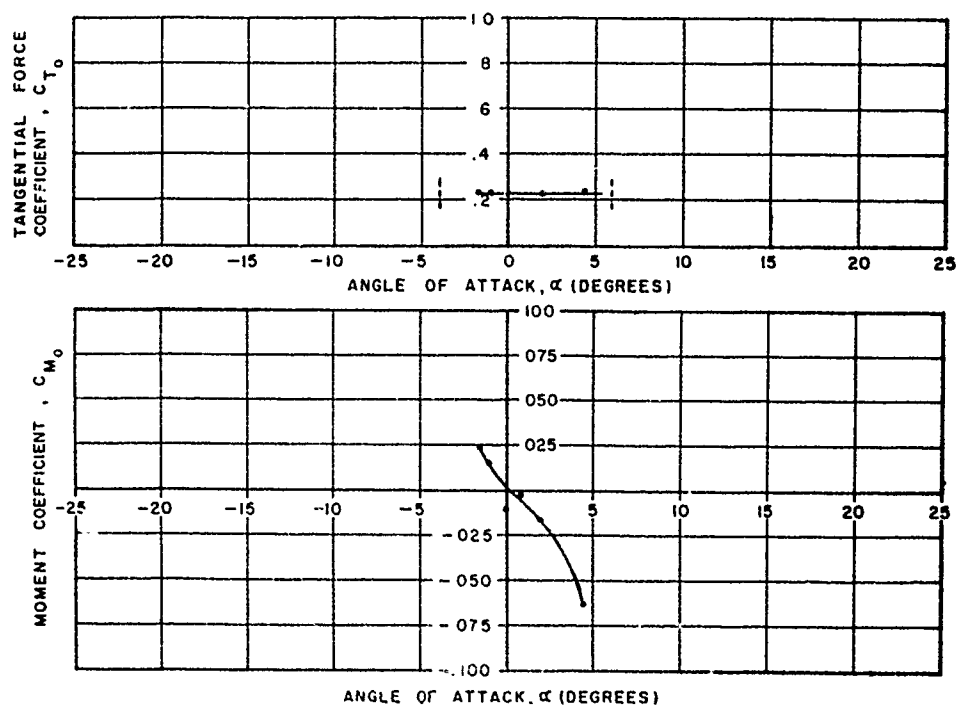


Figure 87. Variation of Tangential Force and Moment Coefficients with Angle-of-Attack: Canopy Type - Ringslot; Cluster - three; Reefing Ratio - 0.3; Riser Length - 0.5 D_0

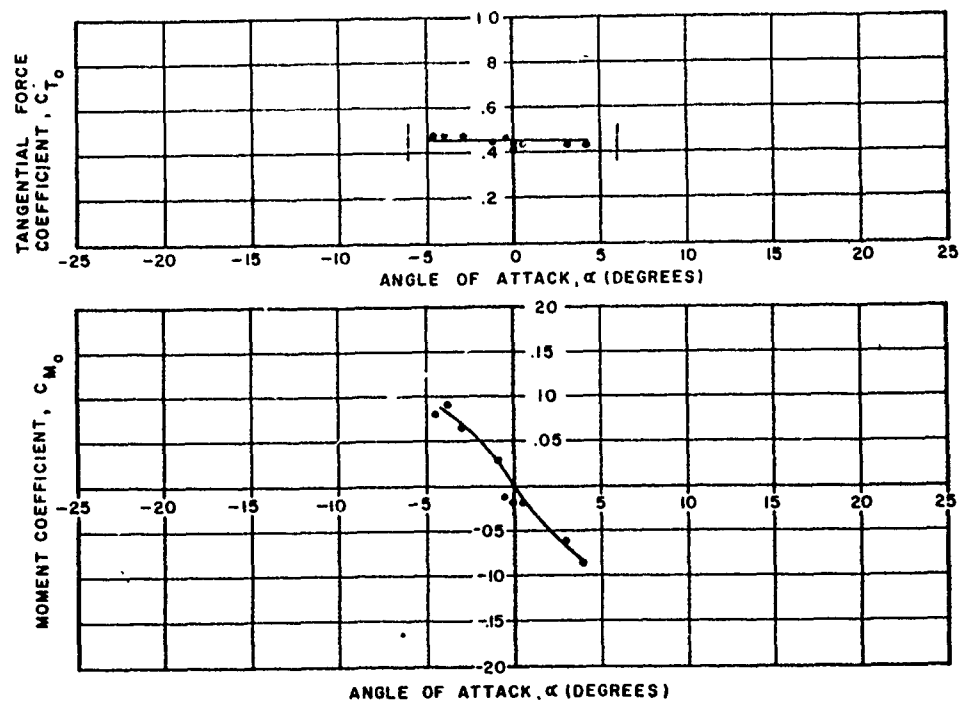


Figure 88. Variation of Tangential Force and Moment Coefficients with Angle-of-Attack: Canopy Type - Ringslot; Cluster - five; Reefing Ratio - none; Riser Length - $1.5 D_0$

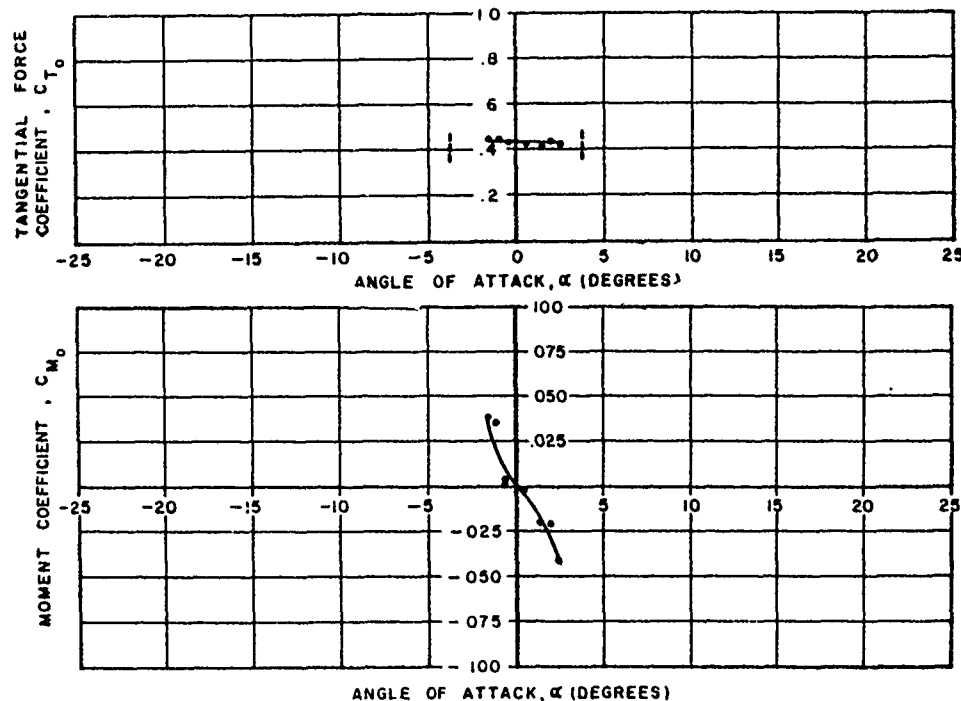


Figure 89. Variation of Tangential Force and Moment Coefficients with Angle-of-Attack: Canopy Type - Ringslot; Cluster - five; Reefing Ratio - none; Riser Length - $1.0 D_0$

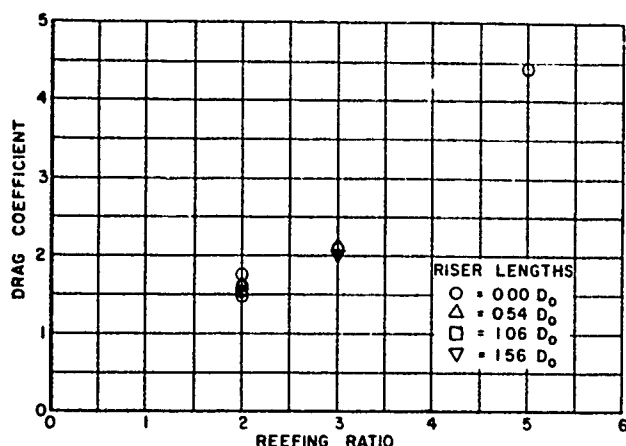


Figure 90. Variation of Drag Coefficient with Reefing Ratio and Riser Length, Equilibrium Test: Canopy Type - Flat Circular; No. of Canopies in a Cluster - one

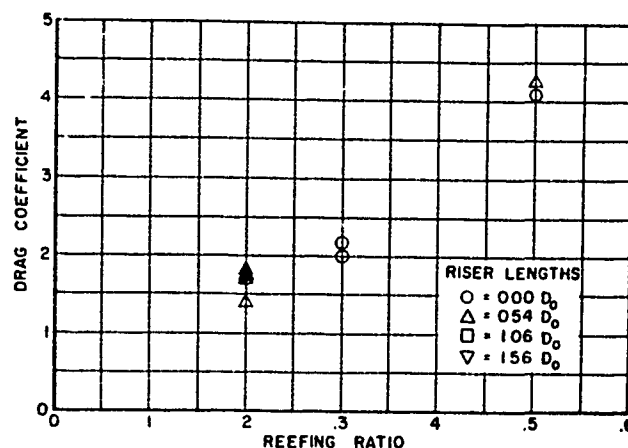


Figure 91. Variation of Drag Coefficient with Reefing Ratio and Riser Length, Equilibrium Test: Canopy Type - Flat Circular; No. of Canopies in a Cluster - two

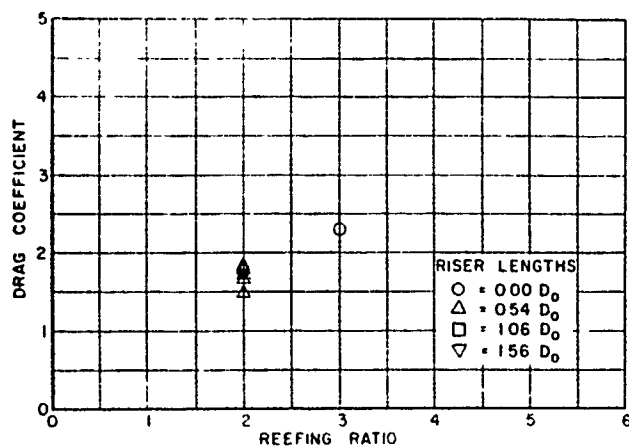


Figure 92. Variation of Drag Coefficient with Reefing Ratio and Riser Length, Equilibrium Test: Canopy Type - Flat Circular; No. of Canopies in a Cluster - three

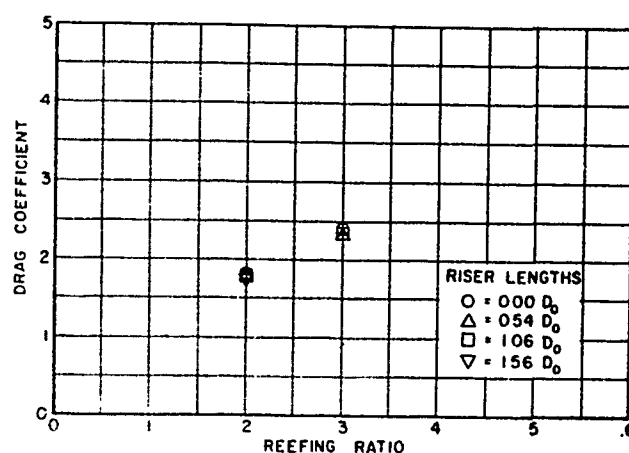


Figure 93. Variation of Drag Coefficient with Reefing Ratio and Riser Length, Equilibrium Test: Canopy Type - Flat Circular; No. of Canopies in a Cluster - four

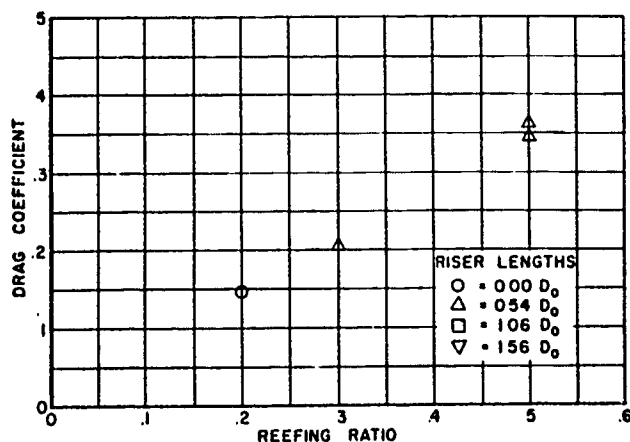


Figure 94. Variation of Drag Coefficient with Reefing Ratio and Riser Length, Equilibrium Test: Canopy Type - Extended Skirt; No of Canopies in a Cluster - one

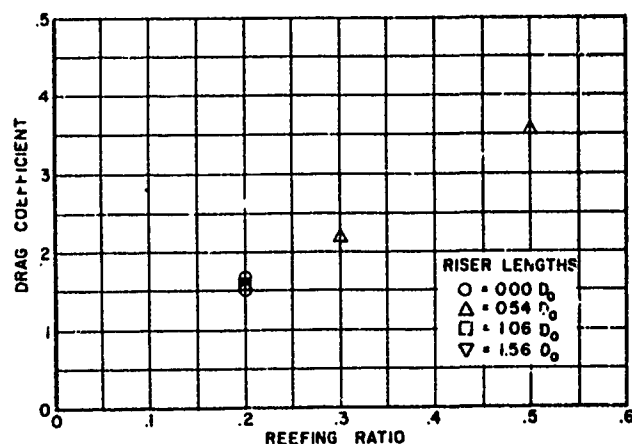


Figure 95. Variation of Drag Coefficient with Reefing Ratio and Riser Length, Equilibrium Test: Canopy Type - Extended Skirt; No. of Canopies in a Cluster - two

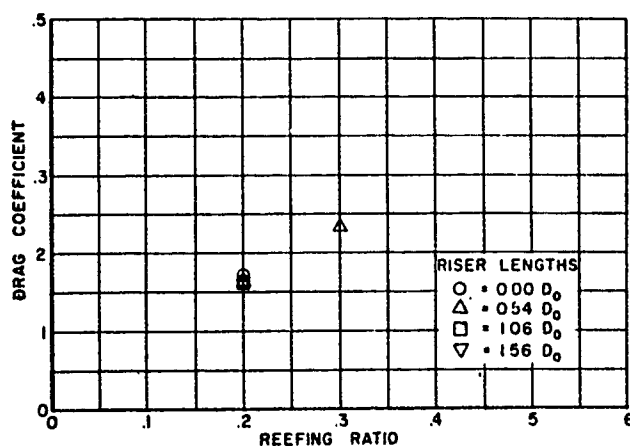


Figure 96. Variation of Drag Coefficient with Reefing Ratio and Riser Length, Equilibrium Test: Canopy Type - Extended Skirt; No. of Canopies in a Cluster - three

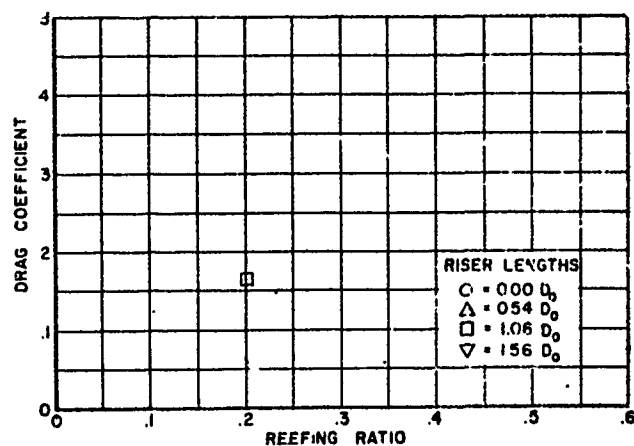


Figure 97. Variation of Drag Coefficient with Reefing Ratio and Riser Length, Equilibrium Test: Canopy Type - Extended Skirt; No. of Canopies in a Cluster - four

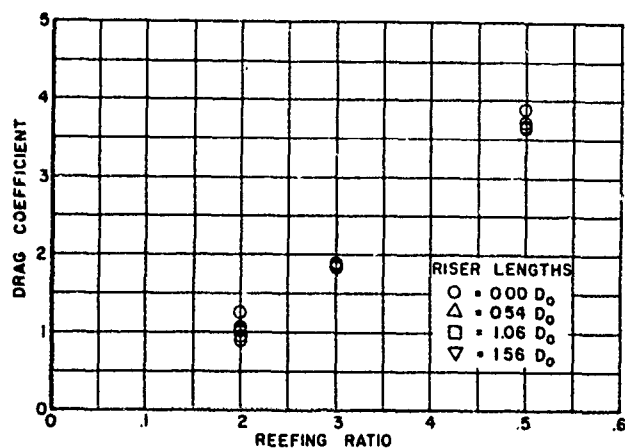


Figure 98. Variation of Drag Coefficient with Reefing Ratio and Riser Length, Equilibrium Test: Canopy Type - Ribbon; No. of Canopies in a Cluster - one

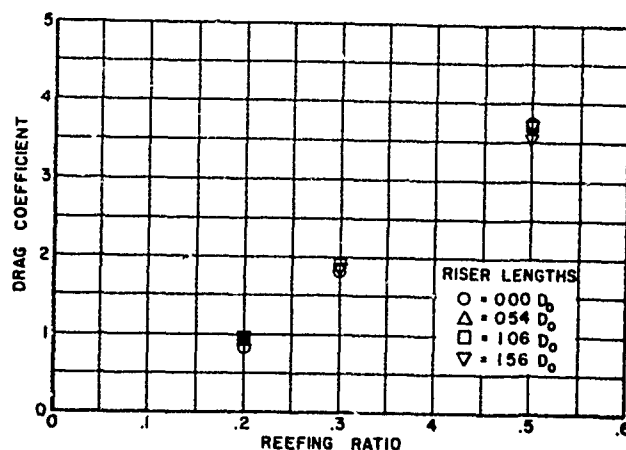


Figure 99. Variation of Drag Coefficient with Reefing Ratio and Riser Length, Equilibrium Test: Canopy Type - Ribbon; No. of Canopies in a Cluster - two

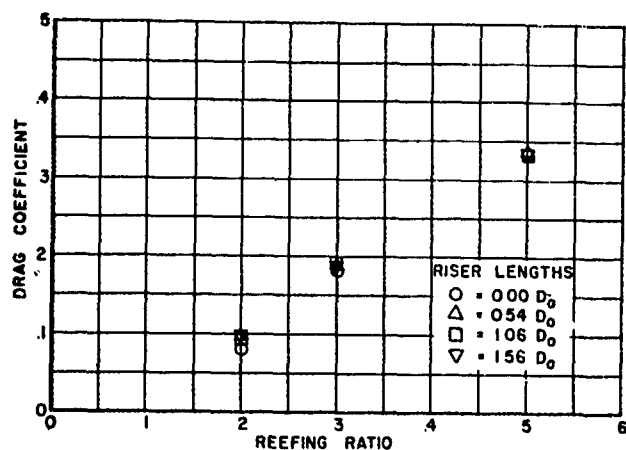


Figure 100. Variation of Drag Coefficient with Reefing Ratio and Riser Length, Equilibrium Test: Canopy Type - Ribbon; No. of Canopies in a Cluster - three

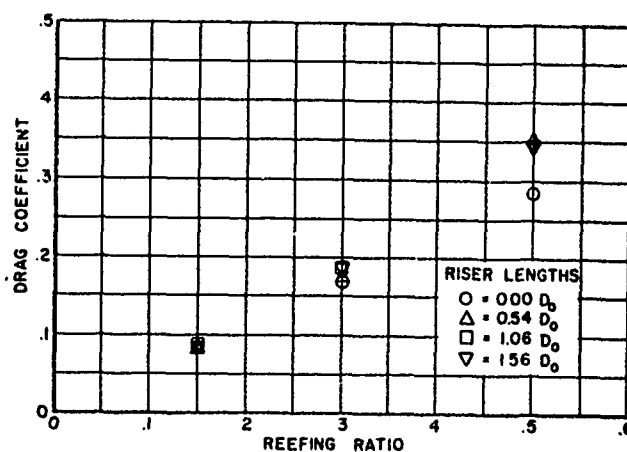


Figure 101. Variation of Drag Coefficient with Reefing Ratio and Riser Length, Equilibrium Test: Canopy Type - Ribbon; No. of Canopies in a Cluster - four

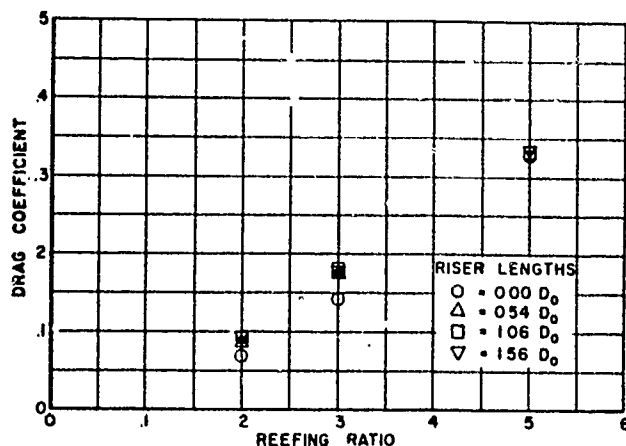


Figure 102. Variation of Drag Coefficient with Reefing Ratio and Riser Length, Equilibrium Test: Canopy Type - Ribbon; No. of Canopies in a Cluster - five

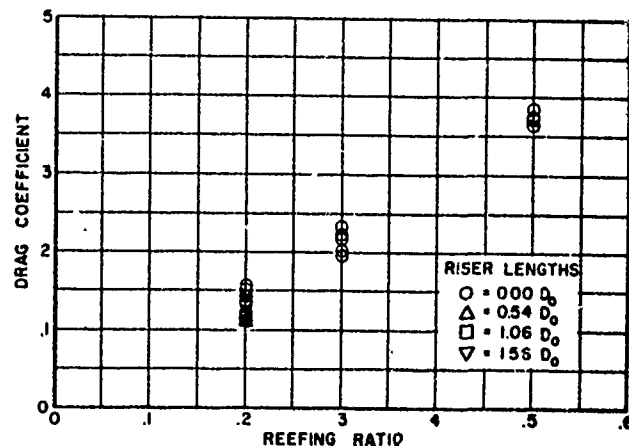


Figure 103. Variation of Drag Coefficient with Reefing Ratio and Riser Length, Equilibrium Test: Canopy Type - Ringslot; No. of Canopies in a Cluster - one

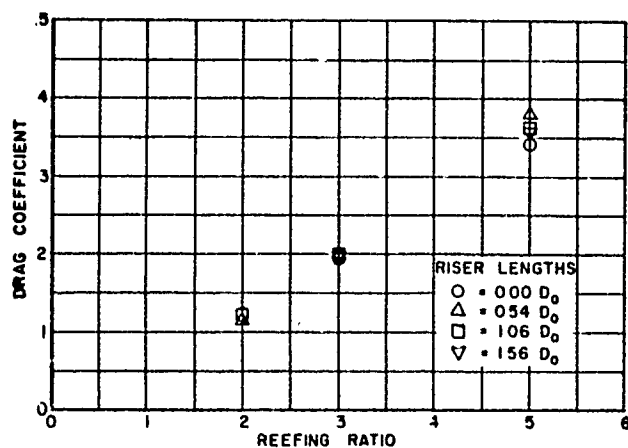


Figure 104. Variation of Drag Coefficient with Reefing Ratio and Riser Length, Equilibrium Test: Canopy Type - Ringslot; No. of Canopies in a Cluster - two

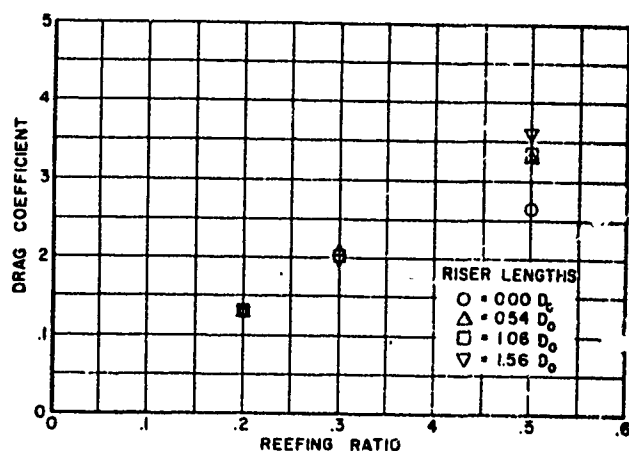


Figure 105. Variation of Drag Coefficient with Reefing Ratio and Riser Length, Equilibrium Test: Canopy Type - Ringslot; No. of Canopies in a Cluster - three

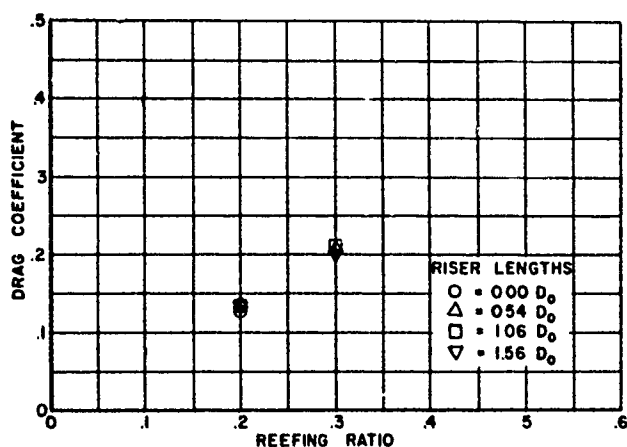


Figure 106. Variation of Drag Coefficient with Reefing Ratio and Riser Length, Equilibrium Test: Canopy Type - Ringslot; No. of Canopies in a Cluster - four

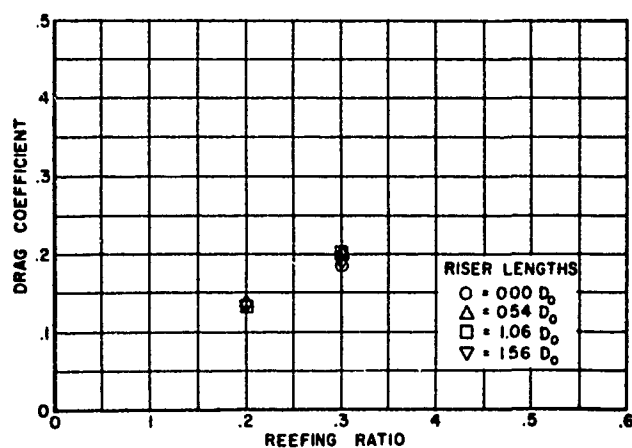


Figure 107. Variation of Drag Coefficient with Reefing Ratio and Riser Length, Equilibrium Test: Canopy Type - Ringslot; No. of Canopies in a Cluster - five

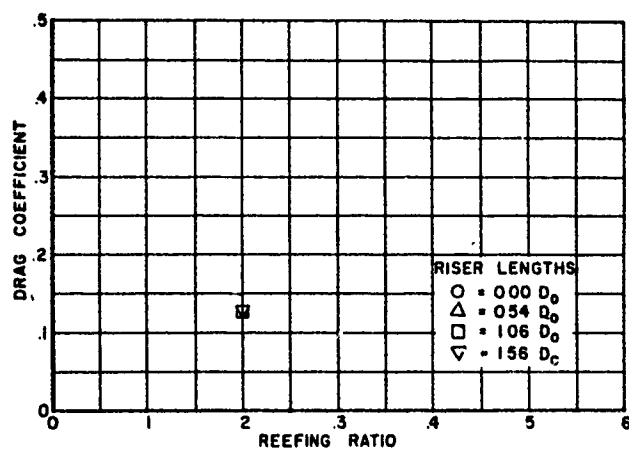


Figure 108. Variation of Drag Coefficient with Reefing Ratio and Riser Length, Equilibrium Test: Canopy Type - Ringslot; No. of Canopies in a Cluster - six

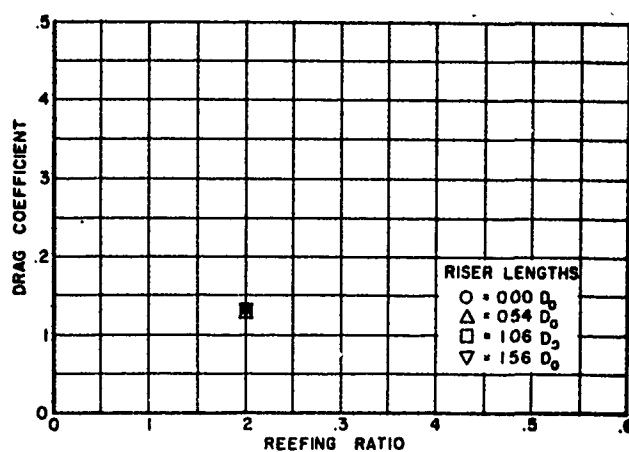


Figure 109. Variation of Drag Coefficient with Reefing Ratio and Riser Length, Equilibrium Test: Canopy Type - Ringslot; No. of Canopies in a Cluster - seven

SECTION 4

DATA DISCUSSION

4.1 General

For a logical consideration of the prime factors in this testing program—types of parachute canopies, number of parachute canopies in a cluster, riser lengths, reefing ratios, and types of testing—this section discusses the following: data accuracy and uncontrollable variables affecting test results, results obtained on each different type of parachute canopy, comparison of equilibrium and captive test results, and general trends common to all parachute canopy types investigated.

4.2 Data Accuracy

4.2.1 Over-all Data Accuracy

Because of several unknown contributing factors, an over-all data accuracy cannot be given. Yet, the instrumentation system demonstrated a repeatability well within one percent of full scale during the dead-weight calibration. The effect of inducing sting vibration on the readings appeared to be negligible. Furthermore, the transducers were utilized as near full scale as practicable during testing to minimize errors due to instrumentation sensitivity.

4.2.2 Raw Data Recordings and Measurements

In general, the raw data accuracy was considered high. The angle-of-attack values, obtained photographically, were ascertained to be within ± 0.25 degree. On the oscillograms, the traces depicting the tangential forces permitted accurate measurements; however, the traces representing the moment had oscillations which reduced somewhat the measurement accuracy. Initially, an average (steady-state) value derived from 0.05-inch increment measurements on 18 randomly selected moment traces was compared with the average obtained from an "eyeball" technique, whose accuracy was found to be within three percent of full scale of the transducer producing the trace.

4.2.3 Dynamic Pressure

Although no accuracy figures of the wind tunnel system operation were obtained during the dynamic pressure survey, the repeatability achieved was excellent. Dynamic pressure measurement inaccuracies

when compared to the dynamic pressure variations were considered inconsequential.

4.2.4 Other Factors Related to Data Accuracy

Other factors which contributed somewhat to inaccuracies in the data are as follows: (1) interference between the sting-balance and the parachute cluster, (2) wake from the airfoil and parachute attachment ring, (3) wind tunnel blockage, and (4) superposition of dynamic forces on steady state. Although all configurations were arranged symmetrically about zero-degrees angle-of-attack, as shown in Figure 8, the resultant asymmetrical distribution of the moment coefficient curves about this axis were caused by inaccuracies in canopy orientation, lack of fabrication exactness among the canopy models, variation in cloth permeability, asymmetrical canopy deformations, differential loading of suspension lines, and inaccuracies in reefing line lengths. Yet, every effort was made to minimize these causes of the asymmetrical data distribution.

The tangential force coefficients obtained in the captive tests with the configurations employing the smaller reefing ratios are low in comparison with the values obtained in the equilibrium tests with the same configurations. The latter values are considered more accurate since the canopies with the smaller reefing ratios in the captive tests were significantly affected by the slight variation of the local flow conditions attributed to the mounting arrangement.

Although the several factors mentioned above caused some scatter and error in the data, the discrepancies are not considered sufficient to affect seriously the validity of either the test results or the conclusions drawn from them.

4.3 Solid Canopies (Circular Flat and Extended Skirt)

The test results presented in Section 3 reveal certain trends which are nearly identical for the Circular Flat and Extended Skirt solid types of canopies. These trends and general observations for both types are discussed in this subsection.

The tangential force coefficient for both types of canopies was not affected by the angle of attack. Any apparent effect is within a small range centered at zero degrees angle of attack only. Although the data of some of the configurations indicate a decrease in the tangential force coefficient through this angle of attack range, the evidence does not warrant a general conclusion since the decrease was

probably due to testing restraints, which is discussed in greater detail in Subsection 4.5. As expected, since wake effects were not included in the investigation, the riser length did not significantly affect the tangential force coefficient or the drag coefficient of the clustered canopies.

The data indicate, as shown in Figures 110 and 111, a decrease in drag coefficient with an increasing number of unreefed canopies in a cluster. However, this effect does not appear in the reefed canopy data. In fact, for the canopies reefed to 0.3 and to 0.2 nominal diameter, the data reveal an increase in drag coefficient with an increasing number of canopies in a cluster. This demonstrates that the percentage changes in the drag coefficient from the unreefed condition to the successively diminishing reefing ratios do not remain the same as the number of canopies in a cluster vary. The drag coefficients from the equilibrium test results and the tangential force coefficients at zero degrees angle of attack from the captive test results were averaged to produce the data for the plotting of the curves in Figures 110 and 111. Some test data were not used to develop these curves since unrealistic trends would have been indicated. The unused data can be summarized according to three test categories as follows: (1) equilibrium tests employing zero riser length which resulted in low drag coefficients due to wake effects, (2) captive tests for single, reefed canopies which displayed low tangential force coefficients due to wake effects from the mounting arrangement, and (3) captive tests which displayed a dip in tangential force coefficient about zero degrees angle of attack.

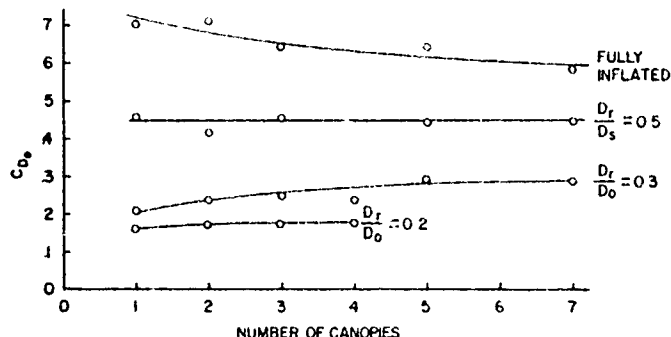


Figure 110. Graph for Flat Circular Type of Canopy Depicting Effect of Reefing Ratio and Number of Canopies in a Cluster on Drag Coefficient

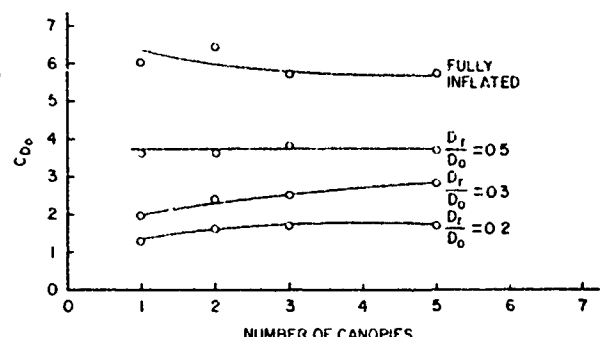


Figure 111. Graph for Extended Skirt Type of Canopy Depicting Effect of Reefing Ratio and Number of Canopies in a Cluster on Drag Coefficient

Since the +5 to -5 degree angle-of-attack range is of primary interest for the study of the static stability characteristics and the moment coefficient data is for practical purposes linear through this range, the data was linearized to derive $C_{M\alpha}$ for the determination of the static stability trends.

The static stability of the Flat Circular and Extended Skirt types of canopies increases as the reefing ratio, D_r/D_o , decreases until a reefing ratio of 0.3 is reached. As shown in Figures 112 and 113, this increase is quite pronounced. Although there is no data for reefing ratios less than 0.3, it appears that the static stability will decrease as the reefing ratio falls below $D_r/D_o = 0.3$.

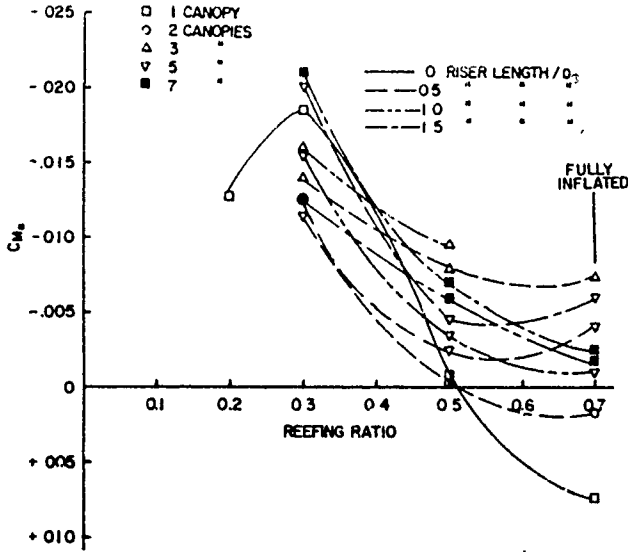


Figure 112. Effect of Reefing Ratio on Static Stability of Flat Circular Type of Canopy Shown Graphically

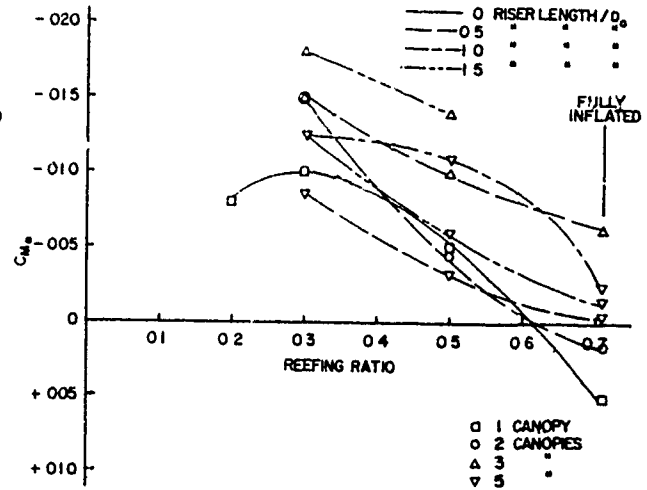


Figure 113. Effect of Reefing Ratio on Static Stability of Extended Skirt Type of Canopy Shown Graphically

The effect of the number of canopies in a cluster upon the static stability of a configuration is shown in Figures 114 and 115: three canopies apparently give the most stable configuration. Although three solid types of canopies, other variables fixed, produce the most stable configuration, no configuration with more than three canopies exhibited instability; however, some configurations with less than three canopies were unstable.

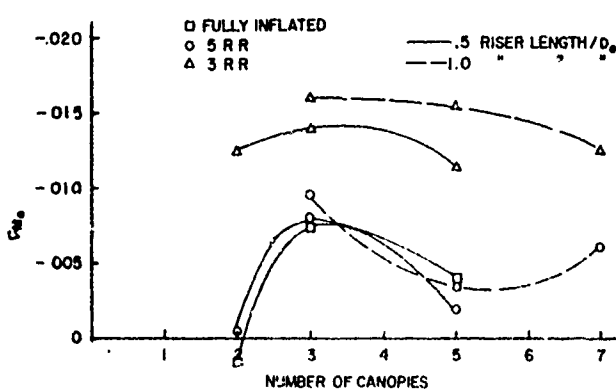


Figure 114. Plot Illustrating Effect of Number of Canopies in a Cluster on Static Stability of Flat Circular Type of Canopy

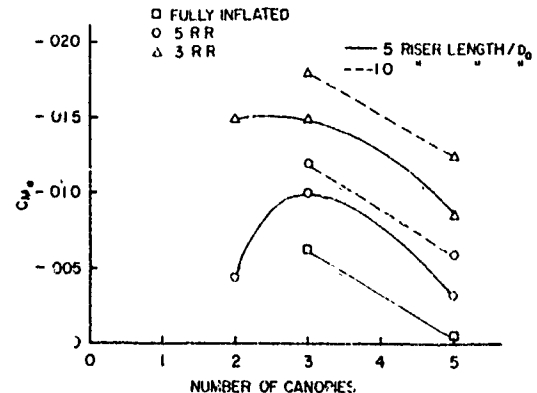


Figure 115. Plot Illustrating Effect of Number of Canopies in a Cluster on Static Stability of Extended Skirt Type of Canopy

As expected, the static stability of a given configuration increased as the riser length increased. But, this increase was not always linear as might have been anticipated. Figures 116 and 117 show the effect of riser length on the static stability and demonstrate quite forcibly that such effects cannot be linearly extrapolated into an unknown region.

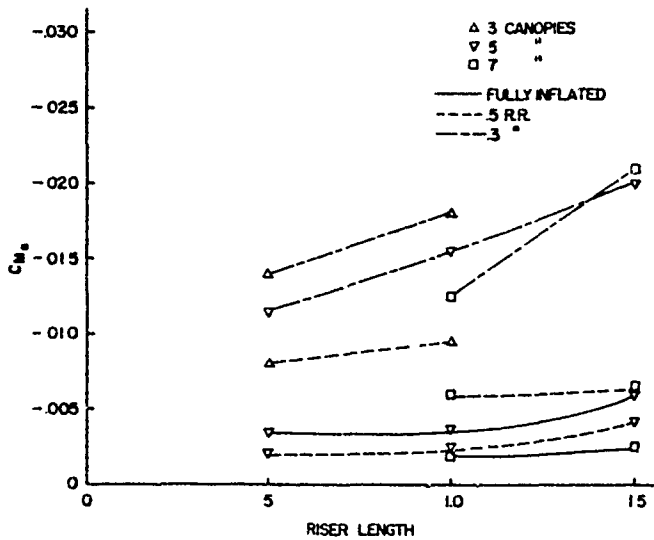


Figure 116. Effect of Riser Length on Static Stability of Flat Circular Type of Canopy Presented Graphically

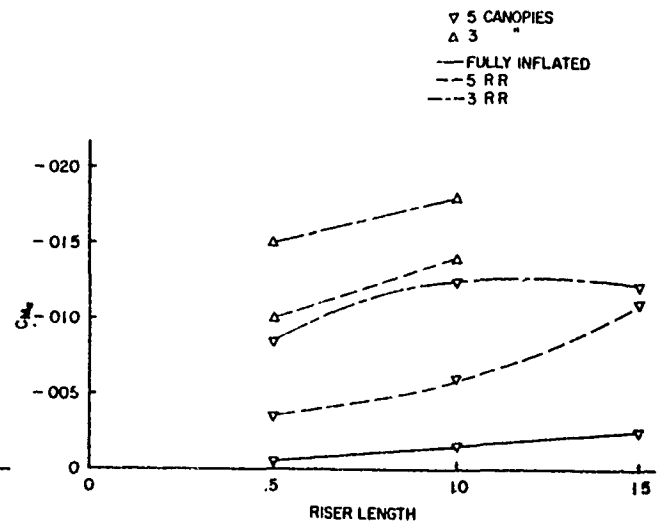


Figure 117. Effect of Riser Length on Static Stability of Extended Skirt Type of Canopy Presented Graphically

4.4 Ribbon Canopies (Circular Flat and Ringslot)

As the Circular Flat and Extended Skirt solid types of canopies were previously discussed together because of their nearly identical trends, so also in this section the Circular Flat Ribbon and Ringslot types of canopies are treated jointly since the latter two types similarly have trends almost identical.

Both riser length and angle of attack did not significantly affect the tangential force coefficient of the ribbon type of canopies. Yet, as shown in Figures 118 and 119, there is a slight decrease, or no change at all, in drag coefficient as the number of canopies in the cluster increases. The more the canopies are reefed, the less pronounced the decrease becomes; as the reefing ratio approaches 0.2, the change appears to be negligible. Nearly the same percentage change in drag coefficient occurs for reefing of the canopies, regardless of the number of canopies in the cluster.

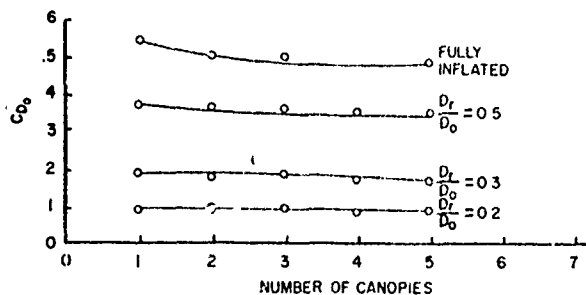


Figure 118. Graph for Ribbon Type of Canopy Depicting Effect of Reefing Ratio and Number of Canopies in a Cluster on Drag Coefficient

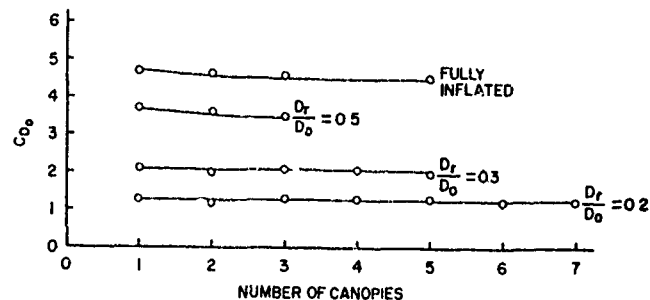


Figure 119. Graph for Ringslot Type of Canopy Depicting Effect of Reefing Ratio and Number of Canopies in a Cluster on Drag Coefficient

The static stability of the ribbon type of canopies appears to peak at a reefing ratio of approximately 0.5. This trend, as demonstrated in Figures 120 and 121, is obvious for the Ringslot type of canopy and possibly could be characteristic of the ribbon type of canopy. Unfortunately, due to the poor inflation properties of the ribbon type of canopies with the smaller reefing ratios, a significant amount of stability data could not be collected. The instability of the ribbon type of canopies for a one-canopy cluster with no reefing or riser exhibited in Figures 120 and 121 is not sufficiently understood to permit an adequate explanation. Yet, the instability could be said to be attributed to wake effects, porosity characteristics, model limitations, or all collectively.

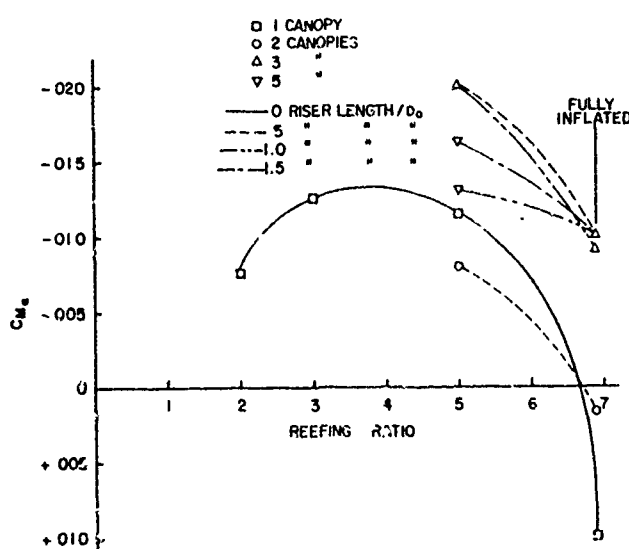


Figure 120. Effect of Reefing Ratio on Static Stability of Ribbon Type of Canopy Shown Graphically

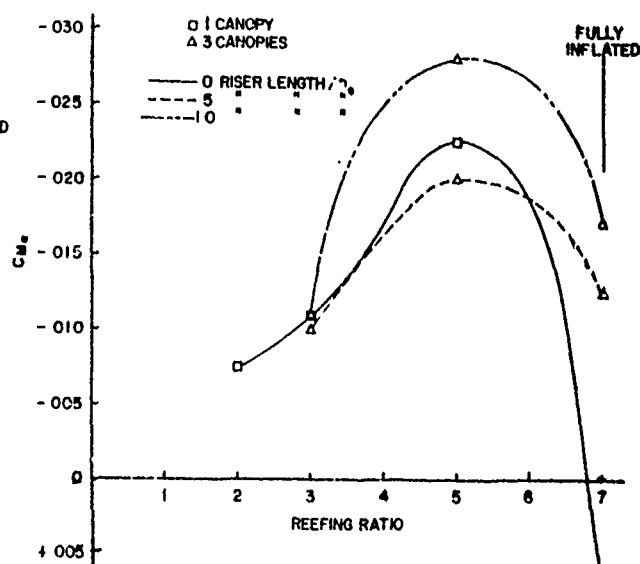


Figure 121. Effect of Reefing Ratio on Static Stability of Ringslot Type of Canopy Shown Graphically

The poor inflation properties of the ribbon type of canopies at the smaller reefing ratios also limited the information on the effects of the number of canopies and riser length on the static stability of these canopies. Still, the data gathered are presented in Figures 122 through 125. Probably the most that can be deduced from these figures is that there is some number of canopies in a given configuration which yields maximum stability and that there is an increase in stability with increasing riser length.

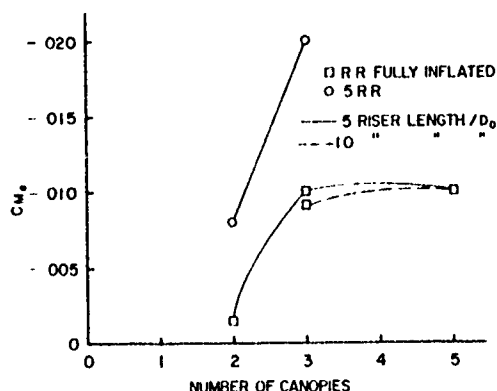


Figure 122. Plot Illustrating Effect of Number of Canopies in a Cluster on Static Stability of Ribbon Type of Canopy

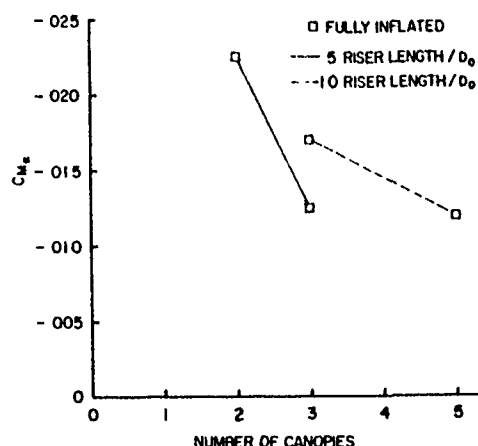


Figure 123. Plot Illustrating Effect of Number of Canopies in a Cluster on Static Stability of Ringslot Type of Canopy

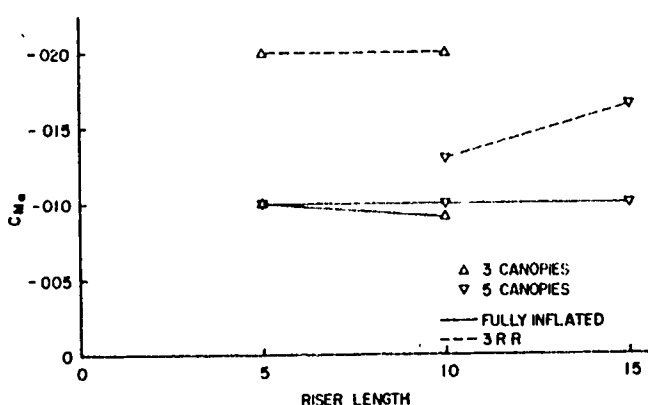


Figure 124. Effect of Riser Length on Static Stability of Ribbon Type of Canopy Presented Graphically

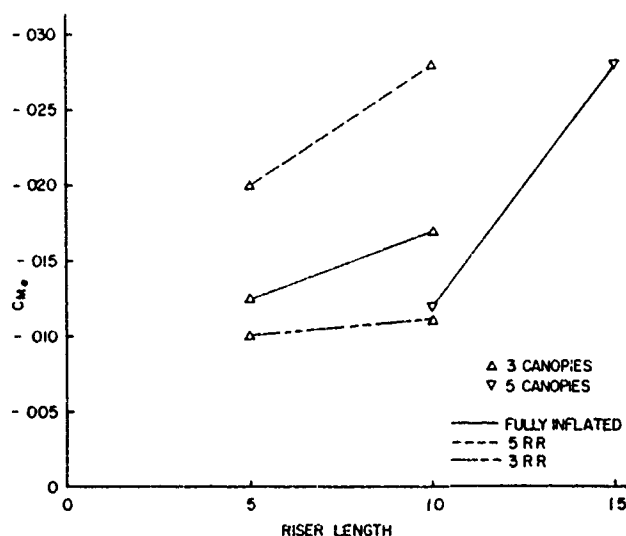


Figure 125. Effect of Riser Length on Static Stability of Ringslot Type of Canopy Presented Graphically

4.5 Over-all Comparisons

Comparing the solid cloth type of canopies with the ribbon type reveals that neither the angle of attack nor the riser length affect the tangential force coefficient. The percentage decrease in drag coefficient for reefing for the ribbon type of canopies remained approximately the same as the number of canopies in the cluster varied while the percentage decrease for the solid cloth type of canopies changed as the number of canopies varied. With unreefed canopies in a cluster, the solid cloth type had a much larger decrease in drag coefficient with increasing number of canopies than the ribbon type. Also, when the solid cloth type of canopies were reefed to 0.3 and 0.2, they had an increase in drag coefficient with an increasing number of canopies in the cluster; whereas the ribbon type of canopies maintained a nearly constant drag coefficient for all variations of the number of canopies in a cluster.

A comparison of the static stability of the solid cloth type of canopies with that of the ribbon type of canopies revealed that the solid cloth type peaked at a reefing ratio of 0.3 while the ribbon type peaked at a reefing ratio of about 0.5. Furthermore, both types of canopies evidenced an increase in stability with increasing riser length.

That the static stability did not exhibit a linear increase with increasing riser length for any of the canopies investigated was undoubtedly due to the interference among the parachutes in a cluster and to the change in the effective angle of attack of each canopy in a cluster as the riser length changed.

No explanation has been attempted for the stability exhibited over the entire angle-of-attack range. Some configurations evidenced positive stability up to an angle of attack and then instability through a particular region, as shown in Figure 20. However, because of the mutual interference present, the stability for a cluster of canopies cannot be predicted from the observation of a single canopy. This interference may account for the unstable region mentioned above. The instability may be also explained partly by the fact that the single canopy is in itself unstable.

It is surmised that the dip or decrease in the tangential force coefficient about zero degrees angle of attack for the captive tests is not representative of the actual performance of a free-falling canopy. This effect, however, occurs only with those unstable configurations which oscillate, cone, and/or glide under free-fall conditions. It, therefore, is concluded that the tangential force coefficient was lower than the true effective drag coefficient because the canopies were restrained.

SECTION 5

CONCLUSIONS AND RECOMMENDATIONS

5.1 Conclusions

The following conclusions are presented:

- (1) For the solid cloth type of canopies, the drag coefficient decreased with an increasing number of unreefed canopies in a cluster, remained nearly constant with the canopies reefed to 0.5, and increased with an increasing number of canopies in a cluster reefed to 0.3 or 0.2.
- (2) For the ribbon type of canopies, the drag coefficient decreased slightly with an increasing number of canopies in a cluster, and the percentage decrease in drag coefficient due to reefing remained almost constant as the number of canopies in a cluster varied.
- (3) Neither the riser length nor the angle of attack affected the drag coefficient in any of the types of canopies investigated.
- (4) The static stability for the solid cloth type of canopies peaked when the reefing ratio was 0.3 and also when three canopies were in a cluster.
- (5) The static stability for the ribbon type of canopies peaked at a reefing ratio of approximately 0.5.
- (6) The static stability for all the types of canopies increased with increasing riser length.
- (7) The more stable configurations exhibited smaller tangential force coefficients and tended to collapse at a lower angle of attack.
- (8) Because of the interference among the canopies in a clustered arrangement, single canopy test results cannot be utilized to predict with certainty the aerodynamic characteristics of clustered configurations.

5.2 Recommendations

The following recommendations are presented:

- (1) Additional wind tunnel tests should be conducted to determine cluster stability characteristics for other orientations.

(2) A theoretical study should be made to attempt to explain the stability characteristics of clustered parachutes.

(3) Tests should be conducted for seven parachutes in a cluster with one of these parachutes positioned in the center.

(4) Tests should be conducted with a more realistic separation between parachutes than the arbitrary 1/2-inch separation used for this program.

(5) Further tests on the ribbon type of canopies should be conducted with a sting which produces less wake effects in order to obtain a more definite description of the static stability with the reefing ratios of 0.3 and 0.2.

APPENDIX I

PARACHUTE INSTRUMENTATION SYSTEM

Introduction

The instrumentation system, described in this text, required the design and construction of a two-component balance and the associated recording equipment employed to measure tangential force, moment, and angle of attack of parachute clusters.

Two-Component Balance

The two-component balances were designed to provide minimum aerodynamic interference over an angle of attack from -25 to $+25$ degrees. Their structural rigidity, however, was such that the induced dynamic load caused by the oscillating parachute clusters would not screen the desired static load parameters.

Figure 126 depicts the major balance assembly for parachute positioning and load sensing. The specially constructed H-beam is housed in the aluminum airfoil. This airfoil affords added stiffness to the H-beam, which is the main support structure for the boom, force sensing element, and angle-of-attack mechanism. The angle of attack was imposed on the parachute clusters by a mechanically linked hydraulic system. The hydraulic cylinder is mounted to the H-beam and plumbed to the hydraulic control console. The hand pump located at the right of this console supplied the pressure to the cylinder. Located in the hydraulic control console are the metering valves, four-way hand operated control valve, and angle-of-attack indicator.

Figure 126.

Illustration of the Balance Assembly for Parachute Positioning and Load Sensing

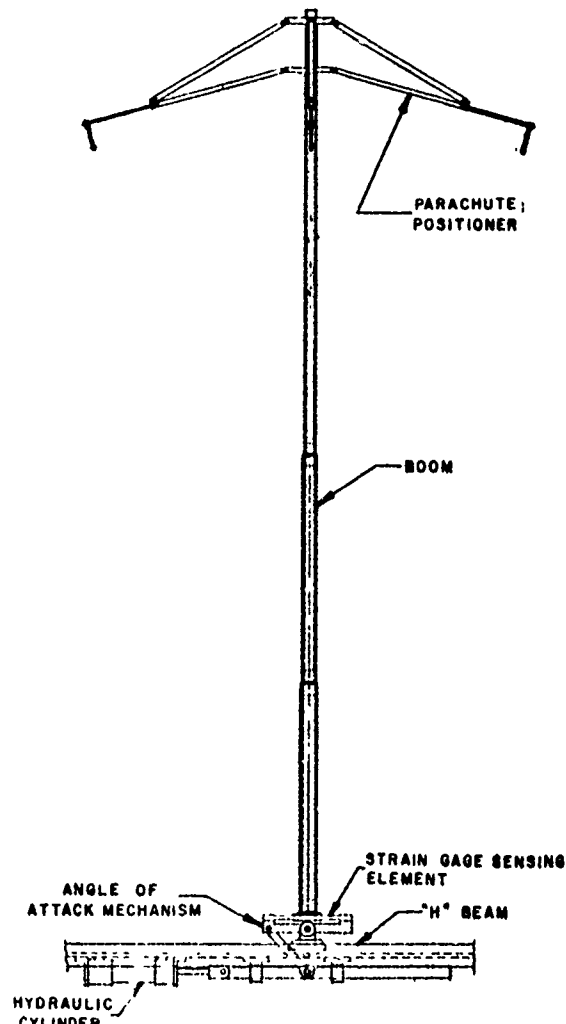


Figure 127 shows the two-component balance and the associated mechanical equipment installed in the Vertical Wind Tunnel. As can be seen, the two parachute force parameters are induced into the force-sensing element by the sting. Eight bakelite-type strain gages were bonded to the force sensing members and were connected into four active arm-bridge circuits. These active arms were wired to eliminate cross-talk between force measurements. Another feature of the two-component balance was the capability of interchanging four different force-sensing elements to cover all testing areas of a configuration with ample sensitivity. See Figure 128.

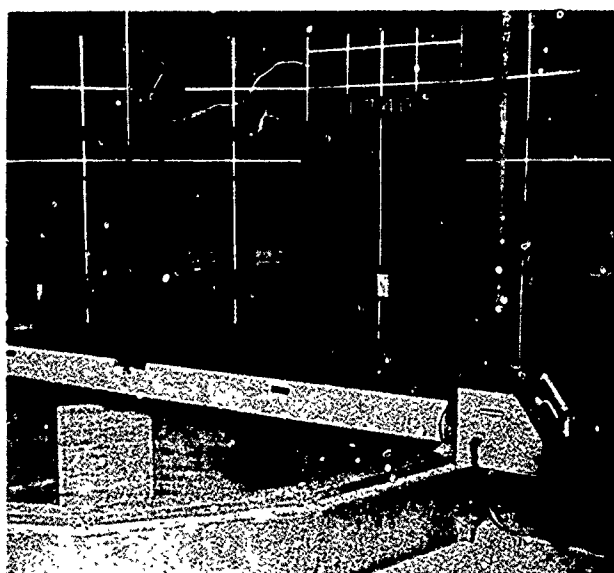


Figure 127.

View Showing Installation of Two-Component Balance with Hydraulic Control Console Seen to the Right

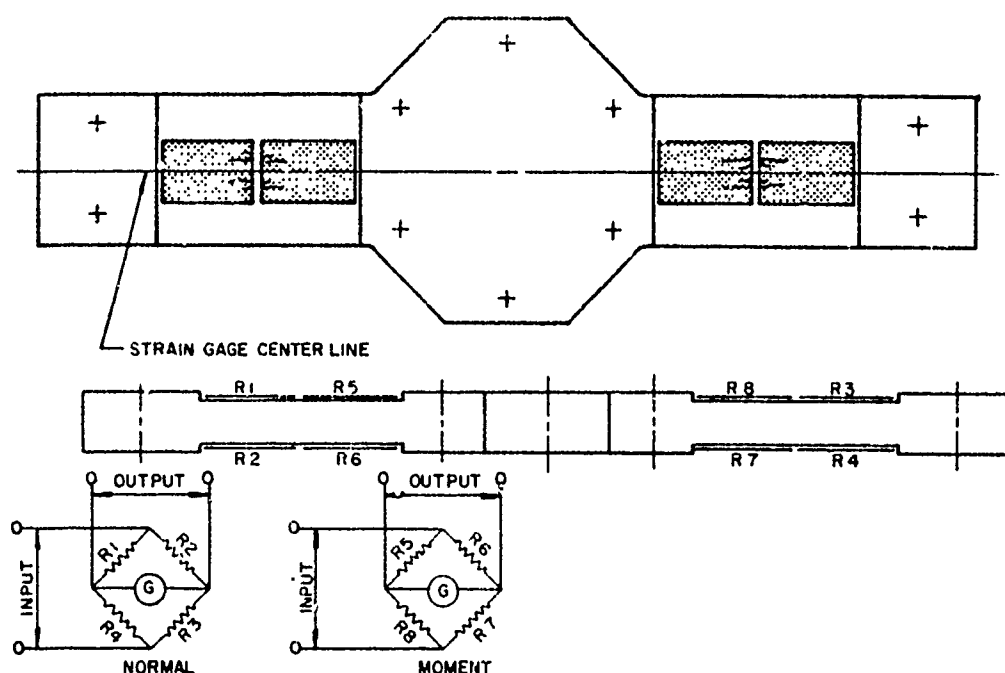


Figure 128. Illustration of Typical Strain Gage Sensing Element

Instrumentation

Figure 129 is a block diagram of the instrumentation system employed to record the parachute cluster parameters. Each force-measuring circuit employed four active arm strain gages with a normal resistance of 350 ohms. The bridge-excitation voltage was supplied by a 12-volt D. C. supply contained in the bridge control unit. Since this excitation voltage was controllable from 0- to 12-VDC, the circuit sensitivity could be increased or decreased. The output signals from the strain gages were recorded on the C. E. C. oscillograph. To eliminate undesirable frequencies, filter networks for both the moment and tangential force were incorporated into the galvanometer input circuit. These filters have a frequency cutoff at approximately six cycles per second.

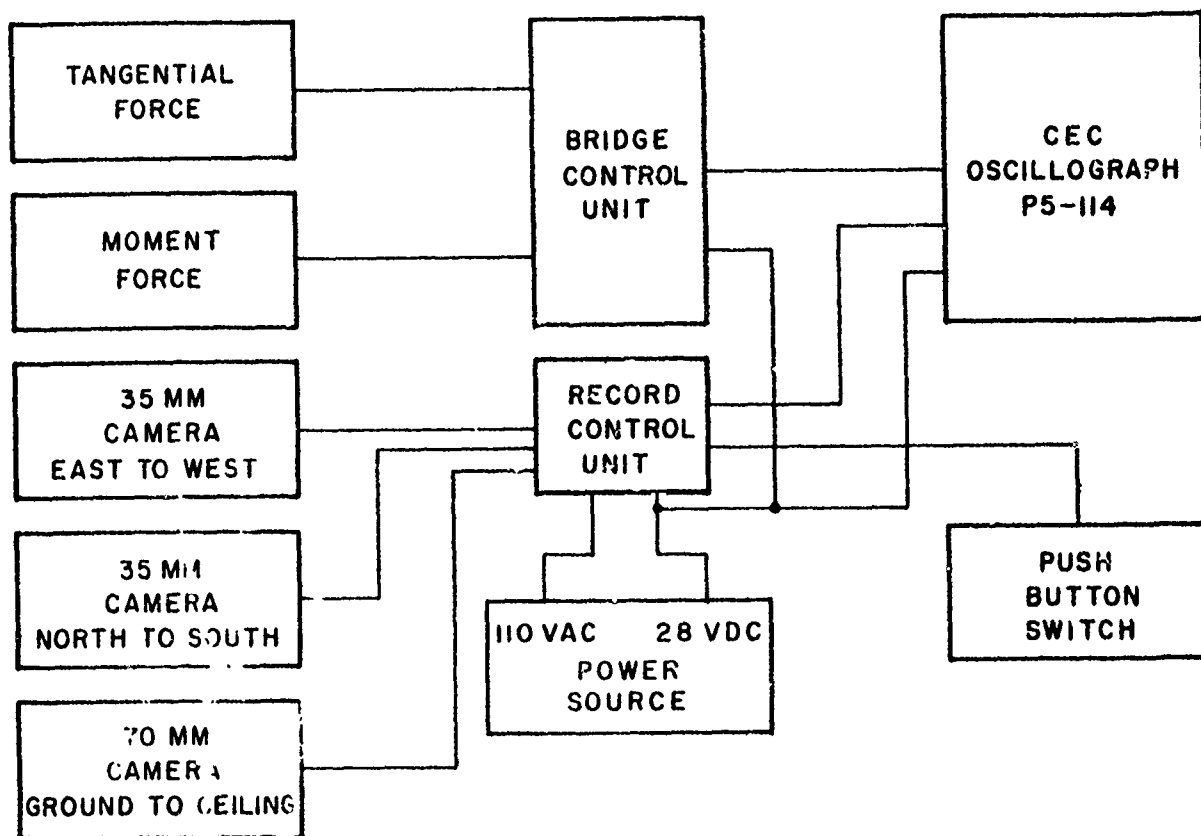


Figure 129. Block Diagram of Recording Instrumentation System

The cameras employed for the testing of the parachute clusters are as follows: two of the 35 mm type and one of the Air Research 70 mm type. The field of view of the two 35-mm cameras were north to south and east to west. The 70-mm camera, located in the throat of the wind tunnel nozzle, had a field of view into the mouth of the wind tunnel nozzle and the test chamber. The location of all three cameras is illustrated in Figure 130.

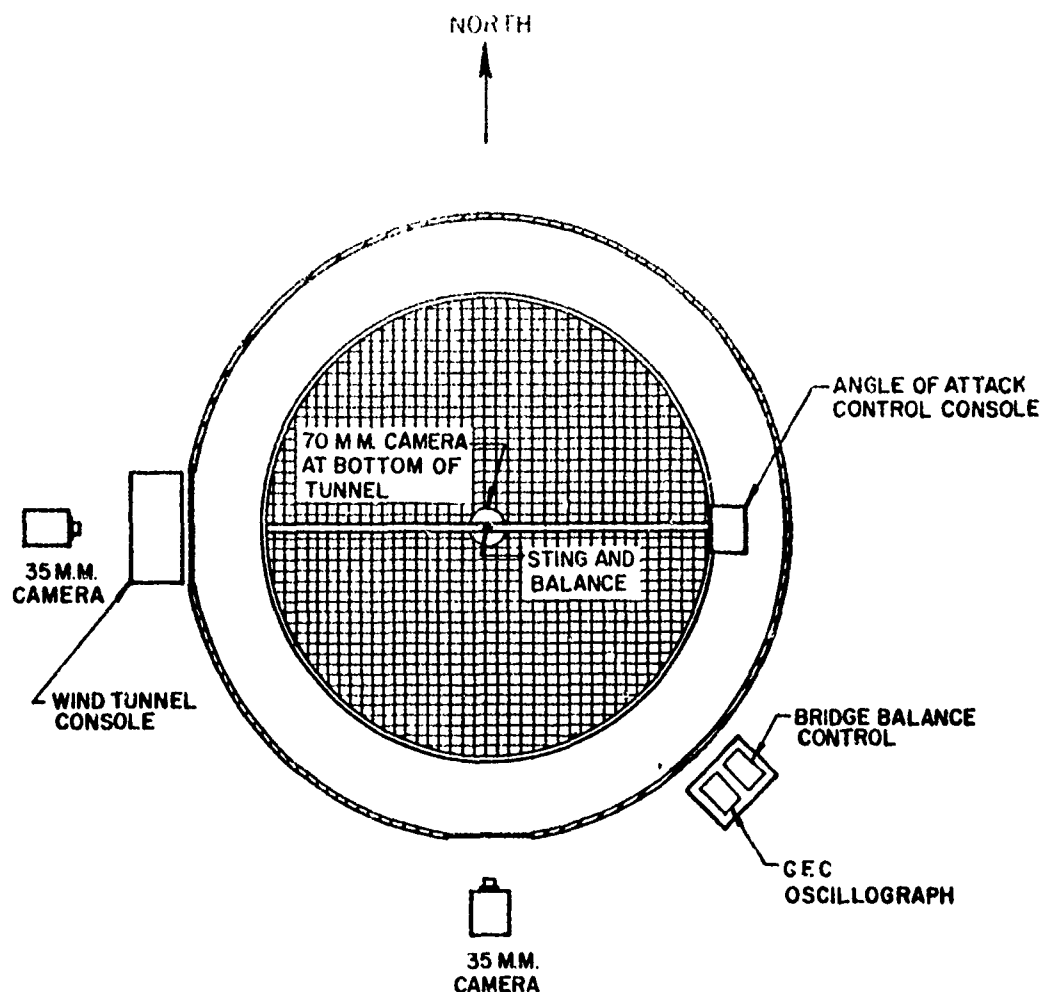


Figure 130. Plan View of Wind Tunnel Indicating Camera Locations as Related to other Equipment

Calibrations were of two types: (1) primary calibrations and (2) secondary calibrations. When primary calibrations were performed, the stimulus was applied to the sensor and the output was recorded under controlled conditions. When the sensors were unbalanced electrically to change the output level, the calibration was a secondary one. The two-component balance sensing elements were calibrated by applying a precision weight through its usable range. As the weight was being applied, its value was recorded by the oscillograph. Calibration runs were made in both directions so that linearity, hysteresis, and repeatability could be determined. Typical calibration curves are illustrated in Figures 131 and 132.

As seen in Figure 133, secondary calibration was accomplished by placing a precision resistor in parallel with one leg of the bridge network. This resistor produces an unbalanced condition to duplicate a mechanical input producing an electrical output level. This output level was the "Cal Pulse" which was equal to the mechanical input per galvanometer deflection. The "Cal Pulse" was a standard in the processing of the test data.

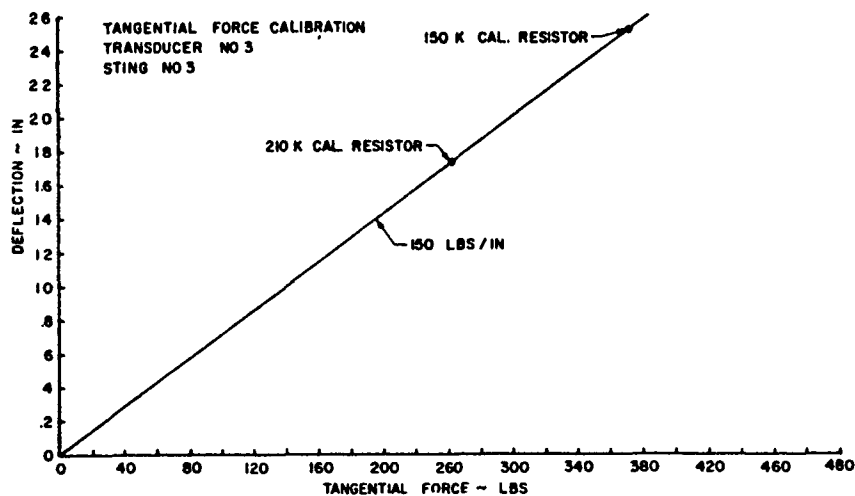


Figure 131. Typical Tangential Force Calibration Curve for Transducer and Sting No. 3

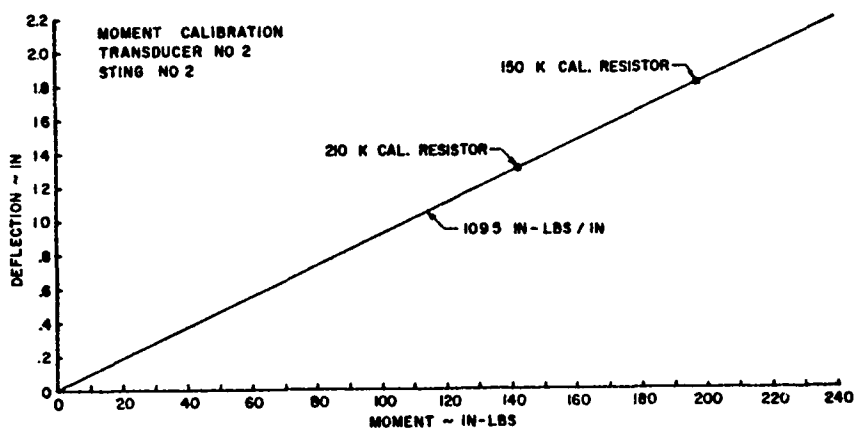


Figure 132. Typical Moment Calibration Curve for Transducer and Sting No. 2

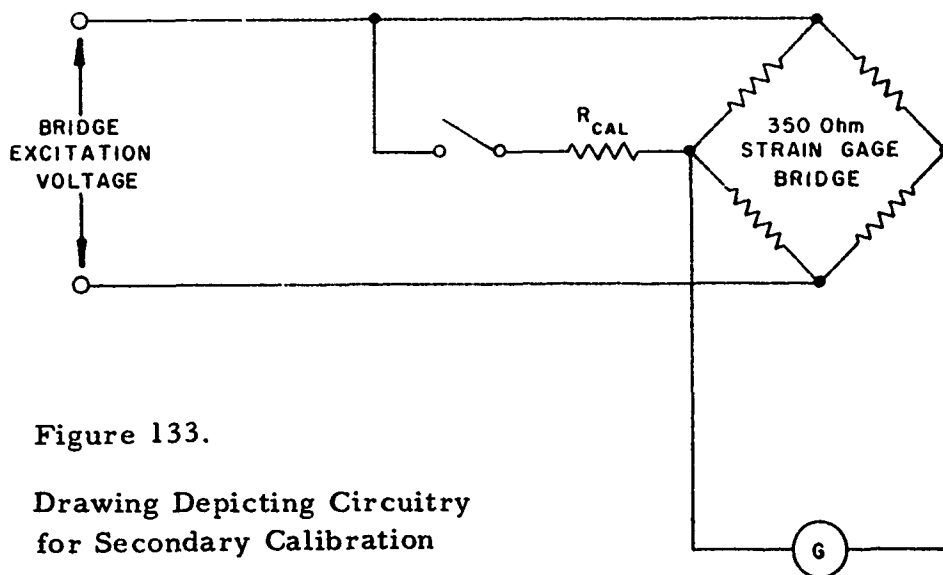


Figure 133.

Drawing Depicting Circuitry
for Secondary Calibration

In order that the "Cal Pulse" would be of a proper magnitude, a special pre-test was prescribed. To insure proper use of the pre-test calibration, the transducer power supply was monitored constantly during each testing sequence. When there was fluctuation only in force-measuring circuit sensitivity, it was detected and noted for incorporation into the data reduction.

Table VI presents the calibrations for the four elements which sensed the tangential forces and pitching moments.

Table VI

Sensing Element Calibrations for Tangential Force and Pitching Moment

<u>Sensing Element</u>	<u>Tangential Force</u>		<u>Pitching Moment</u>	
	<u>Cal. Range</u>	<u>Cal. Slope</u>	<u>Cal. Range</u>	<u>Cal. Slope</u>
1	0 to 60 lb.	29.2 lb. /in.	±200 in. -lb.	97.5 in. -lb. /in.
2	0 to 150 lb.	70.5 lb. /in.	±240 in. -lb.	109.5 in. -lb. /in.
3	0 to 300 lb.	150.0 lb. /in.	±1375 in. -lb.	478.3 in. -lb. /in.
5	0 to 400 lb.	187.5 lb. /in.	±1600 in. -lb.	785.0 in. -lb. /in.

APPENDIX II

MODEL PARACHUTE DESCRIPTION

Parachute Descriptions

Flat Circular, 10% Extended Skirt, Ribbon, and Ringslot are the types of parachutes tested in this program. Presented in Figure 134 are typical gore patterns for the Ribbon and Ringslot parachutes. Since the Flat Circular and 10% Extended Skirt parachutes are defined uniquely by their nominal surface area, no gore patterns are presented for these parachutes. Table I gives a description of each individual parachute.

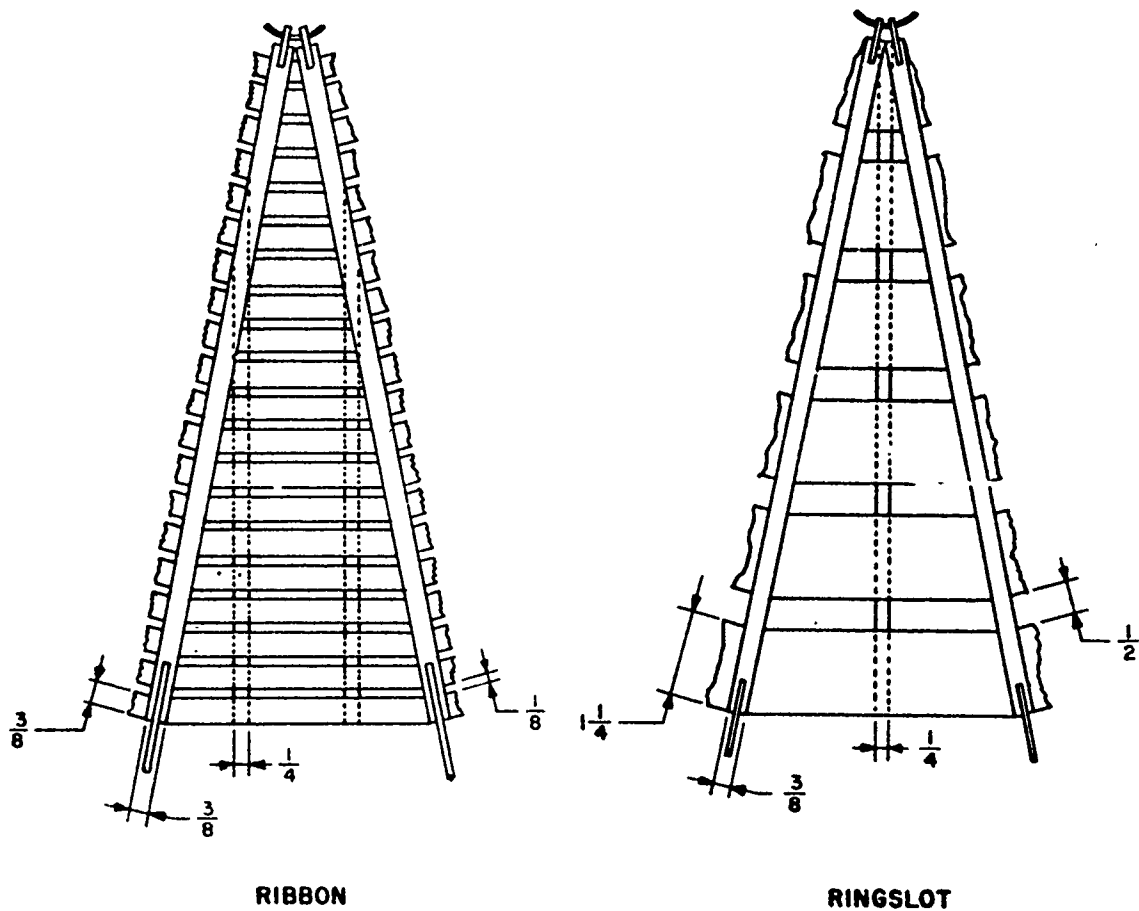


Figure 134. Typical Patterns for Gore Configurations

Measurement Technique

Presented in Figures 135 and 136 is the technique used to obtain the individual parachute geometric characteristics. As illustrated, a circular board slightly larger in diameter than the parachutes was used to stretch the parachute so that each gore of a parachute bore approximately the same amount of tension to eliminate radically different measurements for the nominal diameters in the same parachute. All quoted dimensions are averages of measurements taken at several different locations to negate local inaccuracies inherent in fabrication.

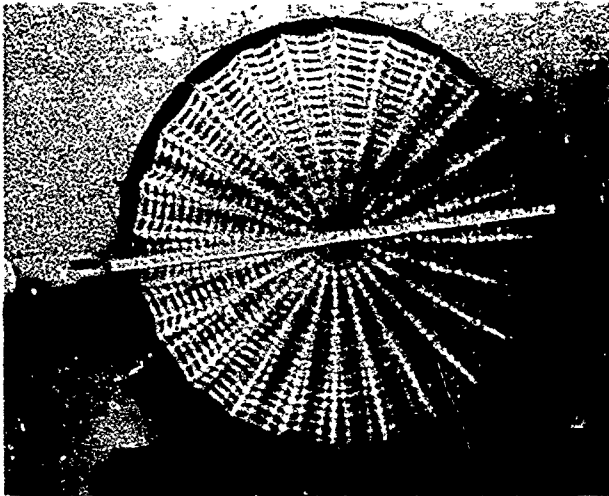


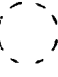
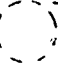






Figure 135. View Showing Measuring Technique for Flat Pattern Canopies



Figure 136. View Showing Measuring Technique for Extended Skirt Canopies

As shown in Figure 136, a slightly different measuring technique was used for the Extended Skirt than for the flat-pattern parachutes. Direct flat-pattern measurements on the Extended Skirt parachute were made by folding back the skirt at approximately the point of skirt extension.

<p>  </p> <p> Aeronautical Systems Division, Dir/Aeromechanics, Flight Accessories Lab, Wright-Patterson AFB, Ohio. Rpt No. ASD-TDR-63-159. WIND TUNNEL STUDY OF PARACHUTE CLUSTERING. Final report, April 63, 80p., incl illus. and tables. Unclassified Report </p> <p> Four types of canopies were tested in a 12-foot ver- tical wind tunnel at a velocity of approximately 100 feet per second to determine the static stability and drag characteristics of multiple canopies in various clustered arrangements under captive and equilibrium test conditions. Solid Flat Circular, Extended Skirt, Ringlot, and Circular Flat Ribbon were the types of canopy tested. Canopies of each type were tested individually and in clusters ranging from two to seven </p> <p>  (over) </p>	<p> 1. Parachute Clusters 2. Equilibrium Velocity </p> <p> I. AFSC Proj 6065, Task 606502 II. Contract No. AF 33(657)-7985 III. Technology Incor- porated, Dayton, O. IV. Braun, J. F., and Walcott, W. B. V. Avail fr OTS VI. In ASTIA collection </p>	<p>  </p> <p> Aeronautical Systems Division, Dir/Aeromechanics, Flight Accessories Lab, Wright-Patterson AFB, Ohio. Rpt No. ASD-TDR-63-159 WIND TUNNEL STUDY OF PARACHUTE CLUSTERING. Final report, April 63, 80p., incl illus. and tables. Unclassified Report </p> <p> Four types of canopies were tested in a 12-foot ver- tical wind tunnel at a velocity of approximately 100 feet per second to determine the static stability and drag characteristics of multiple canopies in various clustered arrangements under captive and equilibrium test conditions. Solid Flat Circular, Extended Skirt, Ringlot, and Circular Flat Ribbon were the types of canopy tested. Canopies of each type were tested individually and in clusters ranging from two to seven </p> <p>  (over) </p>	<p> 1. Parachute Clusters 2. Equilibrium Velocity </p> <p> I. AFSC Proj 6065, Task 606502 II. Contract No. AF 33(657)-7985 III. Technology Incor- porated, Dayton, O. IV. Braun, J. F., and Walcott, W. B. V. Avail fr OTS VI. In ASTIA collection </p>
<p>  </p> <p> canopies per cluster. A special two-component ba- lance was fabricated to measure the pitching moment and tangential force over an angle-of-attack range of ±25 degrees. The effects of riser length, angle-of- attack, reefing ratio, and the number of canopies in a cluster on the tangential force and static stability are discussed. Also, the characteristics peculiar to the solid type of canopies (Solid Flat Circular and Extended Skirt) and to the ribbon type of canopies (Ringlot and Circular Flat Ribbon) are noted. </p> <p>  </p>		<p>  </p> <p> canopies per cluster. A special two-component ba- lance was fabricated to measure the pitching moment and tangential force over an angle-of-attack range of ±25 degrees. The effects of riser length, angle-of- attack, reefing ratio, and the number of canopies in a cluster on the tangential force and static stability are discussed. Also, the characteristics peculiar to the solid type of canopies (Solid Flat Circular and Extended Skirt) and to the ribbon type of canopies (Ringlot and Circular Flat Ribbon) are noted. </p> <p>  </p>	